UNIVERSIDADE FEDERAL DO CEARÁ

CENTRO DE TECNOLOGIA

DEPARTAMENTO DE ENGENHARIA ELÉTRICA

PROGRAMA DE PÓS-GRADUAÇÃO EM ENGENHARIA ELÉTRICA

DOUTORADO EM ENGENHARIA ELÉTRICA

MAGNO PRUDÊNCIO DE ALMEIDA FILHO

CONTRIBUTIONS ON MODEL-BASED CONTROLLERS APPLIED TO DEAD-TIME SYSTEMS

FORTALEZA

2021

MAGNO PRUDÊNCIO DE ALMEIDA FILHO

CONTRIBUTIONS ON MODEL-BASED CONTROLLERS APPLIED TO DEAD-TIME
SYSTEMS

Tese apresentada ao Curso de Doutorado em Engenharia Elétrica do Programa de Pós-graduação em Engenharia Elétrica do Centro de Tecnologia da Universidade Federal do Ceará, como requisito parcial à obtenção do título de doutor em Engenharia Elétrica. Área de Concentração: Engenharia Elétrica

Orientador: Prof. Bismark Claure Torrico, Dr.

Coorientador: Prof. Fabrício G. Nogueira, Dr.

FORTALEZA

2021

MAGNO PRUDÊNCIO DE ALMEIDA FILHO

CONTRIBUTIONS ON MODEL-BASED CONTROLLERS APPLIED TO DEAD-TIME SYSTEMS

<div align="right">

Tese apresentada ao Curso de Doutorado em Engenharia Elétrica do Programa de Pós-graduação em Engenharia Elétrica do Centro de Tecnologia da Universidade Federal do Ceará, como requisito parcial à obtenção do título de doutor em Engenharia Elétrica. Área de Concentração: Engenharia Elétrica

</div>

Aprovada em: 21 de dezembro de 2020.

BANCA EXAMINADORA

_____
Prof. Bismark Claure Torrico, Dr.   (Orientador)
Universidade Federal do Ceará (UFC)

_____
Prof. Fabrício G. Nogueira, Dr.   (Coorientador)
Universidade Federal do Ceará (UFC)

_____
Prof. Tito L. M. Santos, Dr.
Universidade Federal da Bahia (UFBA)

_____
Profa. Michela Mulas, Ph.D.
Universidade Federal do Ceará (UFC)

_____
Prof. Walter Barra Junior, Dr.
Universidade Federal do Pará (UFPA)

Aos meus pais, Magno e Sandra. Às minhas
irmãs, Flávia, Lívia, Fernanda e Larissa. À Titia.
À todos os amigos e amigas. À minha amiga e
companheira, Jarina.

ACKNOWLEDGEMENTS

"If I have seen further it is by standing on the shoulders of giants."

(Isaac Newton)

ABSTRACT

This work addresses the analysis and design of model-based controllers applied to the control of single-input single-output (SISO) and multiple-input multiple-output (MIMO) stable, unstable and integrative dead-time systems. Dead-time, which appears in many industrial processes, is a rather challenging issue in the process control area since the transport delay can lead the closed-loop system to undesired oscillatory behaviour or even instability. The longer the delay, the more difficult it is to cope with it, and one solution to this problem consists of using dead-time compensator (DTC) structures. Thus, initially, this work proposes new guidelines for the tuning of a simplified DTC focusing on industrial processes. The new guidelines employ different poles in the robustness filter of the DTC in order to consider the trade-off between noise attenuation, disturbance rejection performance and overall closed-loop robustness. Furthermore, an extension of the simplified DTC structure for state-space systems is also proposed. The proposed structure has few adjustment parameters and can be applied to both continuous and discrete-time systems. Moreover, it allows improving rejection of both matched and unmatched unknown disturbances for linear time-invariant (LTI) systems with input delay. It is worth to highlight that finite spectrum assignment (FSA) based implementation is used in order to guarantee the internal stability of the proposed state-space controller, which is a novel strategy in the DTC literature for guaranteeing a safe implementation for non Hurwitz open-loop systems. Although the simplified DTC state-space structure is useful for dealing with MIMO systems, it is well known that model predictive controllers (MPCs) can yield some advantages when dealing with such class of processes, specially in the case of non-square and multiple-delay systems. Therefore, a generalized predictive control (GPC) based DTC structure that can deal with aforementioned issues is also developed. Finally, this work also presents a simplified control strategy based on GPC that is applied to two-inputs single-output (TISO) systems in an economic context when the two inputs are from different nature, thus yielding different operating costs. Through simulations and practical experiments, it is shown that the proposed approaches present better results in the control of dead-time processes than other recent works from the literature.

Keywords: Dead-time Systems. Model-based Control. Dead-time Compensator. Generalized Predictive Control.

RESUMO

Este trabalho apresenta a análise e o projeto de controladores baseados em modelos aplicados ao controle de sistemas SISO (entrada e saída únicas) e MIMO (múltiplas entradas e múltiplas saídas), estáveis, instáveis e integradores com atraso de transporte. O atraso de transporte, que aparece em muitos processos industriais, é um problema bastante desafiador na área de controle de processos, já que pode levar o sistema de malha fechada a um comportamento oscilatório ou até mesmo à instabilidade. Quanto mais longo o atraso, mais difícil é lidar com ele, e uma solução para esse problema consiste em usar estruturas compensadoras de tempo morto (DTC). Assim, inicialmente, este trabalho propõe novas diretrizes para o ajuste de um DTC simplificado com foco em processos industriais. As novas diretrizes utilizam diferentes pólos no filtro de robustez do DTC a fim de considerar o compromisso entre atenuação de ruído, rejeição de perturbações e robustez em malha fechada. Além disso, também é proposta uma extensão para espaço de estados da estrutura simplificada do DTC. A estrutura proposta possui poucos parâmetros de ajuste e pode ser aplicada a sistemas de tempo contínuo e discreto. Além disso, permite melhorar a rejeição de distúrbios casados e não-casados para sistemas lineares invariantes no tempo (LTI) com atraso de transporte. Uma implementação baseada em FSA (finite spectrum assignment) é utilizada para garantir a estabilidade interna do controlador proposto em espaço de estados. Essa é uma abordagem inovadora na literatura de DTC para garantir uma implementação internamente estável para sistemas não-Hurwitz em malha aberta. Embora a estrutura simplificada do DTC em espaço de estados seja útil para lidar com sistemas MIMO, os controladores preditivos baseados em modelos (MPCs) possuem algumas vantagens em relação à esse tipo de processos, especialmente para o caso de sistemas MIMO não-quadrados e com múltiplos atrasos. Portanto, este trabalho apresenta uma estrutura DTC baseada no controlador preditivo generalizado (GPC) capaz de lidar com sistemas MIMO não-quadrados e com múltiplos atrasos. Finalmente, este trabalho também apresenta uma estratégia de controle simplificada baseada no GPC e aplicada a sistemas TISO (duas entradas e uma única saída) em um contexto econômico quando as duas entradas são de natureza diferentes, gerando custos operacionais diferentes. Através de simulações e experimentos práticos, mostra-se que as abordagens propostas apresentam melhores resultados em relação ao controle de processos com atraso de transporte do que outros trabalhos recentes da literatura.

Palavras-chave: Sistemas com Atraso de Transporte. Controle Baseado em Modelo. Compen-

sadores de Tempo Morto. Controle Preditivo Generalizado.

LIST OF FIGURES

LIST OF TABLES

LIST OF ABBREVIATIONS AND ACRONYMS

2DOF	two-degree-of-freedom
AP	Artstein predictor
DMC	dynamic matrix control
DTC	dead-time compensator
FIR	finite impulse response
FOPDT	first order plus dead time
FSA	finite spectrum assignment
FSP	filtered Smith predictor
GPC	generalized predictive control
LTI	linear time-invariant
MIMO	multiple-input multiple-output
MPC	model predictive control
MSP	modified Smith predictor
NICU	neonatal intensive care unit
PI	proportional-integral
PID	proportional-integral-derivative
SDTC	simplified DTC
SFSP	simplified filtered Smith predictor
SISO	single-input single-output
SOPDT	second order plus dead time
SP	Smith predictor

LIST OF SYMBOLS

$\mathscr{L}$	Laplace transform
$\mathbb{R}$	The set of real numbers
k	Discrete-time sample
t	Continuous time
ω	Angular frequency
u	Input of a system
y	Output of a system
$\dot{x}$	Derivative of x
$\hat{x}$	Predicted value of x
$x(k+h\|k)$	Value of $x(k+h)$ at instant k
$\bar{\sigma}(\cdot)$	Maximum singular value function
$\Xi(\cdot)$	Minimal state-space realization
H_{yu}	Transfer function from signal u to signal y
I_R, i_R	Robustness indexes
A^T	The transpose of matrix A
A^{-1}	The inverse of matrix A

CONTENTS

1 INTRODUCTION

Dead time, which appears in many industrial processes, is a rather challenging issue in the process control area, since the transport delay can lead the system to undesired oscillatory closed-loop response or even instability. That way, this work proposes the analysis and design of model-based controllers applied to the control of single-input single-output (SISO) and multiple-input multiple-output (MIMO) stable, unstable and integrative dead-time systems. Practical aspects such as tuning rules for set-point tracking, disturbance rejection, noise attenuation and robustness are considered in the design of the controllers. Through simulations and practical experiments, it is shown that the proposed approaches present better results in the control of dead-time processes than other recent works from the literature.

1.1 Motivation

The transport delays, also known as dead times, are commonly found in real process due to multiple sources of communication, mass and energy transport delay, processes containing time-lag associated dynamics, or even by the processing time for sensors or to compute the control laws (NORMEY-RICO; CAMACHO, 2007). Although classical controllers such as proportional-integral (PI) and proportional-integral-derivative (PID) may be used when dead-time is relatively small (MERCADER; BAÑOS, 2017; SEER; NANDONG, 2017; BEGUM *et al.*, 2018), their performance is usually degraded for long time-delayed systems. Processes with large dead-time are quite difficult to control by using conventional feedback controllers because the effects of the perturbations take time to be felt by the controller and, in addition, the control signal does not produce immediate effect on the system output (NORMEY-RICO; CAMACHO, 2008). Furthermore, the longer the delay, the more difficult it is to cope with it.

In process control, the presence of the transport delay in the closed-loop system has two fundamentals characteristics (TORRICO, 2007):

- The dead time reduces the phase margin of the system, which can lead the closed-loop system to undesired oscillatory behaviour or even instability.
- In the continuous case, the input-output relationships become irrational, which increases the difficulty of the controller design.

Most solutions for the control of dead-time systems were initially developed for first order plus dead time (FOPDT) or second order plus dead time (SOPDT) processes; in these cases,

many industrial PID control methods have been designed to handle the presence of dead time (NORMEY-RICO; CAMACHO, 2007). In the late of the 1950's, Smith (1957) proposed the first dead-time compensator (DTC) strategy, also known as the Smith predictor (SP). The main idea of Smith (1957) was simply to use a dynamic model of the delay-free process in order to predict the behavior of the time-delayed system. This approach, which removes the transport delay from the characteristic equation of the controller loop, was able to improve the performance of the closed-loop system for dead-time processes over classical PI or PID controllers. However it presented limitations regarding robustness and disturbance rejection. When the SP was proposed in 1957, its practical implementation was somewhat difficult because of the use of analogue control equipment of the time. However, due to the early 1980's development of digital control platforms, the practical implementation of the DTCs has became a relatively easy task. This motivated researchers to propose in the last decades many extensions and modifications of the DTCs structures in order to overcome the SP drawbacks.

Besides presenting problems of robustness, the Smith predictor also presents a steady-state error due to disturbance for integrating systems and can not control open-loop unstable plants (NORMEY-RICO; CAMACHO, 2007). Lately, the finite spectrum assignment (FSA) (KWON; PEARSON, 1980) and the model reduction (ARTSTEIN, 1982) approaches overcame such issue, however, problems related to numerical instability on the FSA implementation were only definitively solved in Zhong (2004). According to Normey-Rico and Camacho (2008), the advances in the SP are mainly related to: (i) improve its regulatory capabilities for measurable or unmeasurable disturbances; (ii) to allow its use with unstable plants; (iii) to improve the robustness; and (iv) to facilitate the tuning for industrial applications. Palmor (1980) and Palmor and Halevi (1983) analized the stability of the SP and showed that even a small mismatch in the delay model can lead the system to instability if the primary controller is not properly tuned. Simple tuning rules are presented in Hägglund (1996), while Santacesaria and Scattolini (1993) and Lee *et al.* (1996) showed that different tunings of parameters could be used in order to improve the SP robustness. Watanabe and Ito (1981) proposed a modified fast model in the SP in order to improve the disturbance rejection and to control integrative and unstable process. Mataušek and Micić (1996) proposed a modified Smith predictor (MSP) structure for integrating processes with its extension for open-loop unstable systems in Mataušek and Ribić (2012). Another approach, namely filtered Smith predictor (FSP), based on the inclusion of a robustness filter in the feedback path showed itself to be an adequate choice to improve

robustness (NORMEY-RICO *et al.*, 1997; NORMEY-RICO; CAMACHO, 2009). A dead-time compensator for stable and integrating processes considering a reduced model of the process was proposed in García and Albertos (2008). A general structure for long dead-time systems shown to be equivalent to the Smith predictor has been proposed in García and Albertos (2013). Solutions to the problem of processes with multiple delays were presented in Normey-Rico *et al.* (2014) and Torrico *et al.* (2016).

Recently, several works such as those presented in Torrico *et al.* (2013), Torrico *et al.* (2018), Sanz *et al.* (2018), Liu *et al.* (2018b), Liu *et al.* (2018a), Torrico *et al.* (2019), Lima *et al.* (2020), Lima *et al.* (2021), Sá *et al.* (2021), and Castillo and García (2021) have demanded great effort focusing on enhancing some critical characteristics in the control of industrial dead-time processes, such as robustness, disturbance rejection, and noise attenuation.

Majority of the aforementioned works are driven for SISO systems; nevertheless, same concerns are extended for MIMO plants, which may present additional issues such as loop coupling and dominant dead time for each input/output relationship. So that, a generalized structure of the filtered Smith predictor is extended for MIMO square processes in Flesch *et al.* (2011). Additionally, a control procedure able to cope with both multiple delays and unstable MIMO systems was studied in García and Albertos (2010).

Additional issues to deal with MIMO systems may be included if the number of inputs and outputs is not the same, emerging non-square models. For such approach, the work in Flesch *et al.* (2011) was lately devised for non-square plants and multiple delays in Flesch *et al.* (2012) and Santos *et al.* (2014). An extension of the simplified tuning rules presented in Torrico *et al.* (2016) for MIMO systems and capable of dealing with non-square models is presented in Santos *et al.* (2016). An inverted decoupling structure is proposed in Luan *et al.* (2017) which highlights that to control a non-square plant with time delays may be a complex issue.

On the other hand, Richalet *et al.* (1978) incorporated the future process outputs predictions into the control law with the ability to deal with the process constraints. The model predictive control (MPC) paradigm was further elaborated by techniques like generalized predictive control (GPC) (CLARKE *et al.*, 1987) and dynamic matrix control (DMC) (CUTLER; RAMAKER, 1980), which incorporated the dead-time into their process models and consequently, dead-time compensation into the resulting control algorithm (NORMEY-RICO; CAMACHO, 2007). According to Normey-Rico and Camacho (2007), the MPC had a great impact on industrial process control due to its capacity to handle with many situations: it can be

applied to both SISO and MIMO systems; it can include feedback and feedforward actions in a straightforward manner; the input and output constraints can be included in the control law; and it intrinsically compensates the dead time of the process. However, the main characteristic of MPC strategies is that they can compute an optimal control action taking constraints into account (NORMEY-RICO; CAMACHO, 2007).

The model-based controllers continue to be extensively exploited due to their relatively easy implementation in digital controllers and their ability to improve the performance of dead-time systems. Practical aspects such as an ease tuning of parameters and a good trade-off between disturbance rejection, robustness, and noise attenuation are desirable characteristics in the design of any kind of controllers, and any proposals for the improvements of these characteristics are very important for the control of dead-time systems.

1.2 The present work

This work proposes the analysis and design of model-based controllers applied to the control of SISO and MIMO stable, unstable and integrative dead-time systems. Practical aspects such as tuning rules for set-point tracking, disturbance rejection, noise attenuation and robustness are considered in the design of the controllers. Through computational simulations and practical experiments, it is shown that the proposed approaches present better results in the control of dead-time processes than other recent works from the literature.

The rest of this work is organized as follow:

- Chapter 2 introduces the problem of controlling dead-time systems and how model-based controllers can improve the closed-loop performance of such systems. In addition, a review of dead-time compensators (DTCs) and model predictive control (MPC) is presented.

- Chapter 3 is based on Torrico *et al.* (2018), published in *ISA Transactions*, where new guidelines for the tuning of a simplified DTC focusing on industrial processes is introduced. The new guidelines employ different poles in the robustness filter of the DTC in order to consider the trade-off between noise attenuation, disturbance rejection performance and overall closed-loop robustness. Furthermore, it can be applied to control stable, unstable and integrative dead-time systems.

- Chapter 4 is based on Torrico *et al.* (2019), which was published in *ISA Transactions*. This work extends the filtered Smith predictor for state-space systems.

The proposed structure can be applied to both continuous and discrete-time systems and it allows the rejection of both matched and unmatched unknown disturbances for linear time-invariant (LTI) dead-time systems. Moreover, a FSA based implementation is presented in order to guarantee the internal stability for non Hurwitz open-loop systems.

- Chapter 5 proposes a control structure based on generalized predictive control (GPC) able to deal with SISO/MIMO dead-time processes under a unified framework. An equivalent dead-time compensator structure is presented in order to analyze the controller properties, such as set-point tracking, robustness and disturbance rejection. From the equivalent structure, a set of simple tuning rules are derived. Such rules employ a reduced number of parameters which facilitates the tuning of the controller, especially for the case of MIMO processes.

- Chapter 6 presents an extended version of Filho *et al.* (2018), presented at 6th IFAC Conference on Nonlinear Model Predictive Control. This work proposes a control approach for two-input single-output (TISO) processes based on the Generalized Predictive Control (GPC). The proposed strategy is applicable to TISO systems in an economic context when the two inputs are from different nature, thus yielding different operating costs. The main idea comes from mid-ranging controllers, where more than one input is used to control one output. The simplicity of the approach lies in the fact that the operating costs of each input do not need to be precisely specified. Actually, one only needs to know which of the inputs is the most expensive. Furthermore, the proposed strategy is able to deal with the problem when the delays from the two inputs to the output are different.

- Contributions are summarized whereas work in progress is listed in Chapter 7.

1.3 Published and submitted works

The list bellow contains articles developed during the candidate's doctoral program that either have been published or submitted to journals and conferences and are directly or indirectly related to the strategies developed in this work.

- FILHO, M. P. de A.; LIMA, T. A.; TORRICO, B. C.; NOGUEIRA, F. G. Observer Based Approach for the Economic Predictive Control of a TISO System. In: IFAC. **6th IFAC Conference on Nonlinear Model Predictive Control,**

Madison, Wisconsin (USA). [S.l.], 2018.

- TORRICO, B. C.; de Almeida Filho, M. P.; LIMA, T. A.; do N. Forte, M. D.; SÁ, R. C.; NOGUEIRA, F. G. Tuning of a dead-time compensator focusing on industrial processes. **ISA Transactions**, v. 83, p. 189–198, 2018. ISSN 0019-0578.

- TORRICO, B. C.; FILHO, M. P. de A.; LIMA, T. A.; SANTOS, T. L.; NOGUEIRA, F. G. New simple approach for enhanced rejection of unknown disturbances in lti systems with input delay. **ISA Transactions**, 2019. ISSN 0019-0578.

- LIMA, T. A.; TORRICO, B. C.; FILHO, M. P. D. A.; FORTE, M. D. N.; PEREIRA, R. D. O.; NOGUEIRA, F. G. First-order dead-time compensation with feedforward action. In: **2019 18th European Control Conference (ECC)**. [S.l.: s.n.], 2019. p. 3638–3643.

- SOMBRA, A. K. R.; PEREIRA, R. D.; FILHO, M. P. de A.; LIMA, T. A.; TORRICO, B. C.; NOGUEIRA, F. G. A dead-time compensator with dead-beat disturbance rejection response. In: **2019 18th European Control Conference (ECC)**. [S.l.: s.n.], 2019. p. 3613–3618.

- LIMA, T. A.; de Almeida Filho, M. P.; TORRICO, B. C.; NOGUEIRA, F. G.; CORREIA, W. B. A practical solution for the control of time-delayed and delay-free systems with saturating actuators. **European Journal of Control**, v. 51, p. 53–64, 2020. ISSN 0947-3580.

- SÁ, R. C.; SOMBRA, A. K.; TORRICO, B. C.; PEREIRA, R. D.; FORTE, M. D. N.; FILHO, M. P. de A.; NOGUEIRA, F. G. Tuning rules for unstable dead-time processes. **European Journal of Control**, v. 59, p. 250–263, 2021. ISSN 0947-3580.

- LIMA, T. A.; TARBOURIECH, S.; GOUAISBAUT, F.; FILHO, M. P. d. A.; GARCÍA, P. G.; TORRICO, B. C.; NOGUEIRA, F. G. Analysis and experimental application of a dead-time compensator for input saturated processes with output time-varying delays. **IET Control Theory and Applications**, Institution of Engineering and Technology, v. 15, n. 4, p. 580–593, mar. 2021.

2   CONTROL OF DEAD-TIME SYSTEMS

Consider the control structure illustrated in Figure 1, where $G(s)$ represents the dynamic of the process, L is the dead-time, $C(s)$ is a classical controller, such as PI or PID, $r(t)$ is the set-point, $q(t)$ is the input load disturbance, and $n(t)$ is the measurement noise. The input–output closed-loop transfer functions of Figure 1 are

$$H_{yr}(s) = \frac{Y(s)}{R(s)} = \frac{C(s)G(s)e^{-Ls}}{1 + C(s)G(s)e^{-Ls}}, \tag{2.1}$$

$$H_{yq}(s) = \frac{Y(s)}{Q(s)} = \frac{G(s)e^{-Ls}}{1 + C(s)G(s)e^{-Ls}}. \tag{2.2}$$

Note that the dead-time L appears in the characteristic equations, which reduces the phase margin of the closed-loop system. It is well known that the decrease in the phase margin can degrade the system performance, leading to an undesirable oscillatory behavior, or even instability. This effect can be illustrated by an example presented in Normey-Rico and Camacho (2007).

Consider the control structure in Figure 1 applied to the control of a heated tank system with a long pipe described by

$$P(s) = \frac{1}{(1.5s + 1)(0.4s + 1)} e^{-Ls},$$

where $P(s) = G(s)e^{-Ls}$ and $C(s) = k_c \frac{sT_i + 1}{sT_i}$ is a PI controller.

Initially the PI controller was tuned with $K_c = 1$ and $T_i = 1.2$ to obtain a step response with less than 5% of overshoot and faster than the open-loop one. This tuning was proposed by considering $L = 0$, and the blue line in Figure 2 shows the step response for this case. Figure 2 also shows the result obtained for the case of $L = 1.5$ (red line), that is, when the dead time is considered in the process. The presence of the dead time yields a rather oscillatory response. By choosing higher values of T_i and/or lower k_c, the PI controller becomes less aggressive and

Figure 1 – Representation of a control system
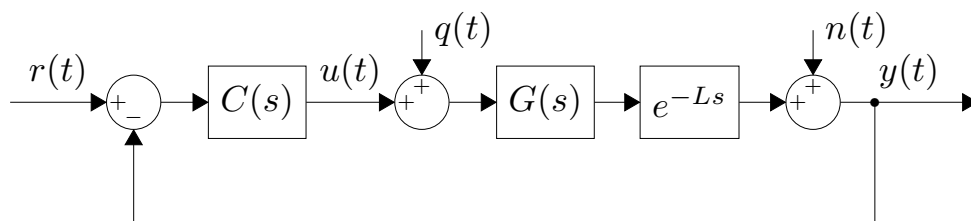
Source: The author.

Figure 2 – Step response and control signal for variations of L, k_c, and T_i
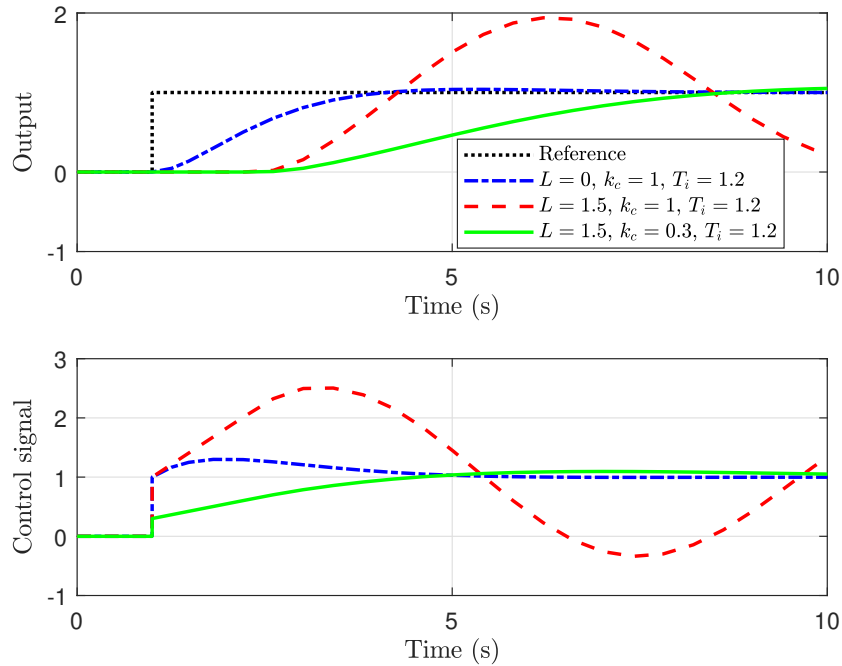
Source: The author.

the undesirable oscillations decrease at the cost of a slower step response, as can be seen by the green line in Figure 2 for the PI tuned with $k_c = 0.3$, and $T_i = 1.2$.

The phase margin and the cross-over frequency of the system are shown in Figure 3. Note the considerable decrease in the phase margin for $L = 1.5$, $K_c = 1$ and $T_i = 1.2$ when compared with the case of $L = 0$. The decrease was of approximately $68°$ in the phase margin, resulting in poor damping. The new tuning of $C(s)$ ($k_c = 0.3$ and $T_i = 1.2$) improved the phase margin of the dead-time system, however, it implied in the decrease of the gain cross-over frequency.

This example shows that closed-loop performance is significantly affected by the presence of the transport delay, and decreasing k_c to avoid oscillatory responses makes the closed-loop response considerably slower.

2.1 Dead-time compensators

The use of classical controller design methods to control dead-time systems requires conservative tunings to ensure the stability of the closed-loop system. To overcome these issues, Smith (1957) proposed the first DTC strategy, the so-called Smith predictor, which will be detailed in the next section.

Figure 3 – Frequency response for variations of L, k_c, and T_i
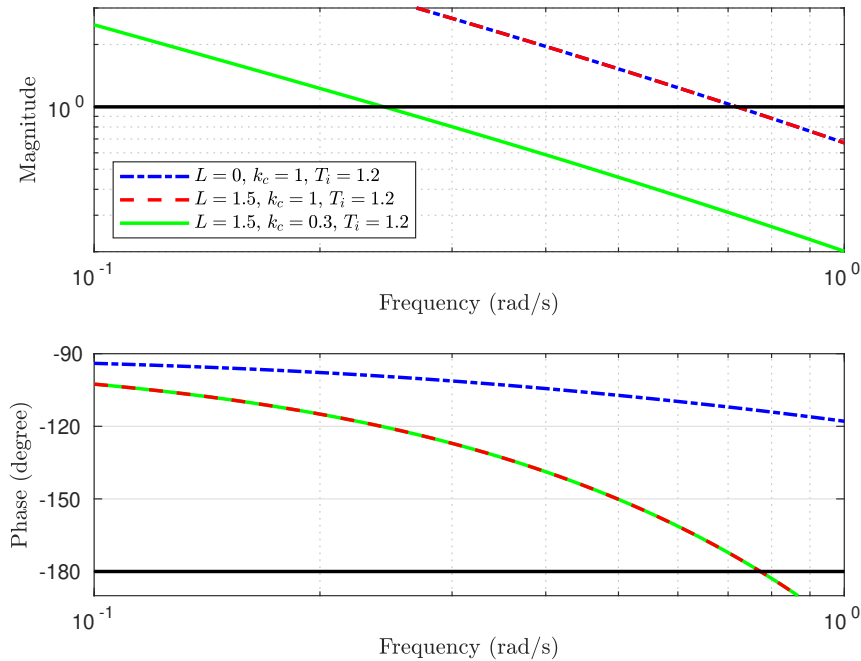
Source: The author.

2.1.1 The Smith predictor

An open-loop predictor based control structure that is able to eliminate the delay of the characteristic closed-loop equations is illustrated in Figure 4. $P(s) = G(s)e^{-Ls}$ and $G_n(s)$ is a dynamic model of the delay-free process $G(s)$, also called fast mode. For the nominal case, i.e. $G_n(s) = G(s)$, the input–output closed-loop transfer functions in Figure 4 are

$$H_{yr}(s) = \frac{Y(s)}{R(s)} = \frac{C(s)G(s)e^{-Ls}}{1 + C(s)G(s)}, \tag{2.3}$$

$$H_{yq}(s) = \frac{Y(s)}{Q(s)} = \frac{G(s)e^{-Ls}}{1 + C(s)G(s)}. \tag{2.4}$$

From (2.3) and (2.4) one can note that the transport delay is no longer part of the control loop. Although the open-loop predictor based control structure is able of removing the transport delay from the control loop, it can not be used in practice because model mismatches, input disturbances and measurement noise are not fed back. Therefore, it is not possible to ensure disturbance rejection or robustness with this structure.

Inspired for the open-loop predictor based control, Smith (1957) proposed the Smith predictor shown in Figure 5. The Smith predictor is composed by the primary controller $C(s)$

Figure 4 – The open-loop predictor based control structure
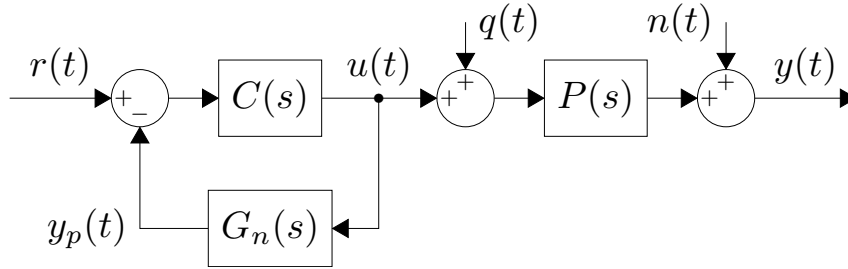
Source: The author.

and the predictor structure, which includes the fast model $G_n(s)$, along with a model of the dead time $e^{-L_n s}$. In order to consider model mismatches, input disturbances and measurement noise, the prediction error $e_p(t) = y(t) - \hat{y}(t)$ is added to the control loop. In the case of no model uncertainty or input disturbance, the prediction error $e_p(t) = 0$ and the predictive output $y_p(t)$ will be the open-loop prediction. Under these conditions, the primary controller $C(s)$ can be tuned as if the plant had no dead time (NORMEY-RICO; CAMACHO, 2008).

Figure 5 – The Smith predictor structure
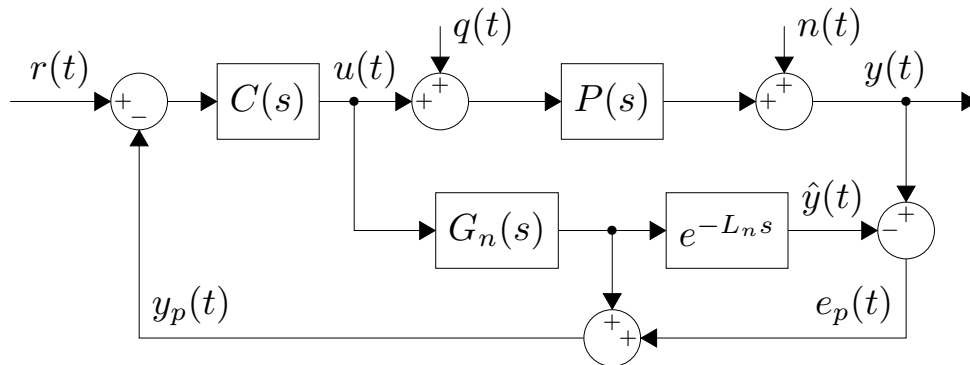
Source: The author.

2.1.1.1 Nominal properties of the SP

The Smith predictor has three fundamental properties for the nominal case ($G_n(s) = G(s)$ and $L_n = L$):

- **Dead-time Compensation:** the transport delay is eliminated from the closed-loop characteristic equation, which avoids the decrease in the phase margin of the system.

- **Prediction:** for the nominal case $e_p(t) = 0$ and $y_p(t) = \hat{y}(t + L)$. In this way, the primary controller $C(s)$ can be tuned for the dead-time system from the delay-free

model.

- **Ideal Dynamic Compensation:** the output $y(t)$ by applying an ideal controller $\frac{C(s)}{1+C(s)G_n(s)} = (G_n(s))^{-1}$ is

$$
\begin{aligned}
y(t) &= r(t - L_n) + G_n(s)e^{-L_n s}\left[q(t) - q(t - L_n)\right] \\
&= r(t - L_n) + G_n(s)e^{-L_n s}\left[1 - e^{-L_n s}\right]q(t) \\
&= r(t - L_n) + \left[G_n(s)e^{-L_n s} - G_n(s)e^{-2L_n s}\right]q(t).
\end{aligned}
$$

This property shows that even using an optimal controller, the SP presents a performance limitation. Note the term $e^{-2L_n s}$ in the input disturbance response. That is, even in the ideal case, if a disturbance is applied at $t = 0$, it is necessary to wait until $t = 2L_n$ to note the effect of the controller on the output.

2.1.1.2 Set-point tracking and disturbance rejection

The input–output relations of the SP for the nominal case are

$$
H_{yr}(s) = \frac{Y(s)}{R(s)} = \frac{C(s)G_n(s)e^{-L_n s}}{1 + C(s)G_n(s)}, \tag{2.5}
$$

$$
H_{yq}(s) = \frac{Y(s)}{Q(s)} = G_n(s)e^{-L_n s}\left[1 - \frac{C(s)G_n(s)e^{-L_n s}}{1 + C(s)G_n(s)}\right]. \tag{2.6}
$$

From (2.6) the disturbance rejection dynamics depends on the open-loop poles of the process, which has three main consequences: (i) the disturbance rejection response cannot be faster than the open-loop one; (ii) the structure in Figure 5 is not internally stable for open-loop unstable or integrative processes; and (iii) the SP can not reject step-like disturbances for integrative processes. In addition, if one adjusts $C(s)$ to get a desired disturbance rejection dynamics, then the SP will not be able to reach the set-point correctly, since it is a controller with only one degree-of-freedom.

2.1.1.3 Stability and robustness

All models are approximations of real processes. That way, the effects of the modeling errors must be considered for the stability and robustness analysis. To account for

model uncertainty it will be assumed that the process is described by a family of transfer functions represented by a unstructured additive or multiplicative uncertainty model. Thus, each model $P_i(s)$ in the family can be written as

$$P_i(s) = P_n(s) + \Delta P_i(s), \tag{2.7}$$

or

$$P_i(s) = P_n(s)(1 + \delta P_i(s)), \tag{2.8}$$

where $P_n(s)$ is nominal process, and $\Delta P_i(s)$ and $\delta P_i(s)$ are the additive and multiplicative errors respectively. $\Delta P(s)$ and $\delta P(s)$ contains the maximum modeling error of the system such that

$$\left| \overline{\Delta P(s)} \right| \geq |\Delta P_i(s)|, \qquad s = j\omega, \qquad \omega > 0, \tag{2.9}$$

$$\left| \overline{\delta P(s)} \right| \geq |\delta P_i(s)|, \qquad s = j\omega, \qquad \omega > 0. \tag{2.10}$$

Consider the closed-loop system in Figure 6, where $C_{eq}(s)$ is the controller and $P(s)$ is the process. Considering the Nyquist criterion along with unstructured additive uncertainties, Morari and Zafiriou (1989) provides the following condition for robust stability

$$|\Delta P(j\omega)| < \frac{\left| 1 + C_{eq}(j\omega)P_n(j\omega) \right|}{\left| C_{eq}(j\omega) \right|}, \qquad \forall \omega > 0. \tag{2.11}$$

Figure 6 – Closed-loop system
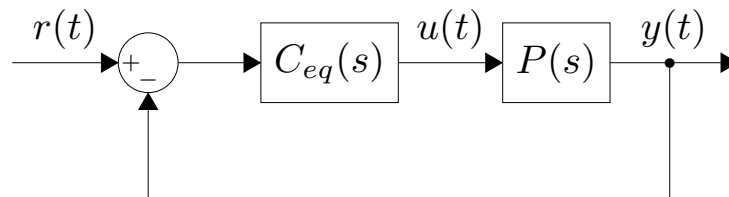
Source: The author.

The robustness index $I_R(\omega)$ can be defined as the second term of (2.11)

$$I_R(\omega) = \frac{\left| 1 + C_{eq}(j\omega)P_n(j\omega) \right|}{\left| C_{eq}(j\omega) \right|} > |\Delta P(j\omega)|, \qquad \forall \omega > 0. \tag{2.12}$$

For the case of unstructured multiplicative uncertainties, the robustness index $i_R(\omega)$ is defined as

$$i_R(\omega) = \frac{\left| 1 + C_{eq}(j\omega)P_n(j\omega) \right|}{\left| C_{eq}(j\omega)P_n(j\omega) \right|} > |\delta P(j\omega)|, \qquad \forall \omega > 0. \tag{2.13}$$

The structure of the SP can be redrawn in a equivalent way to the Figure 6 with

$$C_{eq}(s) = \frac{C(s)}{1 + C(s)(G_n(s) - P_n(s))}. \tag{2.14}$$

Substituting (2.14) in (2.12) and (2.13) one gets the robustness index and the robustness stability condition of the SP for additive and multiplicative uncertainties respectively

$$I_R(\omega) = \frac{|1 + C(j\omega)G_n(j\omega)|}{|C(j\omega)|} > |\Delta P(j\omega)|, \quad \forall \omega > 0, \tag{2.15}$$

$$i_R(\omega) = \frac{|1 + C(j\omega)G_n(j\omega)|}{|C(j\omega)G_n(j\omega)|} > |\delta P(j\omega)|, \quad \forall \omega > 0. \tag{2.16}$$

From (2.15) and (2.16) we can see that the robustness indexes depend on the delay-free model $G_n(s)$ and the primary controller $C(s)$. If the primary controller $C(s)$ is designed for a fast set-point tracking then robustness will be poor, which can lead the system to instability with small modeling errors. In this way, the SP is not able to provide a good set-point tracking performance with high robustness simultaneously.

2.1.1.4 Summary

The SP is a simple and effective controller for dead-time processes. The main advantages and limitations of the SP are the following (NORMEY-RICO; CAMACHO, 2007):

- It eliminates the effect of the dead time in the nominal set-point response.
- It cannot be used properly with integrative and unstable processes.
- The disturbance rejection response cannot be faster than that of the open-loop.

2.1.2 The Artstein predictor

The Artstein predictor (AP) is a state-space DTC strategy that makes use of finite spectrum assignment (FSA) (MANITIUS; OLBROT, 1979) along with the reduction method (ARTSTEIN, 1982). Due to its state space formulation, the Artstein predictor naturally addresses the case of MIMO systems. In addition, unlike the Smith predictor, it is able to control open-loop unstable systems, however, it suffers of some drawbacks, such as its inability to reject disturbances in a straightforward manner.

Consider the following linear time-invariant (LTI) system with single-input delay

$$
\begin{cases}
\dot{x}(t) & = Ax(t) + Bu(t-L) + q(t) \\
u(t) & = \phi(t), \qquad t \in [-L,0) \,, \\
x(0) & = x_0
\end{cases}
\tag{2.17}
$$

where $\phi(t)$ and x_0 define the initial conditions for $t \in [-L,0)$, $x(t) \in \mathbb{R}^n$ is the state vector, $u(t) \in \mathbb{R}^m$ is the control signal, and $q(t) \in \mathbb{R}^n$ is the unknown disturbance.

Assumption 1. *A and B are constant and known and the pair (A,B) is controllable.*

Assumption 2. *The input delay $L > 0$ is constant and known.*

Assumption 3. *The control signal $u(t)$ and the unknown disturbance $q(t)$ are locally integrables.*

In order to compensate the dead time, a prediction $x_p(t) = x(t+L)$ is given by

$$
x_p(t) = e^{AL}x(t) + \int_{t-L}^{t} e^{A(t-\tau)} [Bu(\tau) + q(\tau+L)] d\tau.
\tag{2.18}
$$

The disturbance value is required to compute the integral part of (2.18), however, it is not available at the current instant t for $\tau \in [t-L,t]$. To overcome this issue, the Artstein predictor provides an approximated prediction $\hat{x}_p(t)$ by neglecting the effect of disturbance

$$
\hat{x}_p(t) = e^{AL}x(t) + \int_{t-L}^{t} e^{A(t-\tau)} Bu(\tau) d\tau.
\tag{2.19}
$$

As the disturbance was eliminated from (2.19), the approximate prediction $\hat{x}_p(t)$ will always be different from the exact prediction $x_p(t)$ in the presence of disturbances. Such prediction error, given by

$$
x_p(t) - \hat{x}_p(t) = \int_{t-L}^{t} e^{A(t-\tau)} q(\tau+L) d\tau,
\tag{2.20}
$$

makes it impossible to remove constant disturbances even when integral action is present (SANZ *et al.*, 2016).

Some recent works, such as those presented in Léchappé *et al.* (2015), Sanz *et al.* (2016), and Santos and Franklin (2018) proposed modifications in the Artstein predictor to attenuate or eliminate the disturbance effects.

2.1.3 *The filtered Smith predictor*

An alternative capable of overcoming some of the drawbacks of the SP is the filtered SP (FSP) presented in Normey-Rico *et al.* (1997). The main characteristic of the FSP, shown in Figure 7, is the use of a filter that acts on the prediction error $e_p(t)$. This filter, also known as robustness filter, does not change the set-point tracking response and can be used to improve the robustness or the disturbance rejection capabilities of the system.

Figure 7 – The filtered Smith predictor structure
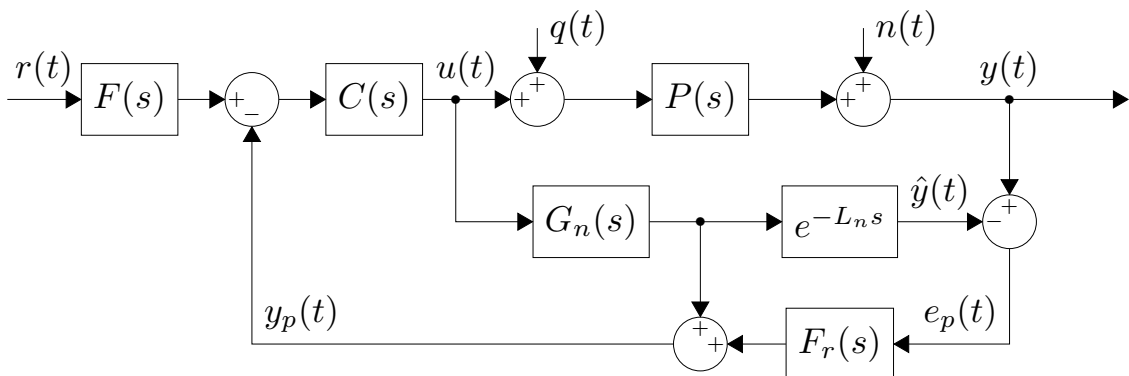
Source: The author.

The presence of the robustness filter leads to the following nominal relations

$$H_{yr}(s) = \frac{Y(s)}{R(s)} = \frac{F(s)C(s)G_n(s)e^{-L_n s}}{1 + C(s)G_n(s)}, \tag{2.21}$$

$$H_{yq}(s) = \frac{Y(s)}{Q(s)} = G_n(s)e^{-L_n s}\left[1 - \frac{F_r(s)C(s)G_n(s)e^{-L_n s}}{1 + C(s)G_n(s)}\right], \tag{2.22}$$

$$i_R(\omega) = \left|\frac{1 + C(s)G_n(s)}{F_r(s)C(s)G_n(s)}\right|_{s=j\omega}, \qquad \forall \omega > 0. \tag{2.23}$$

From (2.21) to (2.23) it is possible to notice three characteristics of the robustness filter $F_r(s)$:

- **It does not act on the set-point tracking response:** the set-point tracking dynamics is defined by $C(s)$ and by a reference filter $F(s)$, which is included in the FSP structure in order to decouple the set-point tracking tuning.

- **It can be tuned on order to eliminate the undesired poles of $G_n(s)$ from the disturbance rejection response:** this allows the FSP to be used to control open-loop unstable and integrative processes. However, the structure in Figure 7 is not

internally stable for open-loop unstable and integrative processes, so that it can only be used for stable processes. A more adequate implementation structure will be seen in the next subsection.

- **It plays an important role in the trade-off between disturbance rejection and robustness:** from (2.22) and (2.23) one can note that $F_r(s)$ appears in the numerator of $H_{yq}(s)$ and in the denominator of $i_R(\omega)$. This means that $F_r(s)$ can be designed considering a trade-off between disturbance rejection and robustness.

2.1.3.1 Designing the FSP

In practice, the implementation of a DTC is performed from a discrete-time control structure with sampling time T_s. The discrete-time model is $P_n(z) = G_n(z)z^{-d_n}$ and $F(z), C(z)$, and $F_r(z)$ are obtained from the discrete design of the reference filter, primary controller and robustness filter respectively. This way, the designing of the FSP will be presented considering the discrete-time domain.

The nominal transfer functions of the discrete-time FSP are

$$H_{yr}(z) = \frac{Y(z)}{R(z)} = \frac{F(z)C(z)G_n(z)z^{-d_n}}{1 + C(z)G_n(z)}, \tag{2.24}$$

$$H_{yq}(z) = \frac{Y(z)}{Q(z)} = G_n(z)z^{-d_n}\left[1 - \frac{F_r(z)C(z)G_n(z)z^{-d_n}}{1 + C(z)G_n(z)}\right], \tag{2.25}$$

$$i_R(\omega) = \left|\frac{1 + C(z)G_n(z)}{F_r(z)C(z)G_n(z)}\right|_{z = e^{j\omega T_s}}, \qquad 0 < \omega < \pi/T_s. \tag{2.26}$$

Consider the two-degree-of-freedom (2DOF) discrete-time control structure in Figure 8. The FSP is equivalent to this structure for

$$C_{eq}(z) = \frac{F_r(z)C(z)}{1 + C(z)G_n(z)\left[1 - F_r(z)z^{-d_n}\right]}, \tag{2.27}$$

$$F_{eq}(z) = \frac{F(z)}{F_r(z)}. \tag{2.28}$$

The reference filter $F(z)$ and the primary controller $C(z)$ are used to obtain the desired closed-loop performance for the nominal process. In order to reject step-like disturbances

Figure 8 – Two-degree-of-freedom (2DOF) control structure
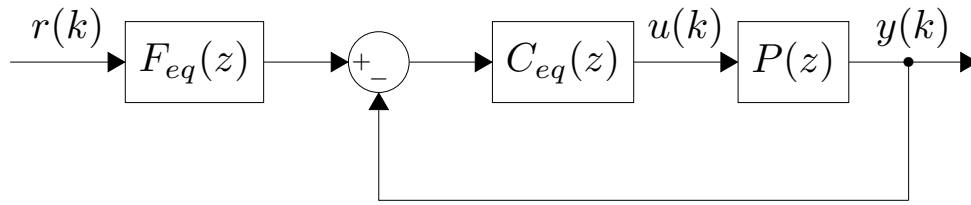
Source: The author.

and to guarantee null steady state error, the following two conditions must be satisfied: (i) $C_{eq}(z)$ must have at least one pole at $z = 1$, and (ii) $F_{eq}(z)\big|_{z=1} = 1$. The first condition is achieved by using a pole at $z = 1$ in $C(z)$, while making $F(z)\big|_{z=1} = 1$ and $F_r(z)\big|_{z=1} = 1$ holds the second condition.

According to Normey-Rico and Camacho (2009), the robustness filter $F_r(z)$ must be chosen to avoid the three main problems of the original SP structure:

- the disturbance rejection properties of the closed-loop system cannot be arbitrarily defined as the open-loop poles are also closed-loop poles of $H_{yq}(z)$;
- if $G_n(z)$ has a unstable pole, then the SP presents a internally unstable closed-loop system;
- for the particular case of integrative processes, the SP cannot reject step-like disturbances.

Thus, the robustness filter is designed with three main objectives: (i) to avoid the appearance of slow or unstable process poles in the disturbance rejection response, (ii) guarantee the disturbance rejection for the case of integrative process, and (iii) to define a trade-off between disturbance rejection and robustness.

One of the main problems of many dead-time compensation design methods for unstable processes is that the obtained controller cannot be implemented in its original structure and an equivalent block diagram should be used (NORMEY-RICO; CAMACHO, 2009). Figure 9 shows the discrete-time implementation structure of the FSP, where $S(z) = G_n(z)\left[1 - F_r(z)z^{-d_n}\right]$. Using this structure and a stable $S(z)$ the controller gives an internally stable system for all cases if $C(z)$ stabilizes the delay-free model $G_n(z)$. In other words, obtaining a stable function $S(z)$ is equivalent to having a stable $H_{yq}(z)$.

For open-loop stable or unstable processes, the robustness filter is designed to avoid the appearance of slow or unstable process poles in the disturbance rejection response. This can

Figure 9 – The filtered Smith predictor discrete-time implementation structure
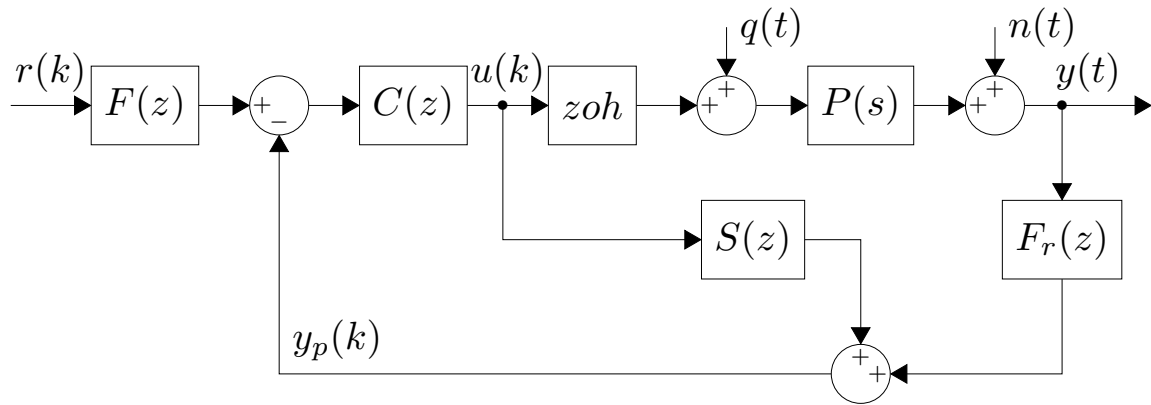
be achieved be considering the following condition

$$\left[1 - F_r(z)z^{-d_n}\right]_{z=p_i} = 0, \tag{2.29}$$

where p_i are the slow or unstable poles of $G_n(z)$.

In the case of integrative process, $F_r(z)$ must be chosen considering

$$\frac{d}{dz}\left[1 - F_r(z)z^{-d_n}\right]_{z=1} = 0. \tag{2.30}$$

The conditions in (2.29) and (2.30) are used in order to define the zeros of $F_r(z)$. The poles of $F_r(z)$ are a tuning parameter chosen to enhance the overall robustness of the system and to reach a compromise between robustness and disturbance rejection performance. If the primary controller is designed to speed-up the closed-loop responses, then the robustness of the system will be poor. This problem can be mitigated by designing $F_r(z)$ as a low pass filter. As $F_r(z)$ is in the denominator of the robustness index (2.26), then small values of $F_r(z)$ in high frequencies are needed in order to enhance the robustness. On the other hand, the disturbance rejection (2.25) becomes slow for small $F_r(z)$ at high frequencies. This means that the poles of $F_r(z)$ must be chosen considering the trade-off between disturbance rejection and robustness.

2.1.4 *The simplified filtered Smith predictor*

Torrico *et al.* (2013) proposed a new and simple design for the FSP. This strategy, namely simplified filtered Smith predictor (SFSP), makes use of gains instead of the reference filter and primary controller and can be applied to stable, unstable and integrative FOPDT models.

The main difference for the FSP, besides a simpler design, is that the primary controller of the SPFP is defined as a gain and does not present explicit integral action. In this way, the robustness filter also assumes the responsibility of disturbance rejection.

The SFSP makes use of the FSP structure by considering $F(z) = k_r$ and $C(z) = k_c$. Note that the reference filter and the primary controller have been replaced by gains, and replacing them in (2.24) to (2.26) yields the following nominal relations for the SFSP

$$H_{yr}(z) = \frac{Y(z)}{R(z)} = \frac{k_r k_c G_n(z) z^{-d_n}}{1 + k_c G_n(z)}, \tag{2.31}$$

$$H_{yq}(z) = \frac{Y(z)}{Q(z)} = G_n(z) z^{-d_n} \left[1 - \frac{k_c F_r(z) G_n(z) z^{-d_n}}{1 + k_c G_n(z)} \right], \tag{2.32}$$

$$i_R(\omega) = \left| \frac{1 + k_c G_n(z)}{k_c F_r(z) G_n(z)} \right|_{z = e^{j\omega T_s}}, \qquad 0 < \omega < \pi/T_s. \tag{2.33}$$

From (2.31) to (2.33) it is possible to notice that k_r and k_c can be adjusted for set-point tracking and $F_r(z)$ for both disturbance rejection and robustness.

The SFSP can also be represented by the 2DOF control structure considering

$$C_{eq}(z) = \frac{F_r(z)}{G_n(z) \left[\frac{1 + k_c G_n(z)}{k_c G_n(z)} - F_r(z) z^{-d_n} \right]}, \tag{2.34}$$

$$F_{eq}(z) = \frac{k_r}{F_r(z)}. \tag{2.35}$$

2.1.4.1 Designing the SFSP

The designing of the SFSP is performed in two steps: (i) k_r and k_c are adjusted for a desired set-point tracking response, and (ii) the robustness filter $F_r(z)$ is tuned considering both disturbance rejection and the trade-off between robustness and disturbance rejection.

Consider the following desired closed-loop set-point tracking response

$$\bar{H}_{yr}(z) = \frac{1 - z_c}{z - z_c} z^{-d_n}, \tag{2.36}$$

where z_c is the tuning parameter that defines a desired close-loop set-point tracking dynamics.

Using the FOPDT model $P_n(z) = \frac{b_0}{z - a_1} z^{-d_n}$ and by making (2.31) equal to (2.36) one gets

$$k_c = \frac{a_1 - z_c}{b_0}, \tag{2.37}$$

$$k_r = \frac{1 - z_c}{a_1 - z_c}. \tag{2.38}$$

The robustness filter of the SFSP has three objectives: i) to guarantee step-like disturbance rejection at steady state; (ii) to eliminate the open-loop pole from (2.32), which implies internal stability for unstable and integrative processes; and (iii) to reach a trade-off between robustness and disturbance rejection performance. In order to achieve these objectives, Torrico *et al.* (2013) proposed the use of the following second-order filter

$$F_r(z) = \frac{b_1 z^2 + b_2 z}{(z - \beta)^2}, \tag{2.39}$$

where b_1 and b_2 are used for the objectives (i) and (ii), and β for the objective (iii).

$C_{eq}(z)$ in (2.34) must have a pole at $z = 1$ for disturbance rejection. In addition, if $C_{eq}(z)$ has no zeros at $z = a_1$, then the plant pole does not appear in $H_{yq}(z)$. For stable and unstable processes ($a_1 \neq 1$), this implies

$$\left. \frac{1 + k_c G_n(z)}{k_c G_n(z)} - F_r(z) z^{-d_n} \right|_{z=1} = 0,$$

$$\left. \frac{1 + k_c G_n(z)}{k_c G_n(z)} - F_r(z) z^{-d_n} \right|_{z=a_1} = 0, \tag{2.40}$$

and for integrative processes ($a_1 = 1$)

$$\left. \frac{1 + k_c G_n(z)}{k_c G_n(z)} - F_r(z) z^{-d_n} \right|_{z=1} = 0,$$

$$\left. \frac{d}{dz} \left[\frac{1 + k_c G_n(z)}{k_c G_n(z)} - F_r(z) z^{-d_n} \right] \right|_{z=1} = 0. \tag{2.41}$$

The coefficients b_1 and b_2 are obtained by means of (2.40) and (2.41). β is the tuning parameter that defines the trade-off between robustness and disturbance rejection performance.

2.2 Model Predictive Control

The model predictive control is a control strategy that explicitly uses a process model to obtain the optimum control signal by minimizing an objective function (CAMACHO; BORDONS, 2007). According to Camacho and Bordons (2007), the main ideas in the MPC control family are:

- the explicit use of a model to predict the output of the process over time (prediction horizon);

- the calculation of the optimal control sequence by minimizing an objective function;

- receding strategy, so that at each instant the horizon is displaced towards the future, which involves the application of the first control signal of the sequence calculated at each step.

There are several predictive control algorithms, and they differ basically in the prediction model, cost function, and the procedure to obtain the optimum control law. The prediction model is used to predict the future plant outputs, based on past and current values and on the proposed optimal future control actions. The control signal is obtained by minimizing a positive definite and usually quadratic cost function, which represents the cost associated with the evolution of the system along the prediction horizon. And finally, the optimizer is an algorithm that minimizes the cost function subject to the constraints of the system variables.

Figure 10 shows the general MPC scheme, and the methodology of all the controllers belonging to the MPC family is characterized by the following control sequence:

1. by using the prediction model, the future outputs of the system are predicted along the prediction horizon N. The predictions $\hat{y}(k+j|k)$ for $j = 1, ..., N$ depend on the past values of inputs and outputs, and the future control signal $u(k+j), j = 0, ..., N-1$.

2. the future reference trajectory $w(k+j), j = 1, ..., N$ is defined;

3. the optimal future control action $u(k+j), j = 0, ..., N-1$ is calculated by minimizing the cost function;

4. only the first element of the control sequence must be applied to the process and the algorithm should return to step 1.

2.2.1 MPC advantages and drawbacks

Some advantages of MPC are (TORRICO, 2007):

- it is particularly attractive to staff with only a limited knowledge of control because the concepts are intuitive;

- it can be used to control a great variety of processes: linear and non-linear, SISO/MIMO, with constraints, with long dead times, stable, unstable, integrative and non-minimum phase.

Figure 10 – General MPC scheme
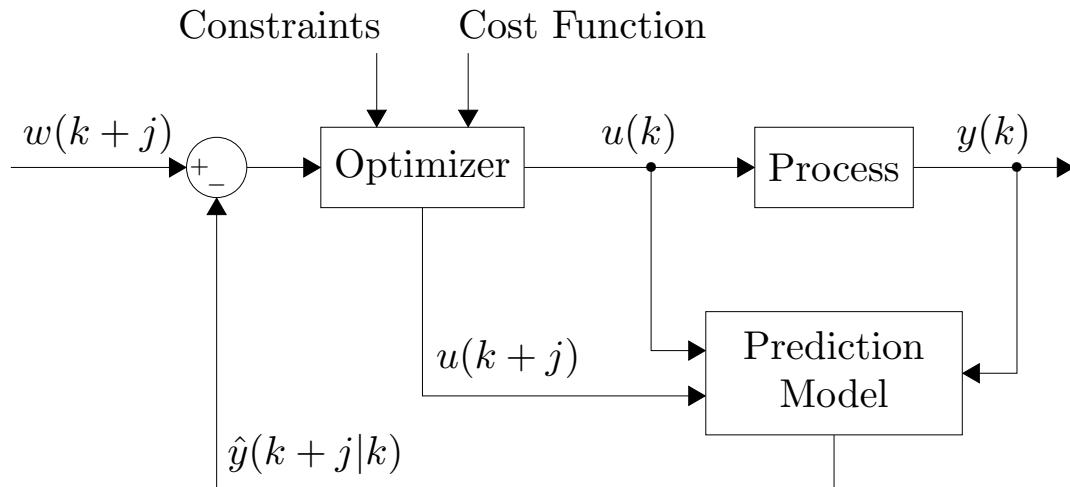
Source: The author.

- the resulting controller is easy to implement;

- it is very useful when future references are known;

- the control law is based on optimal criteria.

Some drawbacks of MPC are:

- it requires a sufficiently precise knowledge of the dynamic model of the system;

- it requires a high computational cost;

- the analysis of stability and robustness becomes complex in case of constraints or non-linear models.

2.2.2 The generalized predictice control

The generalized predictice control (GPC) is a MPC strategy proposed by Clarke *et al.* (1987) and uses the CARIMA (controlled auto-regressive and integrated moving-average) model as prediction model. The CARIMA model for SISO systems is given by

$$A(q^{-1})y(k) = q^{-d}B(q^{-1})u(k-1) + \frac{C(q^{-1})}{\Delta}e(k), \tag{2.42}$$

where $u(k)$ and $y(k)$ are the control signal and output of the model, d is the transport delay, $e(k)$ is a white noise with zero mean,

$$
\begin{aligned}
A(q^{-1}) &= 1 + a_1 q^{-1} + \ldots + a_{na} q^{-n_a}, \\
B(q^{-1}) &= b_0 + b_1 q^{-1} + \ldots + b_{n_b} q^{-n_b}, \\
C(q^{-1}) &= 1 + c_1 q^{-1} + \ldots + c_{n_c} q^{-n_c}, \\
\Delta &= 1 - q^{-1},
\end{aligned}
$$

and q^{-1} is the backward shift operator.

The term $\frac{C(q^{-1})}{\Delta}$ in the CARIMA model is intended to reduce the effects of the prediction errors due to noise, disturbances and model uncertainties. The low frequency disturbances (e.g. step-like disturbance) can be eliminated by the operator Δ, whereas the high frequency errors, which are mainly caused by noise and model mismatches can be mitigated by designing the polynomial $C(q^{-1})$ as a low-pass filter.

The GPC algorithm consists of applying a control signal that minimizes the following cost function

$$min \quad J = \sum_{j=N_1}^{N_2} [\hat{y}(k+j|k) - w(k+j)]^2 + \lambda \sum_{j=0}^{N_u-1} [\Delta u(k+j)]^2, \tag{2.43}$$

where $\hat{y}(k+j|k)$ is the predicted process output j steps ahead of k, $\Delta u(k+j)$ is the variation of control signal, $w(k+j)$ is the future reference, N_u is the control horizon, λ is a weighting variable, and N_1 and N_2 define the prediction horizon. Normally, $N_1 = d+1$ and $N_2 = d+N$, where N is the width of the prediction horizon.

The sequence of future control is obtained from the minimization of (2.43), however, it is necessary to calculate an expression for the predicted output. From (2.42) it is possible to get $y(k)$ so that the output predictions are calculated

$$y(k) = q^{-d}\frac{B(q^{-1})}{A(q^{-1})}u(k-1) + \frac{C(q^{-1})}{\tilde{A}(q^{-1})}e(k), \tag{2.44}$$

where $\tilde{A} = \Delta A$ and the term $\frac{B(q^{-1})}{A(q^{-1})}$ is the discrete transfer function of the process model. For simplicity $C(q^{-1})$ is chosen to be 1, yielding

$$y(k) = q^{-d}\frac{B(q^{-1})}{A(q^{-1})}u(k-1) + \frac{1}{\tilde{A}(q^{-1})}e(k), \tag{2.45}$$

The term $\frac{1}{\tilde{A}(q^{-1})}$ can be represented by the following Diophantine equation

$$1 = E_j(q^{-1})\tilde{A}(q^{-1}) + q^{-j}F_j(q^{-1}). \tag{2.46}$$

Multiplying (2.42) by $\Delta E_j(q^{-1})q^j$ and using the relation in (2.46), one gets

$$\Delta A(q^{-1})E_j(q^{-1})q^j y(k) = q^{-d}E_j(q^{-1})q^j B(q^{-1})\Delta u(k-1) + \frac{\Delta E_j(q^{-1})q^{-j}}{\Delta}e(k),$$

$$\tilde{A}(q^{-1})E_j(q^{-1})y(k+j) = E_j(q^{-1})B(q^{-1})\Delta u(k+j-d-1) + E_j(q^{-1})e(k+j),$$

$$y(k+j) = E_j(q^{-1})B(q^{-1})\Delta u(k+j-d-1) + F_j(q^{-1})y(k) + E_j(q^{-1})e(k+j). \tag{2.47}$$

As the noise components $e(k+j)$ are all in the future, then their best prediction is their mean, that is, zero. Thus, the predicted output is given by

$$\hat{y}(k+j|k) = E_j(q^{-1})B(q^{-1})\Delta u(k+j-d-1) + F_j(q^{-1})y(k). \tag{2.48}$$

It is possible to split the term $E_j(q^{-1})B(q^{-1})$ of (2.48) into two polynomials as follows

$$E_j(q^{-1})B(q^{-1}) = \underbrace{m_0 + \cdots + m_j q^{-j}}_{G_j(q^{-1})} + \underbrace{\cdots + m_{j+nb-2} q^{j+nb-2}}_{q^{-j}H_j(q^{-1})}. \tag{2.49}$$

Thus, (2.48) can be written as

$$\hat{y}(k+j|k) = G_j(q^{-1})\Delta u(k+j-d-1) + F_j(q^{-1})y(k) + H_j(q^{-1})\Delta u(k-1). \tag{2.50}$$

The predicted output of the CARIMA model (2.42) is given by (2.50), which can be written in the matrix form as

$$\hat{\mathbf{y}} = \mathbf{G}\Delta\mathbf{u} + \mathbf{f}, \tag{2.51}$$

where

$$\mathbf{f} = \mathbf{F}y(k) + \mathbf{H}\Delta u(k-1),$$

$$\hat{\mathbf{y}} = \begin{bmatrix} \hat{y}(k+d+1|k) \\ \hat{y}(k+d+2|k) \\ \vdots \\ \hat{y}(k+d+N|k) \end{bmatrix}, \Delta\mathbf{u} = \begin{bmatrix} \Delta u(k) \\ \Delta u(k+1) \\ \vdots \\ \Delta u(k+N_u-1) \end{bmatrix},$$

$$\mathbf{G} = \begin{bmatrix} g_0 & 0 & \dots & 0 \\ g_1 & g_0 & \dots & 0 \\ \vdots & \vdots & \ddots & \vdots \\ g_N & g_{N-1} & \dots & g_0 \end{bmatrix}, \mathbf{F} = \begin{bmatrix} F_{d+1}(q^{-1}) \\ F_{d+2}(q^{-1}) \\ \vdots \\ F_{d+N}(q^{-1}) \end{bmatrix}, \mathbf{H} = \begin{bmatrix} H_1(q^{-1}) \\ H_2(q^{-1}) \\ \vdots \\ H_N(q^{-1}) \end{bmatrix}.$$

The term $\mathbf{G}\Delta\mathbf{u}$ of (2.51) depends on future values and is known as forced response, while $\mathbf{f}$ contains the past control and the present output and is called the free response.

By substituting (2.51) into the cost function (2.43), one gets

$$J = (\mathbf{G}\Delta\mathbf{u} + \mathbf{f} - \mathbf{w})^T (\mathbf{G}\Delta\mathbf{u} + \mathbf{f} - \mathbf{w}) + \Delta\mathbf{u}^T \lambda \Delta\mathbf{u}, \tag{2.52}$$

where $\mathbf{w} = \left[w(k+N_1) \quad \cdots \quad w(k+N_2) \right]^T$.

The minimization of (2.52) assuming no constraints on future controls results in the optimal control sequence

$$\mathbf{\Delta u}^* = \left(\mathbf{G}^T \mathbf{G} + \lambda \mathbf{I} \right)^{-1} \mathbf{G}^T \left(\mathbf{w} - \mathbf{f} \right). \tag{2.53}$$

Due to the receding strategy, only the first element of the control sequence is applied to the process, that is,

$$\Delta u(k) = \mathbf{K} \left(\mathbf{w} - \mathbf{f} \right), \tag{2.54}$$

where $\mathbf{K}$ is the first row of $\left(\mathbf{G}^T \mathbf{G} + \lambda \mathbf{I} \right)^{-1} \mathbf{G}^T$.

3 AN IMPROVED DTC APPROACH

This chapter proposes tuning rules for a simplified dead-time compensator, which is intended to deal with stable, unstable and integrative dead-time processes. The main contribution is the proposal of new guidelines for the tuning of the robustness filter. The new set of rules allow for the use of lower order filters which are able to simultaneously account for closed-loop robustness and noise attenuation. Through illustrative examples, it is shown that the proposed approach provides enhanced disturbance rejection and noise attenuation in the control of industrial processes when compared with other recently published works. Furthermore, the internal temperature of an in-house thermal chamber is controlled to evaluate the applicability of the strategy on real processes.

3.1 Introduction

Dead-time appears in a wide range of industrial processes involving delayed transportation of energy, mass, information or other processes containing time-lag associated dynamics. Although classical controllers such as proportional-integral (PI) and proportional-integral-derivative (PID) may be used when dead-time is relatively small (MERCADER; BAÑOS, 2017; SEER; NANDONG, 2017; BEGUM *et al.*, 2018), their performance is usually degraded for long time-delay systems. Such misfortune can lead to closed-loop instability due to an unwanted extra decrease in the system phase (NORMEY-RICO; CAMACHO, 2007). One solution to this problem consists of using dead-time compensators (DTCs) (NORMEY-RICO; CAMACHO, 2008).

The first DTC strategy was proposed in 1957, known as the Smith Predictor (SP) (SMITH, 1957). Although initially proposed as an improvement over classical PI or PID controllers, it presents limitations regarding robustness and disturbance rejection. In addition, it could not be used to control open loop unstable or integrative processes. Throughout the last decades many modifications have been proposed to overcome these drawbacks. Most of the solutions are intended for processes modeled by first order plus dead time (FOPDT) or second order plus dead time (SOPDT) systems, which are commonly found in industry (ZHENG; GAO, 2014; MATAUŠEK; RIBIĆ, 2012; NOGUEIRA *et al.*, 2011; NOWAK; CZECZOT, 2017). A wide review of these solutions is found in Normey-Rico and Camacho (2007).

Some of the most recent advances in DTCs are reviewed in this paragraph. In

Normey-Rico and Camacho (2009), a unified approach to deal with robustness was presented. In Wang *et al.* (2016), a two-degree-of-freedom (2DOF) design method was proposed based on optimal control and desired disturbance rejection specifications. Several examples showed enhanced performance and robustness when compared to previous works. In Liu *et al.* (2018a), a generalized DTC was presented in order to optimize set-point tracking and disturbance rejection. The structure is based on both an undelayed output prediction and a 2DOF control structure. Although these recent works present good robustness and disturbance rejection, the problem of measurement noise (mainly in unstable processes) is not handled in the design of the controllers.

Noise is commonly found in industrial processes and may cause regulatory performance degradation and increase undesired control signal variation. In Santos *et al.* (2010) a design method for the Filtered SP (FSP) robustness filter was proposed in order to improve noise attenuation. Torrico *et al.* (2013) presented a solution with a simpler way of dealing with robustness, disturbance rejection and noise attenuation when compared to Santos *et al.* (2010). In addition, controller tuning rules were proposed for FOPDT processes. In Mataušek and Ribić (2012) and Ribić and Mataušek (2012) control impairment caused by measurement noise is mitigated by the addition of filters, which increases the order of the equivalent controller. In Torrico *et al.* (2016), the DTC from Torrico *et al.* (2013) was generalized for multiple delay systems, namely simplified DTC (SDTC). Despite good results on noise attenuation, no further analysis was presented in order to improve disturbance rejection properties.

3.1.1 Contribution

This work introduces a new tuning method that simultaneously accounts for closed-loop robustness and noise attenuation for stable, unstable and integrative dead-time processes. It is shown that lower order filters are suitable to satisfy design specifications and provide enhanced performance when compared to more complex controllers from recent literature. In case stronger noise attenuation is required, the method allows to monotonically tune the robustness filter while maintaining desired performance characteristics. More specifically:

- Three different robustness filters are presented. One to deal with FOPDT processes and two which can be tuned for SOPDT industrial processes.
- Each filter presents two adjustment parameters that allow disturbance rejection and noise attenuation to be individually tuned to meet a desired trade-off, while frequency domain analysis of such characteristics is presented.

- Such nice decomposition is achieved by using different poles in the robustness filter $V(z)$ instead of the traditional design of DTCs which employs multiple repeated poles.

3.2 Simplified dead-time compensator

This section presents a the SDTC from Torrico *et al.* (2016) for the case of single-delay SISO systems. The control structure is illustrated in Figure 11, where $P_n(z) = G_n(z)z^{-d_n}$ is the nominal process model, $G_n(z)$ is the nominal process fast model, d_n is the nominal dead-time, $P(z)$ represents the real process, K_r is a constant, $F_1(z)$ and $F_2(z)$ are finite impulse response (FIR) filters and $V(z)$ is the robustness filter. In order to analyze controller properties the input-output relationships and the condition for robust stability are calculated for the nominal case $(P(z) = P_n(z))$

$$H_{yr}(z) = \frac{Y(z)}{R(z)} = \frac{K_r P_n(z)}{1 + F_1(z) + G_n(z)F_2(z)}, \tag{3.1}$$

$$H_{yq}(z) = \frac{Y(z)}{Q(z)} = P_n(z)\left[1 - \frac{P_n(z)V(z)}{1 + F_1(z) + G_n(z)F_2(z)}\right], \tag{3.2}$$

$$H_{un}(z) = \frac{U(z)}{N(z)} = \frac{-V(z)}{1 + F_1(z) + G_n(z)F_2(z)}, \tag{3.3}$$

$$I_r(\omega) = \left|\frac{1 + F_1(z) + G_n(z)F_2(z)}{G_n(z)V(z)}\right|_{z=e^{j\omega T_s}} > \overline{\delta P}(e^{j\omega T_s}), \tag{3.4}$$

where $U(z)$, $Y(z)$, $R(z)$, $N(z)$ and $Q(z)$ are the Z-transform of the following signals: control action, process output, reference, measurement noise, and input load disturbance, respectively; $H_{yr}(z)$, $H_{yq}(z)$, and $H_{un}(z)$ are the input-output transfer functions of the closed loop in Figure 11; $I_r(\omega)$ is defined as robustness index, T_s is the sampling time (with $0 < \omega < \pi/T_s$) and $\overline{\delta P}(e^{j\omega T_s})$ is the upper bound of the multiplicative uncertainty norm.

It is worth to note from (3.1) that K_r, $F_1(z)$ and $F_2(z)$ can be tuned in order to obtain a desired set-point tracking. From (3.2), (3.3), and (3.4), it can be seen that filter $V(z)$ can be used to cancel the effect of slow or unstable poles in the disturbance rejection $H_{yq}(z)$, to attenuate the effect of measurement noise, and/or to obtain a desired robustness index $I_r(\omega)$.

Figure 11 – SDTC conceptual structure
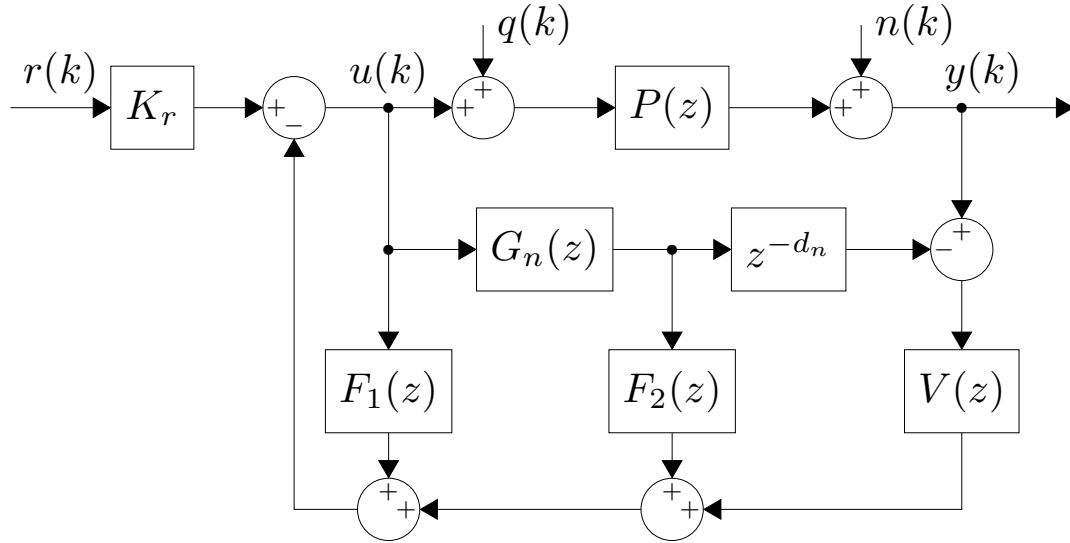
Source: The author.

3.2.1 Designing the SDTC

The tuning of the primary controller, which is defined by K_r, $F_1(z)$, and $F_2(z)$ is realized in order to obtain a desired set-point tracking for the nominal case. For this, consider $F_1(z)$ and $F_2(z)$ as finite impulse response (FIR) filters

$$F_1(z) = f_{1_1}z^{-1} + f_{1_2}z^{-2} + \ldots + f_{1_{n-1}}z^{-n+1}, \tag{3.5}$$

$$F_2(z) = f_{2_0} + f_{2_1}z^{-1} + f_{2_2}z^{-2} + \ldots + f_{2_{n-1}}z^{-n+1}, \tag{3.6}$$

where n is the order of the delay-free process model $G_n(z)$. The coefficients of $F_1(z)$ and $F_2(z)$ are calculated using pole placement by comparing the denominator of (3.1) to a desired closed-loop reference model. In order to find the coefficients of $F_1(z)$ and $F_2(z)$, one must solve an equation of the type $\Phi x = y$, with

$$
\Phi = \underbrace{\begin{bmatrix}
1 & 0 & \ldots & 0 \\
a_1 & 1 & & \vdots \\
\vdots & a_1 & & 0 \\
a_n & \vdots & & 1 \\
0 & a_n & & a_1 \\
0 & 0 & & a_n
\end{bmatrix}}_{n-1}
\underbrace{\begin{bmatrix}
b_1 & \ldots & 0 \\
b_2 & & \vdots \\
\vdots & & 0 \\
b_n & & b_1 \\
0 & & \vdots \\
0 & & b_n
\end{bmatrix}}_{n},
\quad
x = \begin{bmatrix}
f_{1_1} \\
\vdots \\
f_{1_{n-1}} \\
f_{2_0} \\
\vdots \\
f_{2_{n-1}}
\end{bmatrix},
\text{ and } y = \begin{bmatrix}
s_1 - a_1 \\
\vdots \\
s_n - a_n \\
s_{n+1} \\
\vdots \\
s_{2n-1}
\end{bmatrix}, \tag{3.7}
$$

where Φ is a non-singular $2n-1$ square matrix, $a_1 \dots a_n$ and $b_1 \dots b_n$ are the coefficients of

$$G_n(z) = \frac{b_1 z^{-1} + b_2 z^{-2} \dots b_n z^{-n}}{1 + a_1 z^{-1} + a_2 z^{-2} \dots a_n z^{-n}}, \tag{3.8}$$

and $s_1 \dots s_{2n-1}$ are the coefficients of the desired characteristic polynomial

$$1 + s_1 z^{-1} + s_2 z^{-2} \dots s_{2n-1} z^{-2n+1} = (1 - r_1 z^{-1})(1 - r_2 z^{-1}) \dots (1 - r_{2n-1} z^{-1}). \tag{3.9}$$

Therefore, closed-loop poles $r_1 \dots r_{2n-1}$, with $0 \le r_i < 1$, are chosen in order to tune set-tracking point response. For example, if a faster set-point is desired, than smaller values of r_i can be chosen, and *vice-versa*.

Note that in the case of FOPDT systems $F_1(z) = 0$ and $F_2(z) = f_{2_0}$, thus the control structure reduces to the one presented in Torrico *et al.* (2013). K_r is a gain calculated to yield zero steady-state error, then it follows that

$$K_r = \frac{1 + F_1(1) + G_n(1)F_2(1)}{P_n(1)}. \tag{3.10}$$

The SDTC robustness filter is defined as

$$V(z) = \frac{v_0 + v_1 z^{-1} + \dots + v_n z^{-n}}{(1 - \beta z^{-1})^{n+1}}, \tag{3.11}$$

where $v_0 \dots v_n$ are the filter coefficients computed to attend the design requirements and β is a user tuning parameter. The first design requirement is to guarantee rejection of input step-like disturbances in order to assure reference tracking at steady-state. Therefore (3.2) must equal zero for $z = 1$, leading to

$$V(1) = \frac{1 + F_1(1) + G_n(1)F_2(1)}{P_n(1)} = K_r. \tag{3.12}$$

Secondly, the filter is tuned to eliminate slow or unstable modes of the plant model $P_n(z)$ which could appear in the disturbance rejection response (3.2). Consider that p_i are the poles of the process model to be canceled, then the following equations must be satisfied

$$\left[1 - \frac{P_n(z)V(z)}{1 + F_1(z) + G_n(z)F_2(z)} \right]_{z = p_i \ne 1} = 0, \tag{3.13}$$

$$\frac{d}{dz} \left[1 - \frac{P_n(z)V(z)}{1 + F_1(z) + G_n(z)F_2(z)} \right]_{z = p_i = 1} = 0, \qquad i = 1, \dots n, \tag{3.14}$$

where n is the number of undesired poles, generating a set of $n+1$ equations derived from (3.12), (3.13), and (3.14) to calculate robustness filter coefficients $v_0 \dots v_n$. In case it is desired to reject higher order disturbances and/or to follow higher order references (ramps, parabolas, etc.), higher order filters and controllers must be applied (TORRICO; NORMEY-RICO, 2005).

3.3 Proposed tuning rules for the robustness filter

In order to analyse the tuning of $V(z)$, consider the following four equations derived from (3.1), (3.2), (3.3) and (3.4)

$$H_{yr}(\omega) = \mid K_r M(z) \mid_{z=e^{j\omega T_s}},$$ (3.15)

$$H_{yq}(\omega) = \mid G_n(z)\left[1 - M(z)V(z)\right] \mid_{z=e^{j\omega T_s}},$$ (3.16)

$$H_{un}(\omega) = \left| \frac{V(z)M(z)}{G_n(z)} \right|_{z=e^{j\omega T_s}},$$ (3.17)

$$I_r(\omega) = \frac{1}{\mid M(e^{j\omega T_s})V(e^{j\omega T_s}) \mid} > \overline{\delta P}(e^{j\omega T_s}),$$ (3.18)

where

$$M(z) = \frac{N_g(z)}{D_g(z)(1 + F_1(z)) + N_g(z)F_2(z)} z^{-d_n}$$

$$= \frac{N_g(z)}{(1 - r_1 z^{-1})(1 - r_2 z^{-1})\dots(1 - r_{2n-1}z^{-1})} z^{-d_n}$$

with $G_n(z) = N_g(z)/D_g(z)$. Note that the zeros of $M(z)$ are equal to the zeros of the process model while the poles of $M(z)$ are the user defined closed-loop poles for set-point tracking response, thus it can be observed that in industrial processes $M(z)$ has low pass characteristics.

3.3.1 Analysis of the robustness filter effect

3.3.1.1 Disturbance rejection

One can see from (3.16) that it is highly desired that $H_{yq}(\omega)$ approaches to zero for the frequency range $0 < \omega < \pi/T_s$. Unfortunately, it is easy to check that such objective cannot be met at high frequencies ($\omega \to \pi/T_s$) as $M(z)V(z)$ from (3.16) has low pass characteristics. An alternative to deal with this problem is to raise the robustness filter $V(z)$ gain at high frequencies by reducing its number of poles.

3.3.1.2   Noise attenuation

For industrial applications, it is important that the control signal be the least affected by noise measurement as possible. Noise amplification can be responsible for undesired non-linearities in the control loop, such as saturation. Measurement noise tends to occur at high frequencies. Thus, in order to avoid impaired performance due to such phenomenon, robustness filter $V(z)$ in (3.17) must present low gain for $\omega \to \pi/T_s$, indicating the need for higher order $V(z)$ filters. This condition elucidate the trade-off between input disturbance rejection and noise attenuation when tuning the SDTC.

3.3.1.3   Robust stability condition

In general the robust stability condition, given by (3.18), tends to be violated at medium frequencies (NORMEY-RICO; CAMACHO, 2007; ZHENG; GAO, 2014). Low and medium frequency specifications can be attended by low order filters, therefore the order of the robustness filter $V(z)$ is not determinant to achieve desired robustness.

3.3.1.4   Choice of the robustness filter poles

Traditionally, the robustness filter is tuned using a single constant parameter in the filter denominator which defines multiple repeated stable poles. In some cases this parameter is tuned to reach a desired robustness and disturbance rejection (SANZ *et al.*, 2018; WANG *et al.*, 2016), while in other cases the noise attenuation is prioritized by increasing the filter order (ZHENG; GAO, 2014; SANTOS *et al.*, 2010). In this work, a more flexible solution is proposed by using different poles in the robustness filter $V(z)$ to meet a desired trade-off between disturbance rejection and noise attenuation

$$V(z) = \frac{v_0 + v_1 z^{-1} + \cdots + v_n z^{-n}}{(1 - \beta_1 z^{-1})(1 - \beta_2 z^{-1})\ldots(1 - \beta_m z^{-1})}, \tag{3.19}$$

where $m = n + 1$. Note that, if $\beta_1 = \beta_2 = \cdots = \beta_m = \beta$ the the filter reduces to the one in (3.11). Next section presents tuning rules of β_i, $i = 1\ldots m$, for different study cases.

3.3.2 *Study cases*

This work investigates the control of processes modeled by following three transfer functions

$$P_1(s) = \frac{k_n \, e^{-L_n s}}{(\tau_p s - 1)(\tau_u s + 1)}, \tag{3.20}$$

$$P_2(s) = \frac{k_n \, e^{-L_n s}}{s(\tau_u s + 1)}, \tag{3.21}$$

$$P_3(s) = \frac{k_n \, e^{-L_n s}}{(\tau_p s - 1)}, \tag{3.22}$$

where $P_1(s)$ and $P_2(s)$ are second-order plus dead-time (SOPDT) unstable and integrative models, respectively, and $P_3(s)$ is an unstable first-order plus dead-time (FOPDT) model, where $\tau_p > 0$ and $\tau_u > 0$. Such models can represent a wide variety of industrial processes. In Zheng and Gao (2014) it was used to model the concentration of an open loop unstable chemical reactor. The temperature control of an aluminum thin plate is presented in Mataušek and Ribić (2012). Field tests of a damping controller designed to mitigate electromechanical oscillations on an 18-MVA diesel generating unit are presented in Nogueira *et al.* (2011).

3.3.2.1 *Robustness filter for FOPDT processes*

The robustness filter

$$V_1(z) = \frac{v_0 + v_1 z^{-1}}{(1 - \beta_1 z^{-1})(1 - \beta_2 z^{-1})} \tag{3.23}$$

is proposed for the case of FOPDT processes (3.22), where the tuning parameters are chosen as $0 \leq \beta_1 < \beta_2$ and $0 < \beta_2 < 1$. Parameter β_1 is tuned considering a desired noise attenuation response, that is, if noise attenuation is not a priority then β_1 can be chosen close to zero, otherwise, close to β_2. Parameter β_2, on the other hand, is chosen to obtain desired robustness characteristics. That is, as β_2 gets closer to 1, the system overall robustness against uncertainties will increase. On the other hand, slower disturbance rejection will occur, and *vice-versa*.

3.3.2.2 *Robustness filter for SOPDT processes*

Following two filters

$$V_2(z) = \frac{v_0 + v_1 z^{-1} + v_2 z^{-2}}{(1 - \beta_1 z^{-1})(1 - \beta_2 z^{-1})}, \tag{3.24}$$

and

$$V_3(z) = \frac{v_0 + v_1 z^{-1} + v_2 z^{-2}}{(1 - \beta_1 z^{-1})(1 - e^{-\sigma + \Omega i} z^{-1})(1 - e^{-\sigma - \Omega i} z^{-1})} \tag{3.25}$$

are proposed for the case of SOPDT processes, where σ and Ω are free parameters.

The tuning of $V_2(z)$ follows the same procedure as $V_1(z)$, that is, initially β_2 is tuned in order to obtain desired robustness characteristics, then β_1 is set between $0 \leq \beta_1 < \beta_2$.

Another option to deal with measurement noise attenuation is to use filter $V_3(z)$. As shown in Torrico $et\ al.$ (2014), complex poles can improve the relationship between noise attenuation and robustness. In addition, it was shown that the ratio Ω/σ can define the noise attenuation characteristic where $atan(\Omega/\sigma) \leq \pi/3$ is desired (TORRICO $et\ al.$, 2014). Filter $V_3(z)$ is tuned as follows: (i) define a desired ratio $D_r = \Omega/\sigma$, (ii) tune σ to achieve a desired robustness, (iii) set β_1 between $0 \leq \beta_1 < 1$ close to one for improved noise attenuation. In order to illustrate the tuning, consider the plant studied in Normey-Rico and Camacho (2009),

$$G(s) = \frac{0.1}{s(2s + 1)^5}, \tag{3.26}$$

which can be approximated by a second order integrating plant described by the process model (3.21)

$$P(s) = \frac{0.1 e^{-5s}}{s(5s + 1)}. \tag{3.27}$$

Using a sampling time of $T_s = 0.2\ s$, the zero-order-hold method yields the discretized plant

$$P(z) = \frac{0.00039472(z + 0.9868)}{(z - 1)(z - 0.9608)} z^{-25}. \tag{3.28}$$

Consider Dr relation in robustness filter (3.25) is kept fixed at $tan(\pi/3)$, then noise attenuation pole β_1 varies in the range between $0 \leq \beta_1 < 1$. Figure 12 shows the relation between $H_{un}(\omega)$ (3.17) and β_1. From Figure 12 it is possible to notice that the value of $H_{un}(w)|_{w \to \pi/T_s}$ gets lower as β_1 increases, thus obtaining a desired measurement noise gain in the control signal at high frequencies.

3.4 Simulation results

In order to evaluate the performance of the proposed tuning rules, following four examples from recent literature were used. All simulations were compared to recently published

Figure 12 – Relation between $|H_{un}(w)|$ and β_1 with $Dr = tan(\pi/3)$ for (3.28)
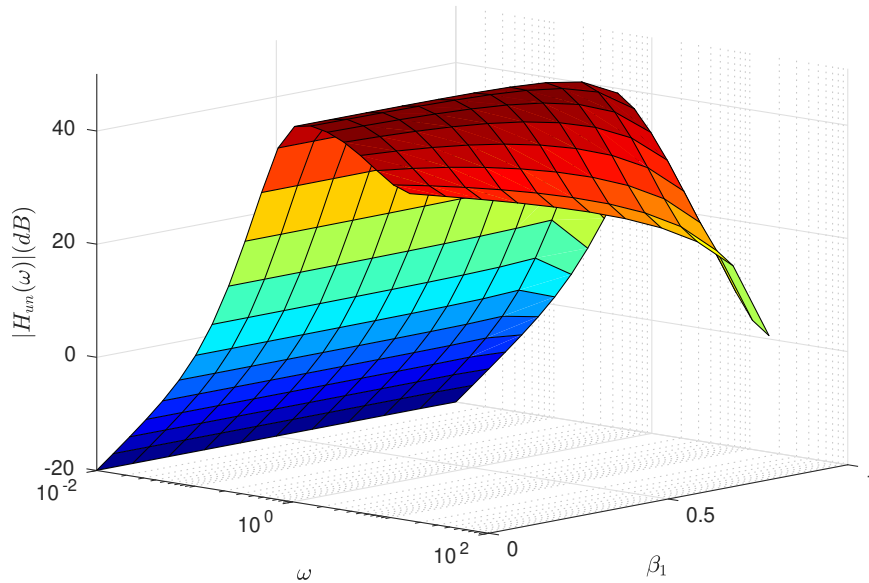
Source: The author.

works that propose tuning for dead-time processes. In order to clearly separate the effects of the input disturbance and of the noise measurement in the output response, the noise is only added in the last seconds of simulation, that is, when the system reaches steady-state, leading to a better analysis.

Example 1

Consider the illustrative process (3.26)-(3.28). Two SDTC controllers were tuned for this example. In order to achieve similar set-point response with compared controllers from Wang *et al.* (2016) and Liu and Gao (2011), primary controller was tuned with $F_1(z) = -0.436z^{-1}$, $F_2(z) = 105.9 - 101.3z^{-1}$ and $K_r = 4.5906$ for both SDTC.

Attenuation of high frequency modes along with fast disturbance rejection are desired for this example. As aforementioned, complex poles exhibit good balance between noise attenuation and robustness, thus initially leading to the adoption of (3.25) as the robustness filter to the SDTC$_1$. By following specified tuning rules from Subsection 3.3.2.2, ratio $D_r = \tan(\pi/3)$ was defined, then $\sigma = 0.0842$ was chosen. Lastly, $\beta_1 = 0.87 \leq 1$ was set, leading to

$$V(z) = \frac{16.03 - 31.06z^{-1} + 15.05z^{-2}}{(1 - 0.87z^{-1})(1 - 1.82z^{-1} + 0.845z^{-2})}. \tag{3.29}$$

A second and more robust proposal is made for the SDTC$_2$ by choosing $\beta_1 = 0.97$

and $\beta_2 = 0.91$ for (3.24), obtaining

$$V(z) = \frac{22.76 - 44.31z^{-1} + 21.56z^{-2}}{(1 - 0.97z^{-1})(1 - 0.91z^{-1})}. \qquad (3.30)$$

Figure 13 shows time responses to a unit step reference. At $t = 50$ s a negative unity step disturbance is applied at the process input. Furthermore, white noise with zero mean and a variance of 0.001 is added to the measured output in the last 10 seconds of simulation. Notice that while possessing faster regulation response than controllers proposed by Wang *et al.* (2016) and Liu and Gao (2011), the SDTC maintained similar noise attenuation.

Suppose now that due to unmodeled dynamics, both the gain and time constant of (3.27) are 20% higher than the nominal case. Figure 14 shows the results for this situation. Similarly to the nominal case, SDTC with uncertainty exhibited fast regulation response with only small oscillations.

Figure 13 – Nominal system responses for example 1
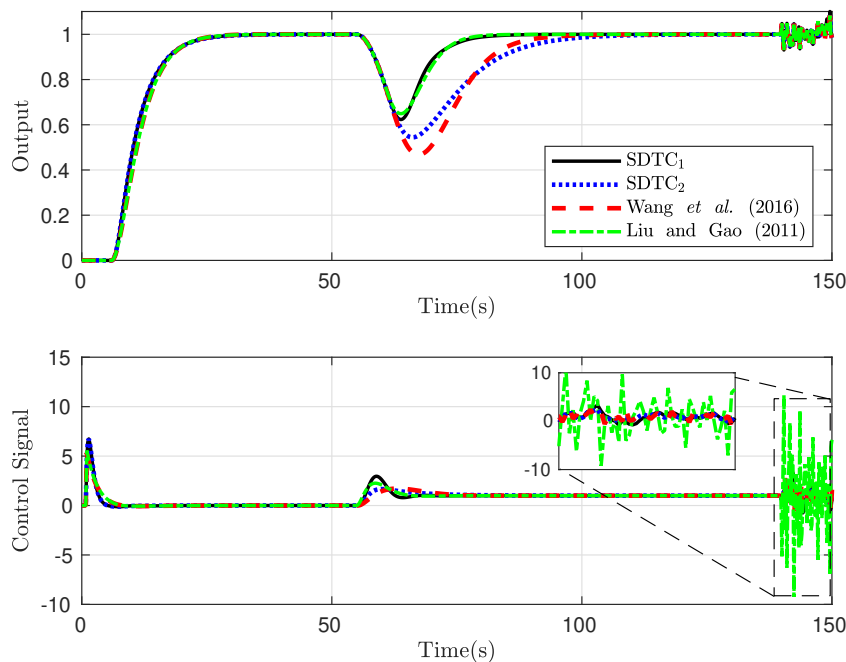
Source: The author.

A second uncertainty case is then considered, with gain 20% higher and time constant 20% lower than the nominal model. Results for this case are presented in Figure 15. In this situation, only the $SDTC_2$ and the controller from Wang *et al.* (2016) were able to remain stable, with slightly better response from the proposed controller, which presented faster disturbance rejection.

Figure 14 – Perturbed system responses for example 1
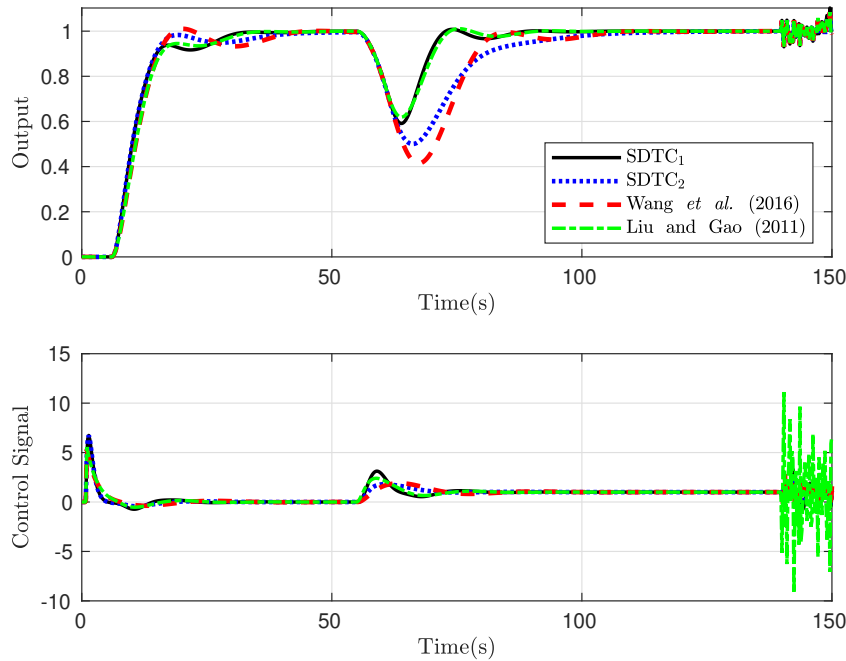
Source: The author.

Example 2

Consider the unstable SOPDT process recently studied in Liu *et al.* (2018a)

$$P(s) = \frac{2}{(10s-1)(2s+1)}e^{-5s}. \tag{3.31}$$

The discrete-time model $P_n(z)$ with long dead-time is obtained using a sampling time of $T_s = 0.1\ s$ is given by

$$P_n(z) = \frac{0.00049342(z+0.9868)}{(z-1.01)(z-0.9512)}z^{-50}. \tag{3.32}$$

For this case, two SDTC controllers were designed. In order to obtain fast set-point tracking, the primary controller of both are tuned with $F_1(z) = -0.8904z^{-1}$, $F_2(z) = 3.433 - 3.268z^{-1}$, and $K_r = 0.1102$.

In addition, both controllers employed (3.25) as the robustness filter model with $\sigma = 0.45$, $\Omega = 1.15$. Fast disturbance rejection was prioritized for the SDTC$_1$, thus $\beta_1 = 0$, leading to

$$V(z) = \frac{296.3 - 576.1z^{-1} + 279.9z^{-2}}{1 - 0.522z^{-1} + 0.4057z^{-2}}. \tag{3.33}$$

In order to improve noise attenuation characteristics while keeping faster disturbance rejection than the controller from Liu *et al.* (2018a), β_1 was increased for the SDTC$_2$, obtaining

Figure 15 – Perturbed system responses for example 1 with gain 20% higher
and time constant 20% lower than the nominal model
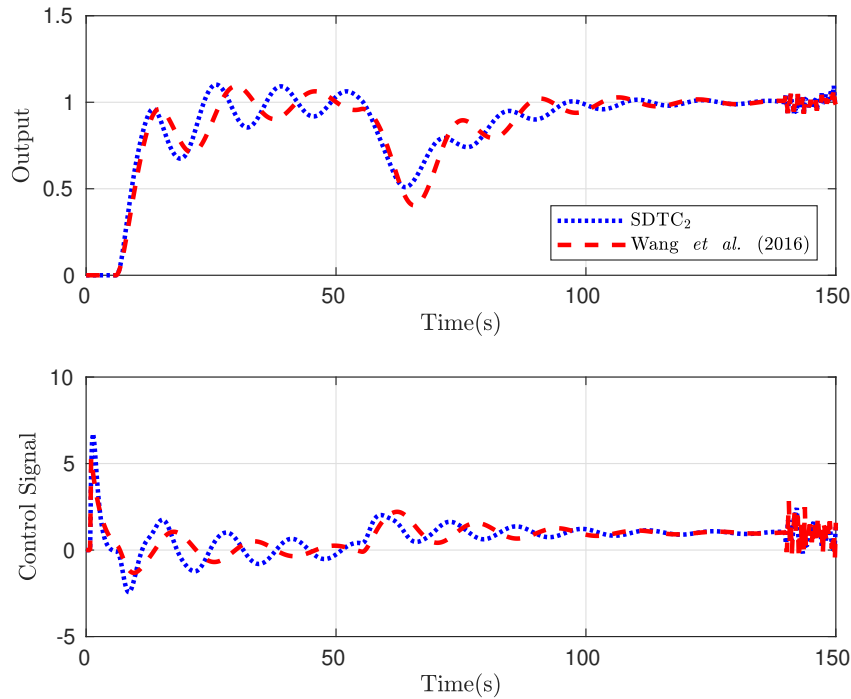
Source: The author.

the following filter

$$V(z) = \frac{34.06 - 66.26z^{-1} + 32.21z^{-2}}{(1 - 0.9z^{-1})(1 - 0.522z^{-1} + 0.4057z^{-2})}. \tag{3.34}$$

Figure 16 shows the relation $|H_{un}(w)|$. It is possible to see that the increase in β_1 for the SDTC$_2$ is an effective design procedure that improves the controller capacity to deal with noise (which occurs at high frequencies).

Two control tests were executed in order to evaluate the SDTC performance. A unity step-change was applied to the system at time $t = 0$ s and a negative constant load disturbance of magnitude 0.2 entered the control signal at time $t = 60$ s. In addition, measurement white noise with zero mean and a variance of 5×10^{-5} was added to the output in the last five seconds of simulation.

Figure 17 shows the results for the nominal case. As it can be seen, both SDTC controllers exhibit faster disturbance rejection than the controller from Liu *et al.* (2018a). Note that, as expected, the SDTC$_2$ achieved the best noise attenuation among all three controllers, making it the most appropriated solution for practical industrial applications.

As in Liu *et al.* (2018a), consider now that the process time delay and proportional gain are actually 5% larger while the stable pole is 5% smaller than the obtained model. Integral

Table 1 – ISE for examples and experiment

| | Example 1 | | | | Example 2 | | |
	SDTC$_1$	SDTC$_2$	Ref. [12]	Ref. [21]	SDTC$_1$	SDTC$_2$	Ref. [13]
Nominal	10.1552	11.7367	12.8919	10.6036	9.8132	9.6574	11.7023
Perturbed 1	10.0866	11.6830	12.9917	10.5032	10.0387	9.7847	11.7279
Perturbed 2	-	11.3755	12.3504	-	-	-	-
	Example 3			Example 4		Experiment	
	SDTC$_1$	SDTC$_2$	Ref. [12]	SDTC	Ref. [12]	SDTC	Ref. [13]
Nominal	7.2601	7.6869	7.4178	2078.6	2100.2	-	-
Perturbed	8.8380	9.7113	8.8668	2273.8	2288.6	130.7141	141.1987

of the square error (ISE) for this situation is shown in Table 1, once more demonstrating the improvement yielded by the proposed strategy.

Figure 16 – Noise sensitivity $|H_{un}(\omega)|$ for example 2
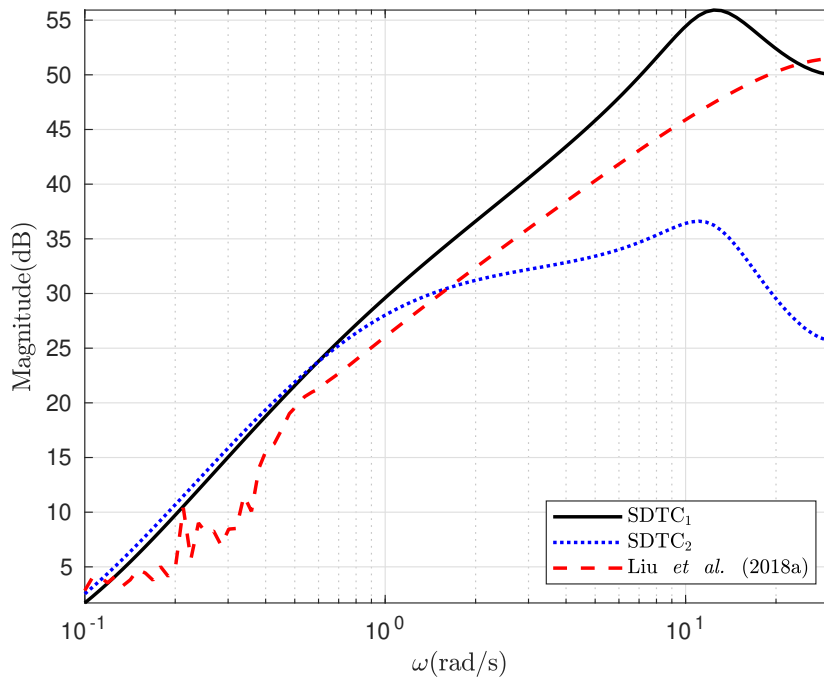
Source: The author.

Example 3

The following process from Wang *et al.* (2016) and García and Albertos (2013) is studied in this example

$$P(s) = \frac{e^{-4s}}{s(s+1)}. \tag{3.35}$$

Using a sampling time $T_s = 0.2\ s$, the discrete time model of the process is given by

$$P_n(z) = \frac{0.018731(z+0.9355)}{(z-1)(z-0.8187)}z^{-20}. \tag{3.36}$$

Figure 17 – Nominal system responses for example 2
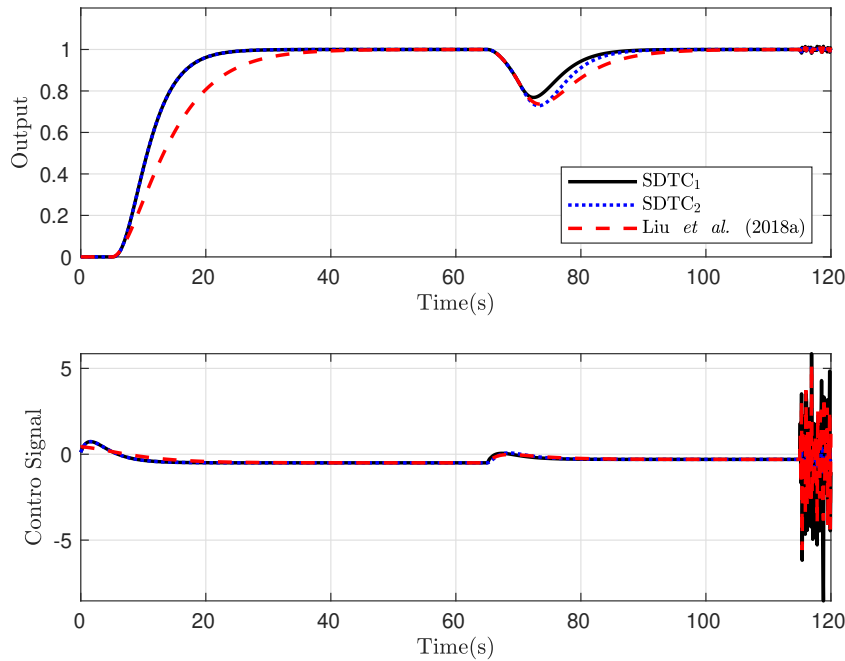
Source: The author.

For comparison purposes, this case includes the traditional SDTC with repeated filter poles, namely $SDTC_2$. The proposed tuning rules are applied in the design of the $SDTC_1$. The primary controllers and robustness filters for both $SDTC_1$ and $SDTC_2$ were designed to yield reference tracking and disturbance rejection performances similar to that presented in Wang *et al.* (2016), thus $F_1(z) = -0.02328z^{-1}$, $F_2(z) = 7.582 - 6.616z^{-1}$, and $K_r(z) = 0.9654$ for both controllers. Disturbance rejection filters were tuned according to (3.24) and (3.11), with $\beta_1 = 0.87$ and $\beta_2 = 0.965$ for the $SDTC_1$, and $\beta = 0.91$ for the $SDTC_2$, leading to

$$V(z) = \frac{1.516 - 2.733z^{-1} + 1.221z^{-2}}{(1 - 0.87z^{-1})(1 - 0.965z^{-1})}, \tag{3.37}$$

and

$$V(z) = \frac{0.2283 - 0.4113z^{-1} + 0.1838z^{-2}}{(1 - 0.91z^{-1})^3}, \tag{3.38}$$

for $SDTC_1$ and $SDTC_2$, respectively.

Control results for the $SDTC_1$, the $SDTC_2$ and the controller proposed by Wang *et al.* (2016) are shown in Figure 18. A unit step reference was introduced at time $t = 0$ s, while a step-like disturbance of -0.1 was added to the control signal at time $t = 65$ s. For analysis purposes, measurement white noise with zero mean and a variance of 0.001 was also added from time $t = 120$ s to the end of the experiment. Furthermore, Figure 19 shows the results of

a second experiment performed in order to evaluate the system robustness in the presence of a 20% error in the process delay model.

From Figures 18 and 19 it is possible to notice that the SDTC$_1$ and the controller proposed by Wang *et al.* (2016) have similar output signals, with slightly better disturbance rejection achieved by the SDTC$_1$. In addition, SDTC$_1$ was able to keep good noise attenuation with faster response than the traditional SDTC$_2$.

Figure 18 – Nominal system responses for example 3
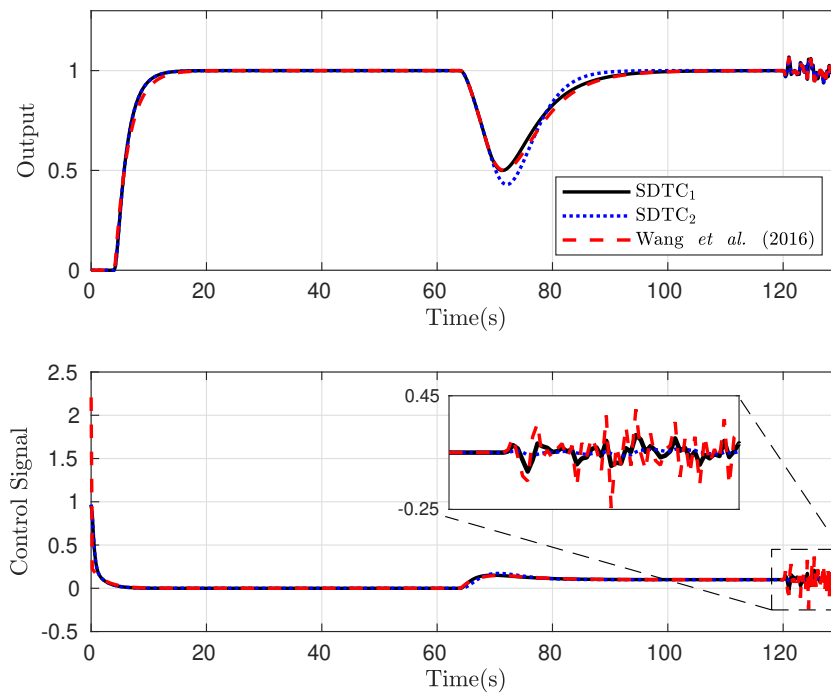
Source: The author.

Example 4

Consider the following first-order unstable process with time-delay of the chemical reactor concentration studied in Wang *et al.* (2016), Torrico *et al.* (2013),

$$P(s) = \frac{3.433e^{-20s}}{101.1s - 1}. \tag{3.39}$$

Using a sampling time $T_s = 0.5$ *s*, the discrete model of the process is given by

$$P_n(z) = \frac{0.016689}{z - 1.00486} z^{-40}. \tag{3.40}$$

In order to obtain similar set-point tracking response with that from Wang *et al.* (2016), the primary controller is tuned with $F_1(z) = 0$, $F_2(z) = 1.742$, and $K_r(z) = 1.451$.

Figure 19 – Perturbed system responses for example 3
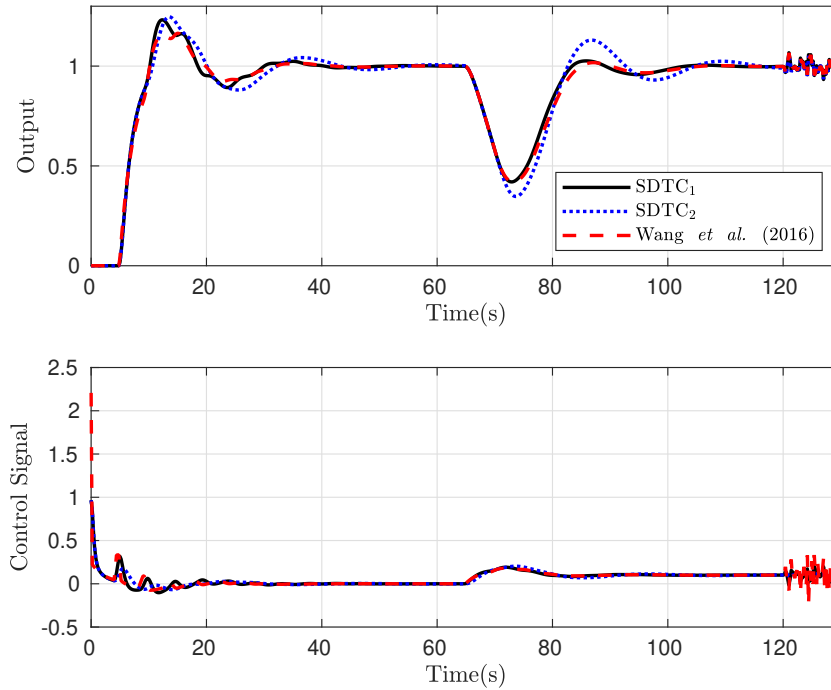
Source: The author.

In order to achieve fast disturbance rejection robustness filter (3.23) with $\beta_1 = 0$ and $\beta_2 = 0.986$ was chosen, yielding

$$V(z) = \frac{4.016 - 3.996z^{-1}}{1 - 0.986z^{-1}}. \tag{3.41}$$

A step reference is applied to the system at time $t = 0$ s while a negative input disturbance of magnitude 1 is applied at time $t = 600$ s. Additionally, white noise with zero mean and a variance of 0.1 is added to the measured output in the last 200 seconds of simulation. Results for this case are shown in Figure 20. Consider now the process delay is actually 30% larger than the modeled one. Figure 21 shows the results for this situation.

Results show that the SDTC was able to achieve faster disturbance rejection for both nominal and perturbed cases. Furthermore, noise attenuation is superior to the controller from Wang *et al.* (2016). Note that such results are obtained by using simples gains in the primary controller, and a monotonically tuned robustness filter.

3.5 Experimental results

The proposed strategy was applied for the temperature control of an in-house thermal chamber, which is shown in Figure 22. The temperature inside the chamber is controlled by

Figure 20 – Nominal system responses for example 4
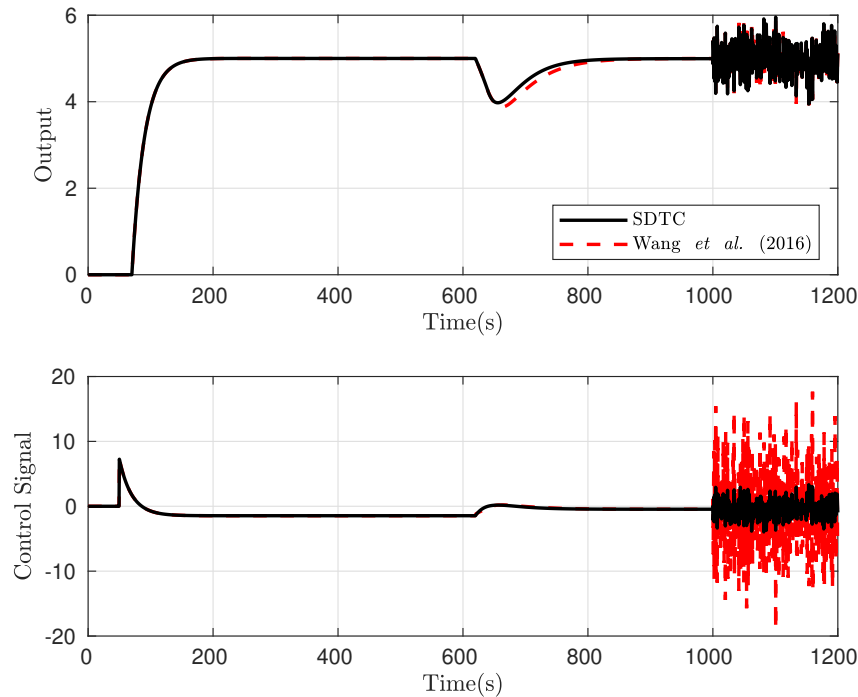
an electrical resistor which provides heat and is situated in an air reservoir right below the acrylic dome. The reservoir is separated only by two openings which allow air to circulate. Additionally, a fan with constant rotational speed provides the internal air flow. This set of actuators is a source of delay and nonlinearities in the system. The control input is limited by the resistor maximum power, which varies in a scale from 0 to 100%, thus the saturation model is included in the control loop, as shown in the control diagram in Figure 23, where subsystem $S(z) = F_1(z) + G_n(z)(F_2(z) - V(z)z^{-d_n})$ is defined to obtain an internally stable implementation of the predictor for any process model (TORRICO *et al.*, 2016). The power delivered to the heating resistor is controlled by the duty cycle of a switching power supply. Furthermore, there are two portholes which can be manually opened in order to disturb the internal temperature by interaction with the external environment. This system can represent a wide variety of industrial and commercial applications, such as thermal control of neonatal incubators and industrial furnaces.

The SDTC is implemented on a supervisory computer. The control signal is sent via Universal Serial Bus (USB) cable to a driving circuit through a Nidaq-USB6009 data acquisition card manufactured by National Instruments. In order to close the control loop, a temperature sensor provides the actual temperature inside the chamber to the acquisition card through an

Figure 21 – Perturbed system responses for example 4
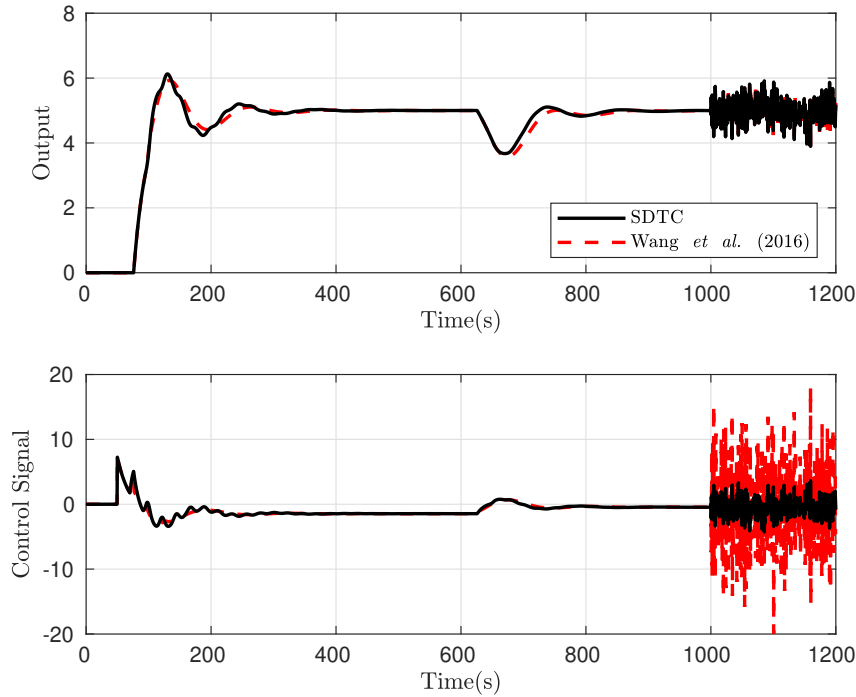
analog digital converter (ADC).

An open-loop identification step test was performed by applying maximum power to the electrical resistor. The temperature response can be view in Figure 24. Practical applications with slow time-constant can be approximated by integrative models (NORMEY-RICO; CAMACHO, 2008). Besides containing less identification parameters, using an integrative model allows to reduce the amount of time required for the identification test, since it is not necessary to reach steady-state regime. Thus, by using the two-parameter method from Aström and Hägglund (1995) the plant was approximated by

$$P(s) = \frac{0.6}{s}e^{-2s}, \tag{3.42}$$

which was discretized by using the zero-order-hold method with $T_s = 0.2$ min, obtaining

$$P(z) = \frac{0.12}{z-1}z^{-10}. \tag{3.43}$$

The SDTC was tuned to produce fast set-point tracking response (3.1) with a time constant of two minutes. Thus, the primary controller was tuned with $F_1(z) = 0$, $F_2(z) = f_{2_0} = 0.8333$, and $K_r = 0.8333$. To provide good disturbance rejection and appropriate noise attenuation, the disturbance filter is given by (3.23)

$$V(z) = \frac{0.2042 - 0.2z^{-1}}{(1 - 0.95z^{-1})(1 - 0.9z^{-1})}. \tag{3.44}$$

Figure 22 – In-house thermal chamber
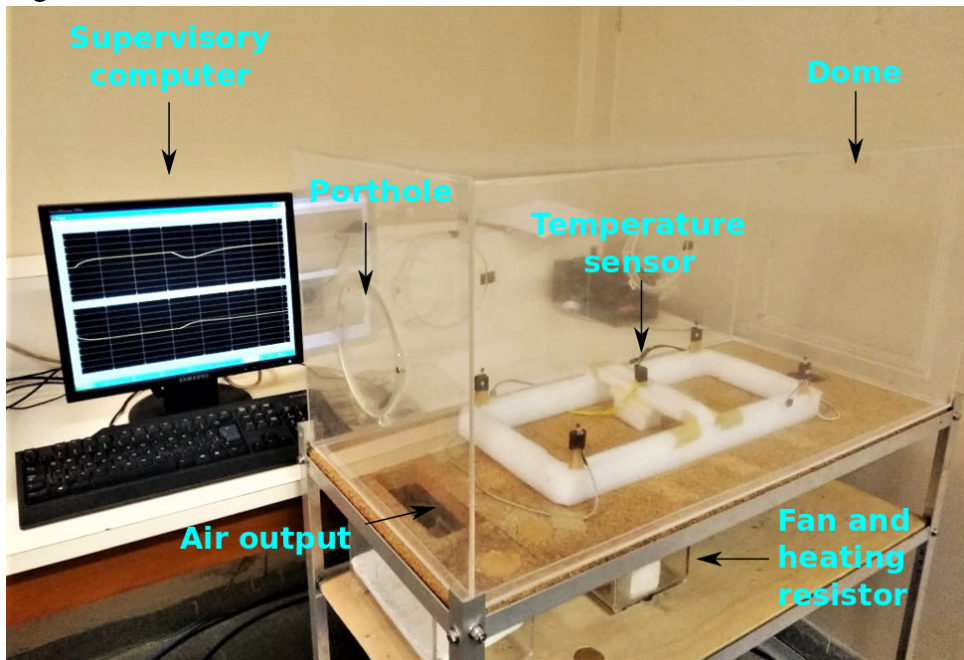
Source: The author.

Figure 25 shows experimental results for a step change on the set-point from 20.7^oC to 26^oC. In order to assess controller robustness, portholes remained opened from $t = 30\ min$ to $t = 40\ min$. For comparison purposes, the control method given in Liu *et al.* (2018a) is also used for implementation with $\lambda = 0.9$, $\lambda_f = 0.96$, $\lambda_s = 0.925$, $m = 1$, $n_h = 0$, $n_d = 2$, $n_f = 2$, $\beta_1 = 2/(1 - \lambda_f)$, and $\beta_2 = 1 - \beta_1$.

Note that both controllers were able to follow the reference without overshoot, and present similar response over the time while the portholes remain open from $t = 30\ min$ to $t = 40\ min$. However, when the portholes were closed at $t = 40\ min$, it is possible to note that, differently from the controller from Liu *et al.* (2018a), the SDTC was capable to reach the set-point once again twenty minutes prior to the compared controller, which kept oscillating for a longer period.

3.6   Discussion

A new set of tuning rules for a simplified dead-time compensator focusing on industrial process has been proposed in this chapter. The set of rules for the poles of the robustness filter has successfully shown its advantages for both robust tuning and measurement noise attenuation. Not merely the proposed tuning rules achieved superior results compared to its classical counterpart, it has also shown to be simpler than recent dead-time process control

Figure 23 – Thermal chamber control diagram
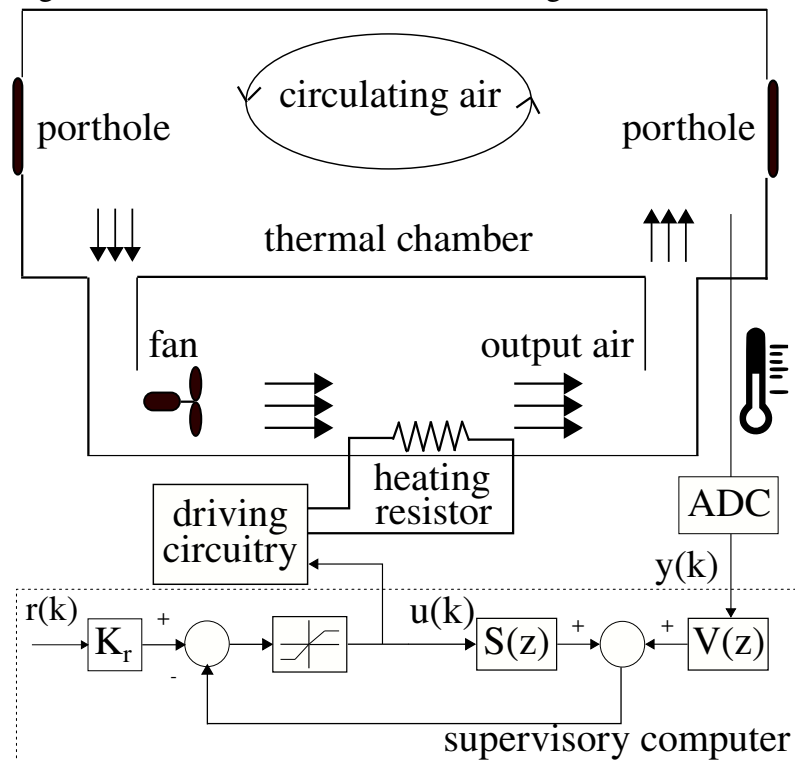
Source: The author.

Figure 24 – Temperature response for process identification
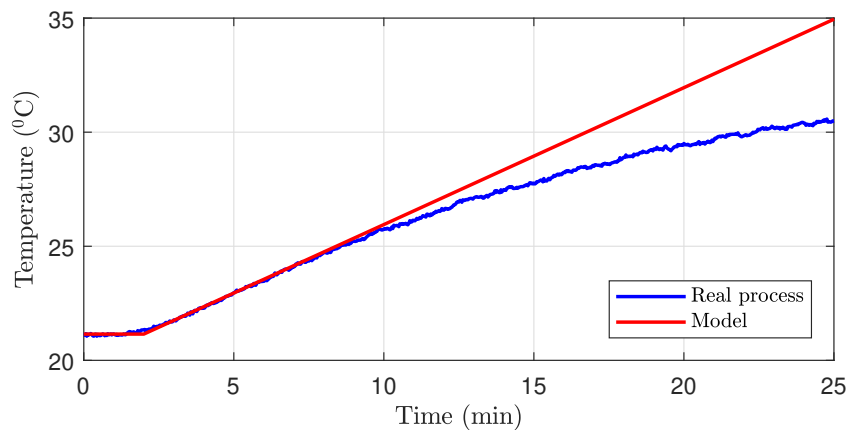
Source: The author.

strategies in the literature (LIU *et al.*, 2018a; WANG *et al.*, 2016).

In general, simplicity is pivotal for controller design implementation and understanding of the tuning rules, which are characteristics clearly achieved by the proposed controller. The variety of simulation examples from different applications (NORMEY-RICO; CAMACHO, 2009; WANG *et al.*, 2016; GARCÍA; ALBERTOS, 2013; PANDA, 2009; LIU *et al.*, 2018a) validates the SDTC versatility, being able to control stable, unstable, and integrative processes even in the presence of modeling uncertainties. The experimental results presented satisfactory performance on the control of a thermal chamber system subjected to modeling mismatch,

Figure 25 – Experimental results
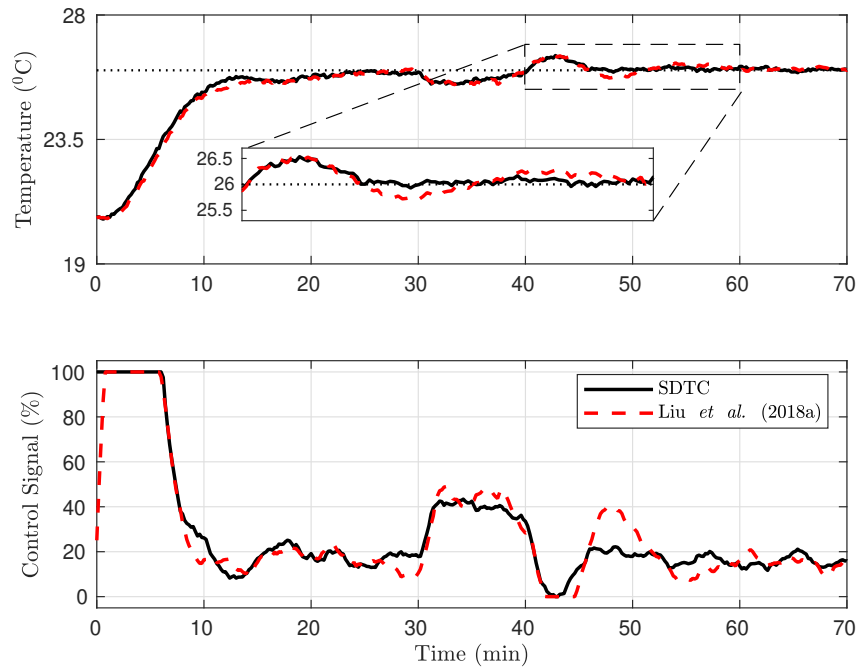
external disturbance, and measurement noise.

4 A STATE-SPACE DTC STRATEGY

This chapter proposes the extension of the simplified filtered Smith predictor for state-space systems to improve rejection of matched and unmatched unknown disturbances in LTI systems with input delay. The proposed structure is simpler than others recently proposed in the literature and can be applied to continuous-time or discrete-time systems. Furthermore, it allows improving rejection of both matched and unmatched disturbances, while also enhancing noise attenuation and robustness characteristics. Finite spectrum assignment (FSA) based implementation is used in order to guarantee the internal stability of the proposed controller. Simulation and experimental results are used to show the usefulness of the proposal.

4.1 Introduction

Since Smith's seminal work (SMITH, 1957), several dead-time compensators have been proposed in order to improve closed-loop performance in the presence of delay.

The Artstein predictor (ARTSTEIN, 1982) is an important state-space based DTC since internal stability is ensured from the nominal closed-loop stability of the delay free model. In this context, the Finite Spectrum Assignment (FSA) is obtained from the combination of the Artstein predictor with a stabilizing state feedback control (MANITIUS; OLBROT, 1979). This idea has been considered from stabilization point of view for several years. Recently, disturbance rejection properties has been analyzed and modified by taking account disturbance effect with respect to the nominal prediction (LÉCHAPPÉ *et al.*, 2015; SANZ *et al.*, 2016; SANTOS, 2016; FURTAT *et al.*, 2018; GIRALDO *et al.*, 2018; SANTOS; FRANKLIN, 2018; LIU *et al.*, 2018b).

In the presence of dead times, control complexity is increased since the control action effect is delayed with respect disturbance outcome (NORMEY-RICO; CAMACHO, 2007). Disturbance compensation properties have been considered in most the Smith predictor-based strategies (NORMEY-RICO; CAMACHO, 2008). However, in contrast to the Artstein predictor, Smith predictor is not internally stable if the open-loop system is unstable. Hence, internal stability of Smith predictor-based strategies depend on a suitable predictor design and implementation. In recent years, several works have provided simplified design and procedures (NORMEY-RICO; CAMACHO, 2009; SANTOS *et al.*, 2010; TORRICO *et al.*, 2013; LIU *et al.*, 2018a; SANZ *et al.*, 2018; TORRICO *et al.*, 2018). These results are quite practical from disturbance rejection point of view since the predictor design problem can be treated from an

unified framework.

In the context of input-output predictors, Normey-Rico and Camacho (2009) proposed a filtered Smith predictor (FSP) where a robustness filter is used to modify disturbance rejection response and to ensure internal stability. A modified robustness filter design was presented in Santos *et al.* (2010) to deal with the trade-off between noise attenuation and disturbance rejection. An improved and simplified design condition was proposed in Torrico *et al.* (2013) in order that a simple proportional primary controller can be used to achieve constant set-point tracking and disturbance rejection. A simplified two degree of freedom strategy based on a finite impulse filter predictor for industrial processes is proposed in Liu *et al.* (2018a). In Sanz *et al.* (2018), the Smith Predictor structure is analyzed in terms of a general predictor in order to preserve disturbance rejection properties of the original controller. Recently, a simplified strategy with a modified structure has been proposed to directly deal with noise attenuation and general disturbance rejection properties (TORRICO *et al.*, 2018).

Motivated by the simplicity and disturbance rejection benefits of Torrico *et al.* (2013), this work extends the advantages of this simplified approach to the dead-time compensation of state-space models. Similarly to Santos and Franklin (2018), several disturbance types can be directly treated, however, based on the Smith predictor approach, matched and unmatched disturbances are considered directly from the prediction error. The main advantage of this approach comes from design and implementation simplicity with guarantees of internal stability.

4.1.1 *Contribution*

The main contribution of this chapter comes from the extension of the SFSP to state-space models. This extension is useful since Artstein based predictors are internally stable, but disturbance rejection performance may be improved due to the combined effect of the additive disturbance and the prediction error. On the other hand, unmeasured disturbance effect appears directly in the predictor error in input-output approaches. Thus, disturbance rejection analysis and predictor design can be simplified in order to achieve an enhanced result. The key advantages are emphasized below:

- Simplified design with few tuning parameters through the FSP approach.
- FSA-based implementation, which provides internal stability for open-loop unstable process.
- Enhanced rejection of disturbances.

4.2 The FSA-based Smith predictor

Along the years, the Smith predictor and the FSA strategy have been explored as two distinct fields of research, so that most researchers on time-delay systems have dedicated to one of these two, but rarely on both. In this section, we show an equivalency between the two approaches.

4.2.1 SFSP - continuous-time approach

Several modifications of the FSP for open-loop unstable or integrative processes were proposed using a discrete-time approach in order to avoid internal instability problems. The simplified FSP proposed by Torrico *et al.* (2013), which is within this category, uses simple gains for the primary controller and the reference filter. Due to its simplicity, robustness, and noise attenuation characteristics, some derived structures (TORRICO *et al.*, 2016; TORRICO *et al.*, 2018) have presented enhanced results in the dead-time literature. Therefore, in this section, the continuous-time SFSP is presented and an internally stable FSA-based implementation structure is proposed for first-order plus dead time (FOPDT) models. The implementation structure of the SFSP is shown in Figure 26. Consider $P_n(s)$ the nominal process of $P(s)$ as

$$P_n(s) = \frac{k_p}{s-a}e^{-hs}, \tag{4.1}$$

where $a \neq 0$. For simplicity, the robustness filter is given by a first-order transfer function

$$V(s) = \frac{v_1 s + v_2}{s - \beta} \tag{4.2}$$

where β is the user tuning parameter. The following conditions to compute filter coefficients v_1

Figure 26 – SFSP implementation structure
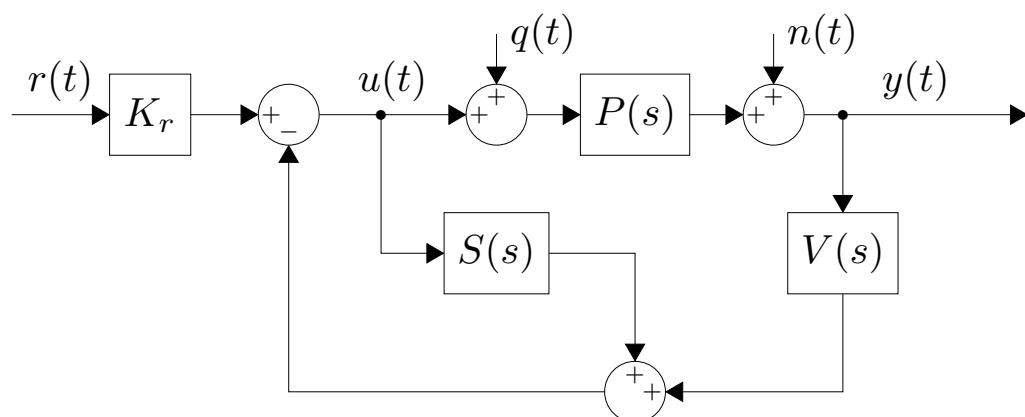
Source: The author.

and v_2 are derived from Torrico *et al.* (2013)

$$V(s)|_{s=0} = K_r, \tag{4.3}$$

$$\left.(K - V(s)e^{-hs})\right|_{s=a} = 0. \tag{4.4}$$

The solutions of (4.3) and (4.4) lead to

$$
\begin{aligned}
v_1 &= \frac{Kk_p(a-\beta)e^{ah}+(Kk_p-a)\beta}{a}, \\
v_2 &= \frac{a-Kk_p}{k_p}\beta.
\end{aligned} \tag{4.5}
$$

Note that, if it is desired to improve the noise attenuation properties then higher order of $V(s)$ can be used. Then, for implementation purposes, it is essential to define a $S(s)$ subsystem in order to avoid internal instability problems

$$S(s) = G_n(s)[K - V(s)e^{-hs}], \tag{4.6}$$

where $G_n(s)$ is the delay-free model of $P_n(s)$. Considering (4.1) and (4.2), and using partial fraction decomposition for the case where $a \neq \beta$, (4.6) can be rewritten as

$$S(s) = \overbrace{\frac{Kk_p}{s-a} - \frac{Kk_pe^{ah}}{s-a}e^{-hs}}^{S_1(s)} - \overbrace{\frac{\Phi}{s-\beta}}^{S_2(s)}e^{-hs}, \tag{4.7}$$

where $\Phi = \dfrac{\beta}{a}[a - Kk_p(e^{ah} - 1)]$.

4.2.2 Extension to state-space systems

The continuous-time representation of the $S_1(s)$ term in (4.7) is

$$S_1(t) = \int_{t-h}^{t} Ke^{a(t-\tau)}k_p u(\tau)d\tau, \tag{4.8}$$

where u is the control signal.

Note that the impulse response of (4.8) is given by

$$
h_{S_1}(t) = \begin{cases} Kk_pe^{at}, & 0 \leq t < h \\ 0, & \text{otherwise} \end{cases},
$$

which is an absolutely integrable function for any $a \in \mathbb{R}$, thus guaranteeing the stability of $S_1(t)$ for open-loop stable, unstable and integrative models. For the discrete-time case, (4.8) is equivalent to a finite impulse response (FIR) filter.

A state-space realization for system (4.1) is given by

$$P_n(s) \sim \left[\begin{array}{c|c} a & k_p \\ \hline 1 & 0 \end{array}\right] = \left[\begin{array}{c|c} \mathrm{A} & \mathrm{B} \\ \hline \mathrm{C} & \mathrm{D} \end{array}\right], \tag{4.9}$$

so that (4.8) becomes

$$S_1(t) = \int_{t-h}^{t} K e^{\mathrm{A}(t-\tau)} \mathrm{B} u(\tau) d\tau, \tag{4.10}$$

which is the matrix counterpart of (4.8) and is valid for systems of any order with the same guarantees of stability of (4.8). Furthermore, note that (4.10) is equivalent to the integral term of the FSA approach and can be implemented as such in Zhong (2004).

4.3   Problem statement

Consider a continuous-time LTI system described by the following nominal state equation

$$\dot{x}(t) = \mathrm{A}x(t) + \mathrm{B}(u(t-h) + w_m(t)) + \mathrm{B}_w w_u(t),$$
$$y(t) = \mathrm{C}x(t), \tag{4.11}$$

where $x(t) \in \mathbb{R}^n$ is the state vector, $u(t) \in \mathbb{R}^n$ is the control input, $y(t) \in \mathbb{R}^m$ is an arbitrary linear combination of the states, w_m and w_u are matched and unmatched disturbances, respectively. Matrices $\mathrm{A} \in \mathbb{R}^{n \times n}$, $\mathrm{B} \in \mathbb{R}^{n \times m}$, $\mathrm{C} \in \mathbb{R}^{m \times n}$ and delay $h > 0$ are all constant and known. Following assumptions are taken:

Assumption 4. *The pair* (A, B) *is controllable.*

Assumption 5. *The unknown disturbance signals are bounded by* $|w_u(t)| < D_u$, $|w_m(t)| < D_m$, *and are locally integrable.*

4.4   Proposal

The proposed control structure is illustrated in Figure 27. It is important to highlight that the proposed structure can overcome the limitation of the SFSP to only deal with FOPDT process. Note that for such strategy, the control law is given as sum of three terms

$$u(t) = u_1(t) - u_2(t) - u_3(t), \tag{4.12}$$

Figure 27 – Proposed structure
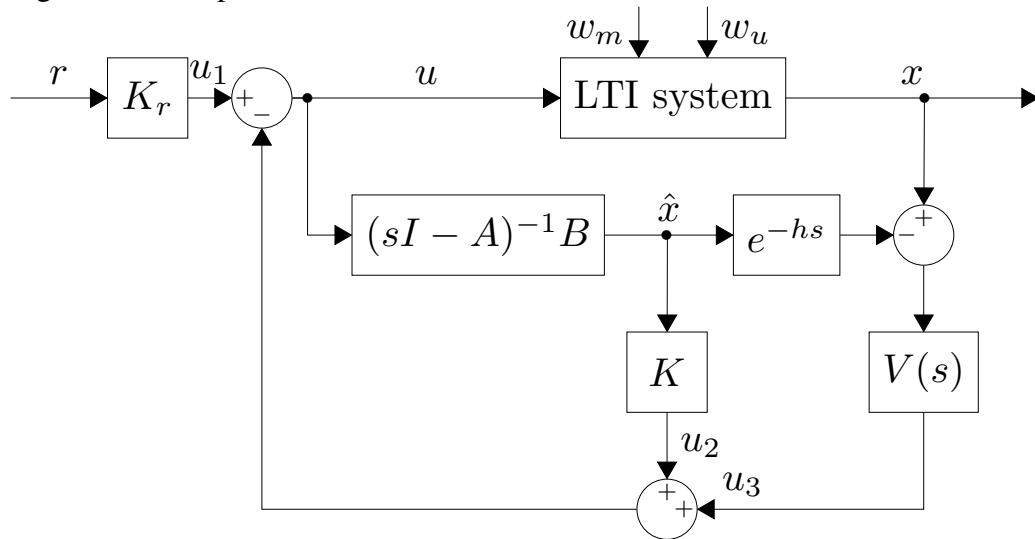
with

$$u_1(t) = \mathrm{K}_r r(t),$$

$$u_2(t) = \mathrm{K}\hat{x}(t), \tag{4.13}$$

$$u_3(t) = \mathscr{L}^{-1}\{\mathrm{V}(s)\mathscr{L}\{x(t) - \hat{x}(t-h)\}\},$$

where $\mathscr{L}$ denotes the unilateral Laplace transform and vector $\mathrm{K} \in \mathbb{R}^n$ is such that the matrix $(\mathrm{A} - \mathrm{BK})$ is Hurwitz. Note that, for the nominal case, with null disturbance signals $w_m(t) = 0$, $w_u(t) = 0$, it is true that $x(t) = \hat{x}(t-h)$, thus (4.12) reduces to the classical state feedback control law with reference tracking

$$u(t) = \mathrm{K}_r r(t) - \mathrm{K}\hat{x}(t), \tag{4.14}$$

where the time delay h is clearly compensated. The Laplace transform of the relation between the reference signals $r(t) \in \mathbb{R}^m$ and the output $y(t)$ is given by

$$H_r(s) = \mathrm{K}_r \mathrm{C}\Psi(s), \tag{4.15}$$

where $\Psi(s) = (s\mathrm{I} - \mathrm{A} + \mathrm{BK})^{-1}\mathrm{B}e^{-hs}$. Therefore, the reference static gain $\mathrm{K}_r \in \mathbb{R}^{m \times m}$ can be calculated in order assure reference tracking at steady-state, leading to

$$\mathrm{K}_r = \left[\mathrm{C}(\mathrm{BK} - \mathrm{A})^{-1}\mathrm{B}\right]^{-1}. \tag{4.16}$$

It is clear then that signal $u_3(t)$ should be calculated in order to compensate the unknown disturbances. Note that the Laplace transform of the relation between $w_u(t)$, $w_m(t)$ and

the plant output $y(t)$ is given by

$$H_u(s) = [I - V(s)\Psi(s)]C(sI - A)^{-1}B_w,$$

(4.17)

$$H_m(s) = [I - V(s)\Psi(s)]C(sI - A)^{-1}B,$$

respectively. From (4.17) note that $V(s)$ can be tuned in order to guarantee rejection of distur-
bances. Then, from the equivalent analysis structure in Figure 28, note that in order to obtain
integral action in $C_{eq}(s) = (I + S(s))^{-1}$, with $S(s) = K(sI - A)^{-1}B - V(sI - A)^{-1}Be^{-hs}$, the
following condition must hold

$$S(s)|_{s=0} = -I = (V(0) - K)A^{-1}B.$$

(4.18)

From (4.18) and (4.16), one has that

$$V(0) = K_r C.$$

(4.19)

Figure 28 – Analysis structure
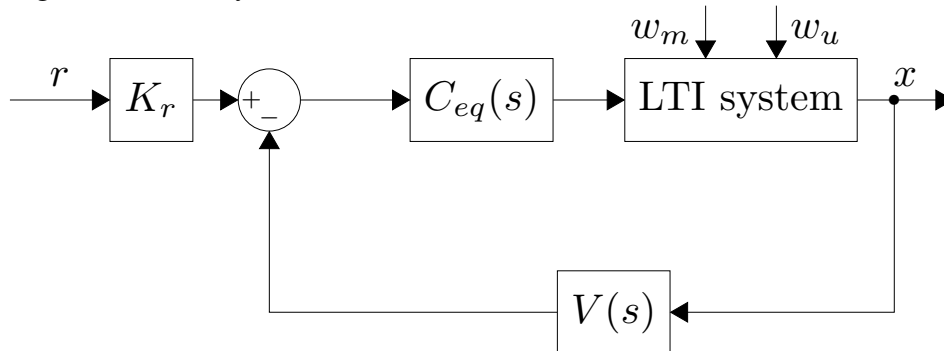
Source: The author.

Condition (4.18) is enough to guarantee rejection of step like matched disturbances
for the controlled states. For rejection of matched sinusoidal disturbances, condition (4.18) must
be expanded to

$$S(s)|_{s=\{0,j\omega,-j\omega\}} = -I,$$

(4.20)

where ω is the frequency of the sinusoidal disturbance wave. Filter $V(s)$ is also used to eliminate
the process dynamics from the disturbance rejection response (4.17). This is translated into the
following equation

$$[I - V(s)\Psi(s)]_{s=\lambda_i \neq 0} = 0,$$

$$\text{for } i = 1, \ldots, p,$$

(4.21)

where λ_i are the p eigenvalues of A. Without loss of generality, let us give some illustrating options for the choice of $V(s)$. Initially, suppose a system with $n = 2$, $m = 1$, and output equal to state x_1. For the rejection of step-like disturbances, we propose the following filter $V(s)$

$$\begin{bmatrix} \dfrac{b_{11}s + b_{12}}{\tau s + 1} & \dfrac{b_{13}s}{\tau s + 1} \end{bmatrix}, \tag{4.22}$$

where τ is the filter tuning parameter. For the case of sinusoidal disturbances, the following format must be used for the filter computation

$$\begin{bmatrix} \dfrac{b_{11}s^3 + b_{12}s^2 + b_{13}s + b_{14}}{(\tau s + 1)^3} & \dfrac{b_{15}(s^2 + \omega^2)s}{(\tau s + 1)^3} \end{bmatrix}. \tag{4.23}$$

This filter format illustrates the simplicity of the proposed strategy. If it is desired to speed up the disturbance rejection response time, smaller values of τ can be chosen, and *vice-versa*.

4.4.1 Robustness analysis

Considering an additive uncertainty

$$P(s) = P_n(s) + \Delta P(s), \tag{4.24}$$

where $\Delta P(s) = W_2(s)\Delta(s)W_1(s)$, $\|\Delta(s)\|_\infty < 1$. The controller structure from Figure 27 can be represented in the $M - \Delta$ form as in Figure 29, where

$$M(s) = W_1(s)M'(s)W_2(s),$$
$$M'(s) = \left[K(sI - A + BK)^{-1}B - I \right] V(s).$$

Then, robust closed-loop stability is given by

$$\bar{\sigma}(\Delta(s)) < \frac{1}{\bar{\sigma}(M(s))}, \tag{4.25}$$

where $\bar{\sigma}(\cdot)$ is the maximum singular value function. Note that (4.25) depends on adjustable controller parts K and $V(s)$. However, K must be prior adjusted for the set-point tracking response (4.15). Therefore, $V(s)$ is left as a valuable option to adjust desired robustness to the closed-loop system. This is done by proper choice of the filter poles τ. Higher values of τ yield enhanced overall robustness to the system, whereas smaller values can be used to speed up disturbance rejection response. This illustrates a trade-off which has to be taken into account when tuning the robustness filter $V(s)$.

Figure 29 – M − Δ structure
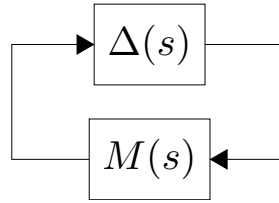
Source: The author.

4.4.2 Effect of the measurement noise

Any feedback control system is affected by measurement noise, which usually occurs at high frequencies. Especially for industrial applications, it is important that the control signal be the least affected as possible by measurement noise. Some common problems could occur in the control loop due to noise amplification in the control signal, such as saturation of the control signal, which could yield undesired windup problems. In order to avoid impaired performance due to such condition, some guidelines can be followed.

Initially, it is important to understand how noise affects the system. For the proposed strategy, noise enters the control loop in the term $u_3(t)$ such that the measured states are given by $x_m(t) = x(t) + n(t)$, where $n(t)$ is the measurement noise. By replacing $x(t)$ by $x_m(t)$ in (4.13), $u_3(t)$ becomes

$$u_3(t) = \mathcal{L}^{-1}\{V(s)\mathcal{L}\{x(t) + n(t) - \hat{x}(t-h)\}\}.$$

It is important to obtain the relationship between the noise $n(t)$ and control signal $u(t)$, which is given in the frequency domain by

$$H_n(\omega) = \bar{\sigma}\left(\left[K(sI-A)^{-1}B + I\right]^{-1}V(s)\right)\Big|_{s=j\omega}. \tag{4.26}$$

Therefore, note that $V(s)$ also plays an essential role at noise attenuation characteristic of the proposed controller. From (4.26), note that in order to mitigate undesired effects, $V(s)$ must present low gain for $\omega \to \infty$. This elucidates a trade-off between noise attenuation and disturbance rejection, e.g. for $\tau \to \infty$ should yield perfect noise attenuation, while $\tau \to 0$ yields faster disturbance rejection.

4.5 Implementation Issues

4.5.1 Continuous-time implementation

The proposed structure in Figure 27 can be directly implemented for the case of open-loop stable plants. However, for non Hurwitz open-loop systems, the structure in Figure 30 must be used in order to ensure internal stability. The subsystem $S_1(s)$ in Figure 30 is given by

$$S_1(s) = K \left(I - e^{-(sI-A)h} \right) (sI - A)^{-1} B, \tag{4.27}$$

which can be implemented in a similar fashion to (4.10). For more details on the implementation of (4.27) one can see (ZHONG, 2004).

Figure 30 – Implementation structure
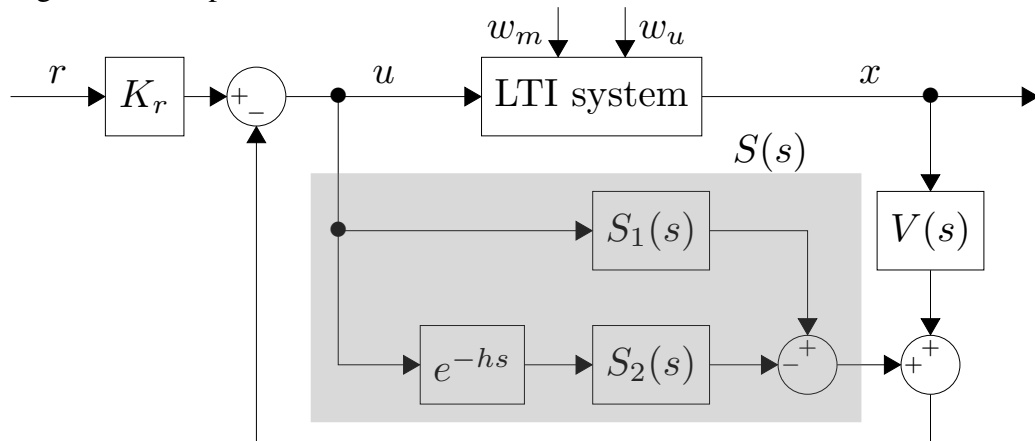
Source: The author.

The subsystem $S_2(s)$ is defined as

$$S_2(s) = \Xi \left(\left(V(s) - K e^{Ah} \right) G_n(s) \right), \tag{4.28}$$

where $\Xi(\cdot)$ is the minimal state-space realization for a LTI system. Although $S_2(s)$ depends on $G_n(s)$, the poles of $G_n(s)$ are not part of it, thus no instability issues are presented. This is better formulated in the following proposition.

Proposition 1. *If the condition* (4.21) *is satisfied, then $S_2(s)$ is stable for open-loop unstable process.*

Proof. Consider the following assumption

Assumption 6. *If the minimal representation of a LTI system $\Gamma(s)$ is finite valued at $\Gamma(\gamma)$, then γ is not an eigenvalue of the state matrix of the state-space realization of $\Gamma(s)$.*

Now, consider that λ_i are the eigenvalues of matrix A. From (4.21), one can find that

$$V(\lambda_i) = \mathrm{B}^{-1}(\lambda_i \mathrm{I} - \mathrm{A} + \mathrm{BK})e^{h\lambda_i}. \tag{4.29}$$

By substitution of (4.29) into (4.28), it follows that

$$S_2(\lambda_i) = e^{h\lambda_i} + \mathrm{K}\left(e^{h\lambda_i} - e^{h\mathrm{A}}\right)(\lambda_i \mathrm{I} - \mathrm{A})^{-1}\mathrm{B}. \tag{4.30}$$

From the Taylor series expansion

$$\begin{cases} e^{h\lambda_i} & = \mathrm{I} + \sum_{n=1}^{\infty} \frac{h^n(\lambda_i \mathrm{I})^n}{n!}, \\[2mm] e^{h\mathrm{A}} & = \mathrm{I} + \sum_{n=1}^{\infty} \frac{h^n \mathrm{A}^n}{n!}, \end{cases}$$

then

$$e^{h\lambda_i} - e^{h\mathrm{A}} = \sum_{n=1}^{\infty} \frac{h^n(\lambda_i \mathrm{I} - \mathrm{A})^n}{n!}.$$

This way, the term $(e^{h\lambda_i} - e^{h\mathrm{A}})(\lambda_i \mathrm{I} - \mathrm{A})^{-1}$ in (4.30) can be rewritten as

$$\sum_{n=1}^{\infty} \frac{h^n(\lambda_i \mathrm{I} - \mathrm{A})^{n-1}}{n!},$$

leading to

$$S_2(\lambda_i) = e^{h\lambda_i} + \mathrm{K}\left(\sum_{n=1}^{\infty} \frac{h^n(\lambda_i \mathrm{I} - \mathrm{A})^{n-1}}{n!}\right)\mathrm{B}. \tag{4.31}$$

Note that the singular term $(\lambda_i \mathrm{I} - \mathrm{A})^{-1}$ of (4.30) was canceled in (4.31), thus $S_2(\lambda_i)$ is finite valued, so that by means of **Assumption 6**, λ_i is not an eigenvalue of the state matrix of the minimal state-space realization of $S_2(\lambda_i)$, thus the proof is completed. $\square$

4.5.2 Discrete-time implementation

Consider the discretized model of (4.11)

$$\begin{aligned} x(k+1) &= \mathrm{A_d}x(k) + \mathrm{B_d}(u(k-d) + w_m(k)) + B_{d_w}w_u(k), \\ y(k) &= \mathrm{C_d}x(k), \end{aligned} \tag{4.32}$$

obtained for a sampling time $T_s > 0$ such that $d = h/T_s$ is an integer. In order to obtain a pure full discrete-time implementation some steps must be followed. **1.)** Design a vector $\mathrm{K} \in \mathbb{R}^n$ such that

the matrix $A_d - B_d K$ is Schur stable. **2.)** Find $K_r = \left[C_d (I + B_d K - A_d)^{-1} B_d \right]^{-1}$ in order to ensure set-point tracking at steady-state. **3.)** For the design of a discrete-time disturbance filter $V(z)$, consider $S(z) = K(zI - A_d)^{-1} B_d - V(zI - A_d)^{-1} B_d z^{-d}$ and make $S(z_i) = -I|_{z_i = \{1, e^{T_s j\omega}, e^{-T_s j\omega}\}}$. Also consider the ϕ_i eigenvalues of A_d and make sure that

$$[I - V(z)\Psi(z)]_{z=\phi_i \neq 1} = 0, \tag{4.33}$$
$$\text{for } i = 1, \dots p,$$

where $\Psi(z) = (zI - A_d + B_d K)^{-1} B_d z^{-d}$.

4.6 Simulation results

Case 1 - Benchmark problem

This subsection presents a study case of a benchmark problem which has been proposed by Léchappé *et al.* (2015) and used for comparison in Santos and Franklin (2018), Sanz *et al.* (2016). The model of the aforementioned works is an open-loop unstable LTI system with input delay:

$$\dot{x}(t) = \begin{bmatrix} 0 & 1 \\ -9 & 3 \end{bmatrix} x(t) + \begin{bmatrix} 0 \\ 1 \end{bmatrix} (u(t-h) + w_m(t)) + \begin{bmatrix} 1 \\ 1 \end{bmatrix} w_u(t). \tag{4.34}$$

As in Léchappé *et al.* (2015), Santos and Franklin (2018), Sanz *et al.* (2016) the state feedback control action considering no disturbances or delay is defined with $u(t) = \begin{bmatrix} 45 & 18 \end{bmatrix} x(t)$. In addition, for the chosen output $y(t) = \begin{bmatrix} 1 & 0 \end{bmatrix} x(t)$, the static gain $K_r = 54$ is obtained to yield zero set-point tracking error in steady-state.

Simulations are performed for both constant and sinusoidal disturbances.

Constant disturbances

For this example, $V(s)$ is calculated using (4.18) and (4.21). Two different tuning for the disturbance rejection filters with $\tau = 0.5$ and $\tau = 0.1$ have been considered, yielding respectively

$$V(s) = \begin{bmatrix} \dfrac{-80.06s + 54}{0.5s + 1} & \dfrac{56.55s}{0.5s + 1} \end{bmatrix}, \tag{4.35}$$

and

$$V(s) = \begin{bmatrix} \dfrac{-18.24s + 54}{0.1s + 1} & \dfrac{29.85s}{0.1s + 1} \end{bmatrix}. \tag{4.36}$$

For practical implementation purpose the values of $S_2(s)$ for $\tau = 0.5$ and $\tau = 0.1$ are

$$S_2(s) = \frac{23.174}{0.5s + 1} \tag{4.37}$$

and

$$S_2(s) = \frac{23.174}{0.1s + 1} \tag{4.38}$$

respectively, which confirms the results from **Proposition 1**. In this example, comparison against the strategies from Léchappé *et al.* (2015) and Santos and Franklin (2018) is presented. Simulation results are shown in Figure 31 where unit-step matched and unmatched disturbances are applied at $t = 5$ s and $t = 15$ s, respectively.

Figure 31 – Output response: step-like disturbance
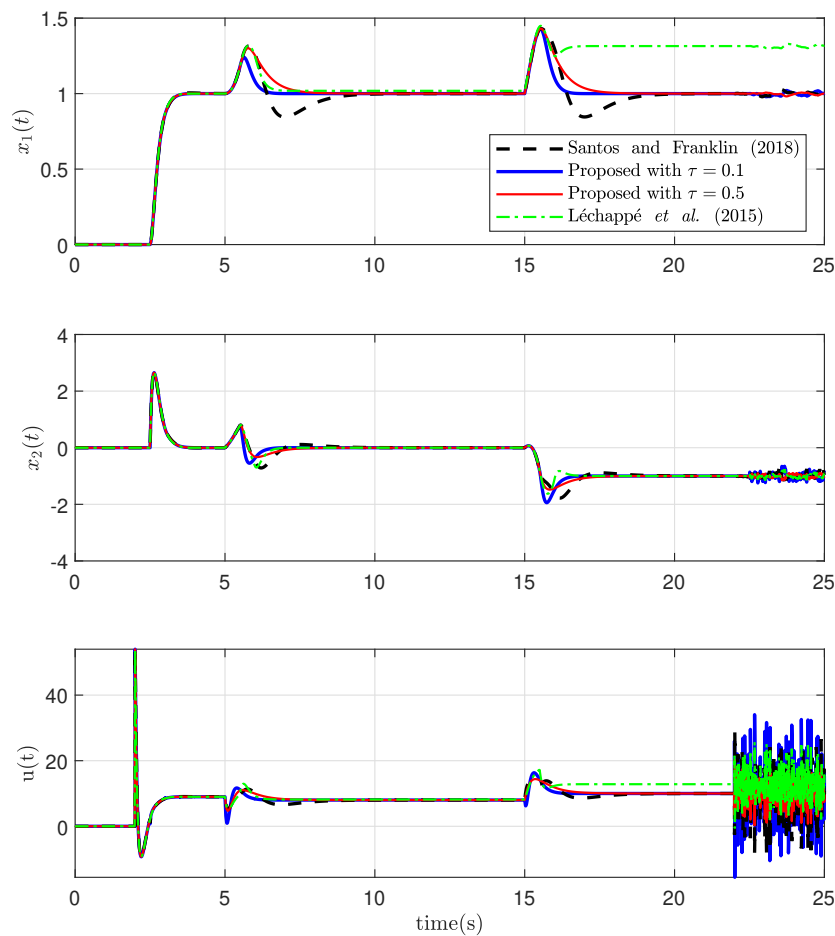
Source: The author.

Note from Figure 31 that for the filter adjusted with $\tau = 0.5$, which is the same time constant used for the filter of the compared strategy in Santos and Franklin (2018), the proposed controller was able to achieve faster rejection of both disturbances. Additionally, on contrary to Santos and Franklin (2018), no undershoots appear in the response for the output state $x_1(t)$. Furthermore, as expected, the response for the filter adjusted with $\tau = 0.1$ presents the overall fastest rejection of the disturbances, while undershoots are still avoided. In order to further evaluate the proposed control system characteristics, white noise with zero mean and variance $\sigma^2 = 0.005$ has been added in the last three seconds of simulation. As a measure of performance, the variance of the control signal has been calculated. Note that for the filter adjusted with $\tau = 0.5$ the noise has been the least amplified in the control signal, with variance $\sigma^2 = 13.1$. For the compared strategy in Santos and Franklin (2018), the calculated calculated variance was $\sigma^2 = 45.6$, which further illustrates the advantages of the proposed strategy. As expected, the system with $\tau = 0.1$ has presented the highest variance value with $\sigma^2 = 79.2$, which confirms the aforementioned trade-off between noise attenuation and disturbance rejection from Subsection 4.4.2. When better noise attenuation is required, higher order filters can be used. Analysis of this condition has been further studied in Torrico *et al.* (2018). It is fair to mention that Santos and Franklin (2018) were concerned only with the disturbance rejection and they did not present any qualitative comparison with other strategies.

Sinusoidal disturbances

Consider now, similarly to Santos and Franklin (2018), the case with $w_m(t) = 0$ and $w_u(t) = (0.5 + sin(t))(t - 10)$. For this scenario, the disturbance filter is adjusted with $\tau = 0.3$. By using (4.20), (4.21) and (4.28), following filter V(s) and subsystem $S_2(s)$ are obtained as

$$\text{V}(s) = \left[\frac{3.73s^3 + 58.97s^2 + 66.22s + 54}{(0.3s + 1)^3} \quad \frac{12.88(s^3 + s)}{(0.3s + 1)^3} \right], \tag{4.39}$$

and

$$\text{S}_2(s) = \frac{11.08s^2 + 23.12s + 23.17}{(0.3s + 1)^3}, \tag{4.40}$$

respectively. Since the approach of Santos and Franklin (2018) already presented improved performance compared to previous works, such as the one in Léchappé *et al.* (2015), it will be the only strategy considered for comparison from now on. From Figure 32 the proposed controller was once again able to achieve better disturbance rejection characteristics, with smaller overshot,

undershoot and response time for output state $x_1(t)$. For state $x_2(t)$, similar response has been achieved.

Figure 32 – Output response: sinusoidal disturbance
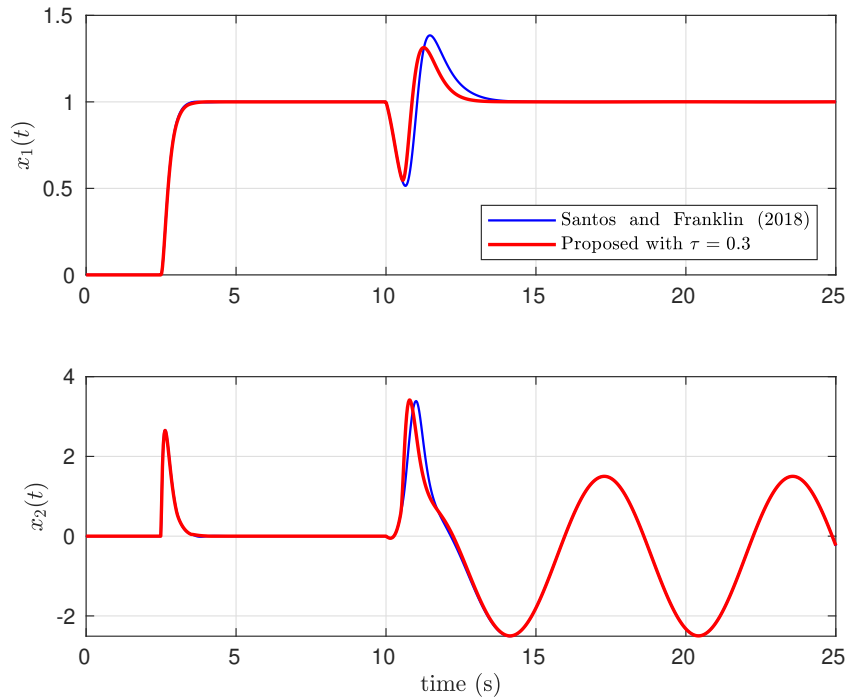
Source: The author.

Case 2 - DC-DC boost converter

Consider now the DC-DC boost converter presented in Santos and Franklin (2018), with average non-linear model given by

$$\dot{\xi}(t) = \begin{bmatrix} -(1 - u(t-h))\frac{\xi_2(t)}{L} + \frac{V_s(t)}{L} \\ (1 - u(t-h))\frac{\xi_1(t)}{C} - \frac{\xi_2(t)}{RC} \end{bmatrix}, \tag{4.41}$$

where $\xi(t) = \begin{bmatrix} I(t) & V_o(t) \end{bmatrix}'$, $I(t)$ is the inductor current, $V_o(t)$ represents the capacitor voltage, $u(t)$ is the duty-cycle, $L = 500 \times 10^{-6}$ H, $C = 200 \times 10^{-6}$ F, $R = (24)^2/100$ Ω, and $V_s = 20$ V. As in Santos and Franklin (2018), the linearized model was obtained considering $x_1(t) = \xi_1(t) - I^*$ and $x_2(t) = \xi_2(t) - V_o^*$, where $V_o^* = 24$ V is the desired equilibrium output voltage, $I^* = (V_o^*)^2/(V_s^*R)$, yielding $u^* = 1 - (V_o^*/I^*)/(R)$. This way, the linearized model is given by

$$\dot{x}(t) = \begin{bmatrix} 0 & -\frac{1-u^*}{L} \\ \frac{1-u^*}{C} & -\frac{1}{RC} \end{bmatrix} x(t) + \begin{bmatrix} \frac{V_0^*}{L} \\ -\frac{I^*}{C} \end{bmatrix} (u(t-h) - u^*), \tag{4.42}$$

where $h = 10$ ms. This DC-DC boost converter model was obtained based on automotive applications.

Considering the discrete-time implementation of the proposed controller in sub-section 4.5.2, $K = \begin{bmatrix} -0.1336 & 0.0230 \end{bmatrix}$ was obtained by classical pole placement in order to speedup the disturbance rejection, yielding $K_r = 0.0020$ and the following robustness filter $V(z)$

$$V(z) = \begin{bmatrix} \dfrac{0.00080(z-1)}{z-0.95} & \dfrac{0.00099(z-0.8963)}{z-0.95} \end{bmatrix}.$$

Figure Figure 33 shows the response when considering the average non-linear model (4.41) in the simulations. Similarly to Santos and Franklin (2018), the voltage source V_s was varied from 20 to 16 V at 0.05 s as a way of introducing unmatched disturbances. Note that in this scenario, the proposed controller achieved faster rejection of the disturbance.

Figure 34 shows the response for a similar scenario, however this time the DC-DC boost converter was simulated within Matlab/Simulink using inductors, capacitors, diodes, mosfets and voltage sources in order to evaluate the proposed controller under the uncertainties of caused by these components. Once again the proposed controller presented better results.

Figure 33 – Output response: DC-DC boost converter with average non-linear model
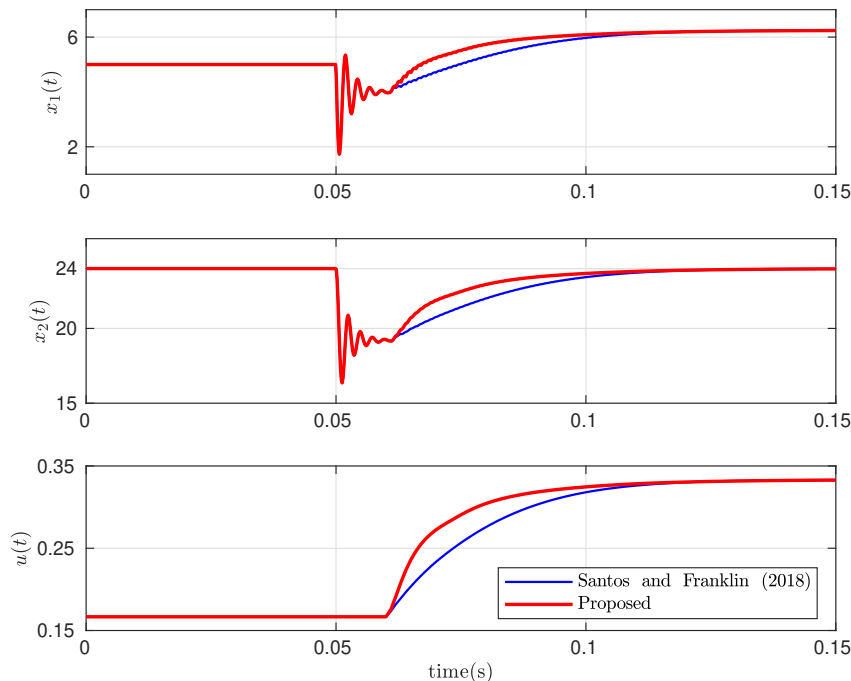
Source: The author.

Figure 34 – Output response: DC-DC boost converter with non-linear switching model
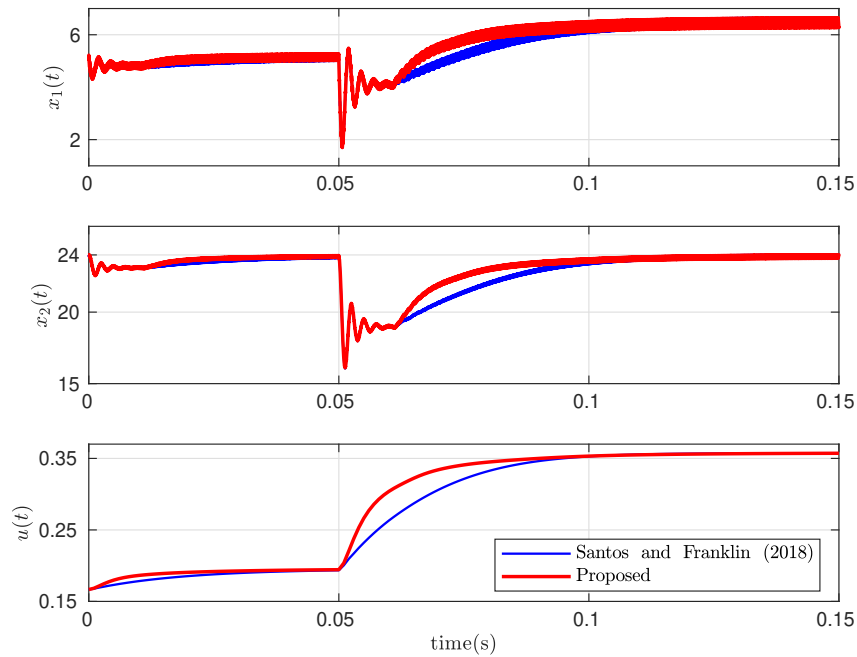
Source: The author.

Table 2 – Output MSE and control variance for simulation cases

Case 1 - constant disturbance						Case 1 - sinusoidal disturbance	
Output signal MSE			Control signal variance			Output signal MSE	
$\tau = 0.1$	$\tau = 0.5$	Santos and Franklin (2018)	$\tau = 0.1$	$\tau = 0.5$	Santos and Franklin (2018)	$\tau = 0.3$	Santos and Franklin (2018)
0.0323	0.0354	0.0366	20.1248	13.8333	17.1079	0.0338	0.0481

Case 2 - average non-linear model				Case 2 - non-linear switching model			
Output signal MSE		Control signal variance		Output signal MSE		Control signal variance	
Proposed	Santos and Franklin (2018)	Proposed	Santos and Franklin (2018)	Proposed	Santos and Franklin (2018)	Proposed	Santos and Franklin (2018)
2.6811	3.3991	0.0058	0.0055	3.0131	3.8542	0.0058	0.0059

Table 2 summarizes the results for the simulations cases. The mean squared error (MSE) of the output signal and the control signal variance were calculated. In most scenarios, the proposed controller presents better results.

4.7 Experimental results

In order to evaluate the proposed controller in a practical situation, the control of the internal temperature of a neonatal intensive care unit (NICU) was carried out. The NICU, shown

Figure 35 – Neonatal intensive care unit (NICU)

Source: The author.

in Figure 35, has been identified as

$$
\dot{x}(t) = \begin{bmatrix} -0.11206 & 1 \\ -0.00120 & 0 \end{bmatrix} x(t) + \begin{bmatrix} 0 \\ 0.00027 \end{bmatrix} u(t-6.29),
$$

$$
y(t) = \begin{bmatrix} 1 & 0 \end{bmatrix} x(t),
$$

(4.43)

where the time is measured in minutes and the control is constrained within the range from 0 to 100 % as it is the current flowing through a heating resistor, which is limited by its maximum power.

The following discrete-time model was obtained for a sampling time of $T = 0.2$ min

$$
x(k+1) = \begin{bmatrix} 0.97781 & 0.19777 \\ -0.00023 & 0.99997 \end{bmatrix} x(k) + \begin{bmatrix} 5.5 \times 10^{-6} \\ 5.54 \times 10^{-5} \end{bmatrix} u(k-31),
$$

$$
y(k) = \begin{bmatrix} 1 & 0 \end{bmatrix} x(k).
$$

(4.44)

The state feedback gain was designed as $K = \begin{bmatrix} -2.87 & 231.04 \end{bmatrix}$, the static gain was calculated as $K_r = 27.37$, and the following $V(z)$ was obtained considering a second-order filter with poles $\beta = 0.98$

$$
V(z) = \begin{bmatrix} \dfrac{90.85z^2 - 179.4z + 88.51}{(z-0.98)^2} & 0 \end{bmatrix}.
$$

Figure 36 shows the results for a step change on the temperature set-point from 22.1°C to 28°C. The portholes remained opened from t = 85 min to t = 95 min in order to insert disturbances in the system and assess controller robustness. As the acrylic dome does not provide

a good level of thermal isolation between the internal and external environment, the external temperature, which was kept around 19°C, can also be considered as an unmodeled disturbance.

Note that the temperature reaches the desired set-point without oscillations or over-shoot. Even when the disturbance was applied by opening the portholes, the controlled variable smoothly reached the set-point again.

Figure 36 – Experimental results
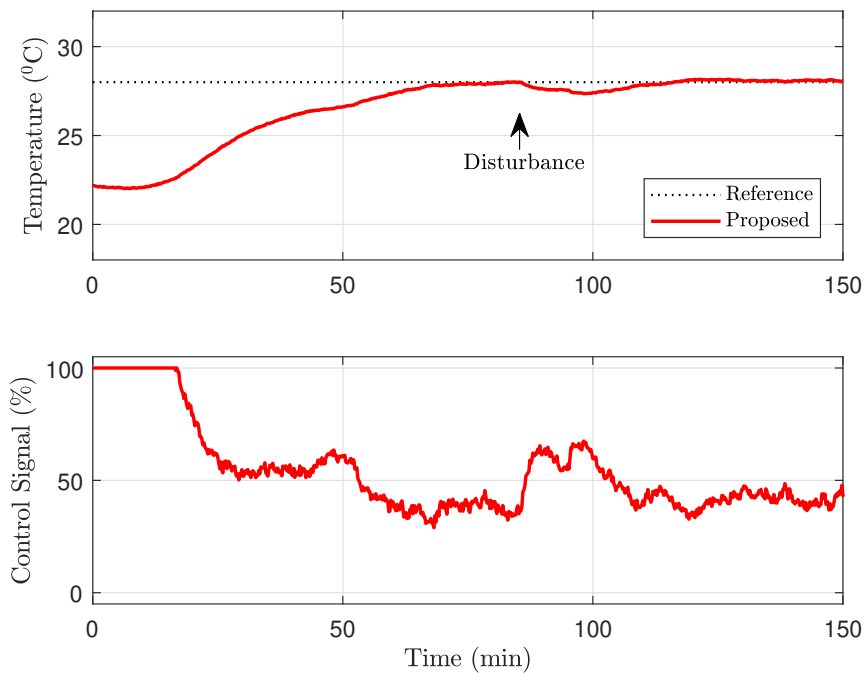
Source: The author.

4.8 Discussion

A new dead-time compensator with enhanced performance has been proposed for LTI systems with input delay. The main advantage of the proposed strategy is that the robustness filter can be designed directly to deal with both matched and unmatched unknown disturbances. Thus, design and implementation are conceptually equivalent to that of a simplified DTC based on the filtered Smith predictor. Furthermore, implementation is realized by means of an integral term equivalent to the FSA, which facilitated the extension of the strategy to state-space systems and avoided the undesirable pole-zero cancellation effects of others strategies based on the FSP. The simulation case study effectively assured that the proposed controller presents better disturbance rejection performance when compared to the tuning presented in a recent strategy based on the Artstein predictor with two-layer feedforward (SANTOS; FRANKLIN, 2018).

The good results and simplicity show a great potential for further extensions, as for the case of systems with both state and input delays. Another challenging study cases would be the control of integrative systems, which would require a modification in the robustness filter computation condition (4.21). The control of non-squared systems, such as when there are more inputs than outputs, also fall within the scope of desired future work cases.

5 THE MULTIPLE DELAY MIMO CASE

This chapter proposes a control structure based on generalized predictive control (GPC) able to deal with SISO/MIMO dead-time processes under a unified framework. An equivalent dead-time compensator structure is presented in order to analyze the controller properties, such as set-point tracking, robustness and disturbance rejection. From the equivalent structure, a set of simple tuning rules are derived. Such rules employ a reduced number of parameters which facilitates the tuning of the controller, especially for the case of MIMO processes. Simulation results show the enhanced performance of the proposed strategy when compared with other recent SISO and MIMO literature examples. An experiment was performed to show the effectiveness of the proposed strategy on the temperature and humidity control of an in-house thermal chamber.

5.1 Introduction

Many industrial processes exhibit input and/or output time delays, also known in the control community as dead-times. In some cases, the dead-time is much smaller than the time constant of the process to be controlled. In this case, a PID controller should be able to stabilize the closed-loop since the dead-time is non-dominant. On the other hand, the difficult in controlling such systems with classical control rules increases as the delay becomes bigger (NORMEY-RICO; CAMACHO, 2007). A dead-time compensator (DTC) structure may then be required.

Within this context, Smith proposed in 1957 a control structure able to properly compensate the dead-time, which is well known as the Smith predictor (SP) (SMITH, 1957). Although it became a seminal work in the control community, some drawbacks of the proposal were evident. Its inability to deal with open-loop unstable plants and steady-state errors caused by disturbances in the case of integrating processes are two of the main weaknesses of the original proposal (NORMEY-RICO; CAMACHO, 2007). Later, the Finite Spectrum Assignment (FSA) (KWON; PEARSON, 1980) and the model reduction (ARTSTEIN, 1982) approaches overcame such issues.

However, problems related to numerical instability on the FSA implementation were only definitively solved much later by (ZHONG, 2004). This issue motivated the search for solutions using SP derived structures, currently known as DTCs. (WATANABE; ITO, 1981)

proposed a modified fast model in the SP in order to improve the disturbance rejection and to control integrative and unstable processes. A modified Smith predictor (MSP) structure was proposed for integrating plants (MATAUŠEK; MICIĆ, 1996) with its extension for open-loop unstable systems in (MATAUŠEK; RIBIĆ, 2012). Another approach, namely filtered SP (FSP), based on the inclusion of a robustness filter in the feedback path showed itself to be an adequate choice to improve robustness (NORMEY-RICO *et al.*, 1997; NORMEY-RICO; CAMACHO, 2009). A dead-time compensator for stable and integrating processes considering a reduced model of the process was proposed in (GARCÍA; ALBERTOS, 2008). A general structure for long dead-time systems shown to be equivalent to the Smith predictor has been proposed in (GARCÍA; ALBERTOS, 2013).

Recently, the control community has spent great effort to enhance critical characteristics in the control of dead-time processes, such as robustness, disturbance rejection, and noise attenuation (TORRICO *et al.*, 2013; NORMEY-RICO *et al.*, 2014; TORRICO *et al.*, 2016; SANZ *et al.*, 2018; TORRICO *et al.*, 2018; LIU *et al.*, 2018a; LIU *et al.*, 2018b).

Majority of the aforementioned works were developed for the special case of single-input single-output (SISO) systems; nevertheless, improved solutions for the control of multivariable plants, which may present additional issues such as loop coupling and different dead-times for each input/output, also deserve attention. With this aim, a generalized structure of the filtered Smith predictor was extended for MIMO square processes in (FLESCH *et al.*, 2011). Additionally, a control procedure able to cope with both multiple delays and unstable MIMO systems was studied in (GARCÍA; ALBERTOS, 2010).

Additional issues to deal with MIMO systems may appear if the number of inputs and outputs is different, emerging non-square models. For such cases, the work in Flesch *et al.* (2011) was later extended for non-square plants and multiple delays in Flesch *et al.* (2012) and Santos *et al.* (2014). An extension of the simplified tuning rules presented in Torrico *et al.* (2016) for MIMO systems and capable of dealing with non-square models is presented in Santos *et al.* (2016). An inverted decoupling structure is proposed in Luan *et al.* (2017) which highlights that to control a non-square plant with time delays may be a complex issue.

On the other hand, Model-based Predictive Control (MPC) is pointed out as a natural choice for practical applications to deal with SISO and MIMO time-delayed (GIRALDO *et al.*, 2018) and delay-free (TORRICO *et al.*, 2014; SILVA *et al.*, 2017) processes. Although some works have approached dead-time systems with a state space GPC formulation (WANG, 2009;

ROSSITER, 2003), the problem of long dead times has not been robustly approached. This is probably due to two reasons: (i) It has been enhanced in the literature that the GPC controller is highly dependent on an accurate model, mainly for long dead-time processes, which may provoke lack of robustness when there is model mismatch (GIRALDO *et al.*, 2018; PAWLOWSKI *et al.*, 2017); (ii) There is a previously reported relation between closed-loop robustness impairment as the process dead-time increases (NORMEY-RICO; CAMACHO, 2007; NORMEY-RICO; CAMACHO, 2000a).

Another barrier in the use of the GPC is that the complexity of the tuning can grow proportionally to the complexity of the system to be controlled (especially in the MIMO case), which leads to non-intuitive tuning rules (WANG *et al.*, 2019). The work in (NORMEY-RICO; CAMACHO, 2000b) has been one of the first to consider the robust design of the generalized predictive controller (GPC) for processes with time delay. However, the approach was not developed on state-space equations but rather on Diophantine equations, which may complicate analysis and tuning for the MIMO case.

5.1.1 Contribution

This work proposes a general approach for controlling SISO/MIMO dead-time processes using the GPC. The approach employs state-space models for prediction while the control structure is in an observer-based form with two feedback gains, which implies the simplicity of the approach. Furthermore, an equivalent dead-time compensator structure for analysis purposes is presented, which yield some advantages over previously proposed strategies:

- A unified framework for the control of SISO/MIMO square/non-square processes with dead time. The controller order of the proposed implementation structure is equivalent to that one of dead-time compensators.
- A simplified tuning approach is proposed for the GPC-based strategy. In the proposed strategy, the number of tuning parameters is reduced to three and can be chosen by intuitive rules.
- Such nice obtained tuning rules yield enhanced set-point tracking, robustness, and disturbance rejection properties when compared to recently proposed DTC structures for the control of dead-time processes. Furthermore, results have shown that the effect of coupling between the process variables is reduced in the proposed strategy.

5.2 Proposed GPC based control structure

5.2.1 Model for prediction

Without loss of generality, this paper considers processes with m inputs and n outputs, where $m \geq n$. The $i-$th output $y_i(k)$ can be represented by a CARIMA model:

$$A_i y_i(k) = B_{i,1}\Delta u_1(k - d_{i,1}) + \ldots + B_{i,m}\Delta u_m(k - d_{i,m}) + C_i e_i(k), \tag{5.1}$$

where $u_j(k)$ is the $j-$th input, d_j is the delay associated with each input, $e_i(k)$ is a white noise with zero mean,

$$
\begin{aligned}
A_i &= 1 + a_{i,1}q^{-1} + \ldots + a_{i,n_{a_i}}q^{-n_{a_i}}, \\
B_{ij} &= b_{ij,1}q^{-1} + \ldots + b_{ij,n_{b_i}}q^{-n_{b_i}}, \\
C_i &= 1 + c_{i,1}q^{-1} + \ldots + c_{i,n_{c_i}}q^{-n_{c_i}}, \\
\Delta &= 1 - q^{-1},
\end{aligned}
$$

and q^{-1} is the backward shift operator.

For simplicity, from this point on, the following nomenclature is adopted for the time dependent variables $y_{i_k} \leftarrow y_i(k)$, $\Delta u_{j_k} \leftarrow \Delta u_j(k)$, and $e_{i_k} \leftarrow e_i(k)$. The CARIMA model from (5.1) can be written as a state space representation for each output in observable canonical form

$$
\begin{aligned}
x_{i_{k+1}} &= \mathrm{A}_i x_{i_k} + \mathrm{B}_{i,1}\Delta u_{i_k} + \ldots + \mathrm{B}_{i,m}\Delta u_{m_k} + \mathrm{D}_i e_{i_k} \\
y_{i_k} &= \mathrm{H}_i x_{i_k} + e_{i_k}
\end{aligned}, \tag{5.2}
$$

where

$$
\mathrm{A}_i = \begin{bmatrix}
-a_{i,1} & 1 & 0 & \ldots & 0 \\
-a_{i,2} & 0 & 1 & \ldots & 0 \\
\vdots & \vdots & \vdots & \ddots & \vdots \\
& & & & 1 \\
-a_{i,p_i} & 0 & 0 & \ldots & 0 \\
0 & 0 & 0 & \ldots & 0 \\
\vdots & \vdots & \vdots & \vdots & \vdots \\
0 & 0 & 0 & 0 & 0
\end{bmatrix}_{v_i \times v_i},
\mathrm{B}_{ij} = \begin{bmatrix}
0 \\
\vdots \\
0 \\
b_{ij,1} \\
b_{ij,2} \\
\vdots \\
b_{ij,p_i}
\end{bmatrix}_{v_i \times 1},
\mathrm{D}_i = \begin{bmatrix}
c_{i,1} - a_{i,1} \\
c_{i,2} - a_{i,2} \\
\vdots \\
c_{i,p_i} - a_{i,p_i} \\
0 \\
\vdots \\
0
\end{bmatrix}_{v_i \times 1},
$$

$$\mathrm{H}_i = \begin{bmatrix} 1 & 0 & \ldots & 0 \end{bmatrix}_{1 \times v_i},$$

with $p_i = max(n_{a_i}, n_{b_i}, n_{c_i})$, and $v_i = p_i + max(d_{i,1}, \ldots, d_{i,m})$. In this formulation, the input dead times are implicitly represented in the state-space representation, therefore augmenting the system overall order.

The complete state-space representation of the process model for all outputs i from 1 to n is given by

$$
\begin{aligned}
x_{k+1} &= Ax_k + B\Delta u_k + De_k \\
y_k &= Hx_k + e_k
\end{aligned},
$$
(5.3)

where

$$
\Delta u_k = \begin{bmatrix} \Delta u_{1k} & \ldots & \Delta u_{mk} \end{bmatrix}^T, e_k = \begin{bmatrix} e_{1k} & \ldots & e_{nk} \end{bmatrix}^T,
$$

$$
y_k = \begin{bmatrix} y_{1k} & \ldots & y_{nk} \end{bmatrix}^T, A = diag(A_1, \ldots, A_n),
$$

$$
D = diag(D_1, \ldots, D_n), H = diag(H_1, \ldots, H_n),
$$

$$
B = \begin{bmatrix}
B_{11} & B_{12} & \ldots & B_{1m} \\
B_{21} & B_{22} & \ldots & B_{2m} \\
\vdots & \vdots & \ddots & \vdots \\
B_{n1} & B_{n2} & \ldots & B_{nm}
\end{bmatrix}.
$$

5.2.2 Output predictions

The predicted output $\hat{y}_{k+i}$, along the prediction horizon N, $i = 1, \ldots, N$, can be computed recursively by using the state-space model from (5.3). Since e_k is a white noise with null mathematical expectation, its best predicted value is zero, yielding

$$
\begin{aligned}
\hat{y}_{k+1} &= HAx_k + HDe_k + HB\Delta u_k, \\
\hat{y}_{k+2} &= HA^2x_k + HADe_k + HAB\Delta u_k + HB\Delta u_{k+1}, \\
&\vdots \\
\hat{y}_{k+N} &= HA^Nx_k + HA^{N-1}De_k + HA^{N-1}B\Delta u_k + HA^{N-2}B\Delta u_{k+1} + \ldots + HB\Delta u_{k+N-1},
\end{aligned}
$$
(5.4)

which can be written in the following matrix form

$$
Y = G\Delta U + Fx_k + Ee_k,
$$
(5.5)

where $\Delta\mathbf{U} = \begin{bmatrix} \Delta u_k & \Delta u_{k+1} & \dots & \Delta u_{k+N-1} \end{bmatrix}^T$, and

$$\mathbf{Y} = \begin{bmatrix} \hat{y}_{k+1} \\ \hat{y}_{k+2} \\ \dots \\ \hat{y}_{k+N} \end{bmatrix}^T, \mathbf{F} = \begin{bmatrix} \mathrm{HA} \\ \mathrm{HA}^2 \\ \vdots \\ \mathrm{HA}^N \end{bmatrix}, \mathbf{E} = \begin{bmatrix} \mathrm{HD} \\ \mathrm{HAD} \\ \vdots \\ \mathrm{HA}^{N-1}\mathrm{D} \end{bmatrix}, \mathbf{G} = \begin{bmatrix} \mathrm{HB} & 0 & \dots & 0 \\ \mathrm{HAB} & \mathrm{HB} & \dots & 0 \\ \vdots & \vdots & \ddots & \vdots \\ \mathrm{HA}^{N-1}\mathrm{B} & \mathrm{HA}^{N-2}\mathrm{B} & \dots & \mathrm{HB} \end{bmatrix}.$$

Equation (5.5) can also be written as

$$\mathbf{Y} = \mathbf{G}\Delta\mathbf{U} + \mathbf{f}, \tag{5.6}$$

where the term $\mathbf{f} = \mathbf{F}x_k + \mathbf{E}e_k$ is known as the free response of the system. Note that for dead-time systems, the first $n \times d_{min}$ rows of matrix $\mathbf{G}$ are null, where d_{min} is the smallest delay associated to each output. Thus, these rows can be eliminated in order to reduce control calculation efforts.

5.2.3 Optimization procedure

A matrix approach of the GPC strategy consist on minimizing the following cost function

$$J = (\mathbf{Y} - \mathbf{W})^T \Psi (\mathbf{Y} - \mathbf{W}) + \Delta\mathbf{U}^T \Lambda \Delta\mathbf{U}, \tag{5.7}$$

where $\mathbf{W} = \begin{bmatrix} r_{k+1} & r_{k+2} & \cdots & r_{k+N} \end{bmatrix}^T$ is the future desired output reference, $\Lambda_{(N_u m \times N_u m)}$, and $\Psi_{(Nn \times Nn)}$ are diagonal weighting matrices, N is the prediction horizon, and N_u is the control horizon. For simplicity, in this work is defined $\Lambda = \lambda \mathrm{I}_{(N_u m \times N_u m)}$, where λ is a positive scalar used as a tuning parameter (CAMACHO; BORDONS, 2007). The first term of (5.7) guarantees output set-point tracking whereas the second one ensures that the variations in control signals go to zero, i.e., control signal asymptotically goes to a bounded final value. For the unconstrained case minimizing J leads to the optimum control sequence

$$\Delta\mathbf{U} = \left(\mathbf{G}^T \Psi \mathbf{G} + \Lambda\right)^{-1} \mathbf{G}^T \Psi (\mathbf{W} - \mathbf{f}). \tag{5.8}$$

Nevertheless, only the first m elements of $\Delta\mathbf{U}$ are used, so the optimal control sequence is given by

$$\Delta u_k = \mathbf{K}(\mathbf{W} - \mathbf{f}), \tag{5.9}$$

where $\mathbf{K}$ contains the first m rows of $\left(\mathbf{G}^T \Psi \mathbf{G} + \Lambda\right)^{-1} \mathbf{G}^T \Psi$.

In the case where constraints need to be taken into account, the optimal control requires the solution of a quadratic programming problem which has been extensively studied in the literature (WANG, 2009).

5.2.4 *Closed loop analysis*

By substituting $\mathbf{f} = \mathbf{F}x_k + \mathbf{E}e_k$ from (5.6) into (5.9), one gets

$$\Delta u_k = \mathbf{K}(\mathrm{W} - \mathbf{F}x_k - \mathbf{E}e_k). \tag{5.10}$$

In the case where future reference remains constant the above equation turns into

$$\Delta u_k = \mathrm{K}_r r_k - \mathrm{K}_F x_k - \mathrm{K}_E e_k, \tag{5.11}$$

where $\mathrm{K}_r = \left[\sum_{i=1}^{N} \mathbf{K}_{1i} \quad \sum_{i=1}^{N} \mathbf{K}_{2i} \quad \cdots \quad \sum_{i=1}^{N} \mathbf{K}_{N_u i} \right]^T$, $\mathrm{K}_F = \mathbf{KF}$, $\mathrm{K}_E = \mathbf{KE}$ are constant matrices of dimensions $m \times n$, $m \times nv$, and $m \times n$, respectively, with $v = max(v_i)$, $i = 1, ..., n$.

Figure 37 – Proposed implementation structure
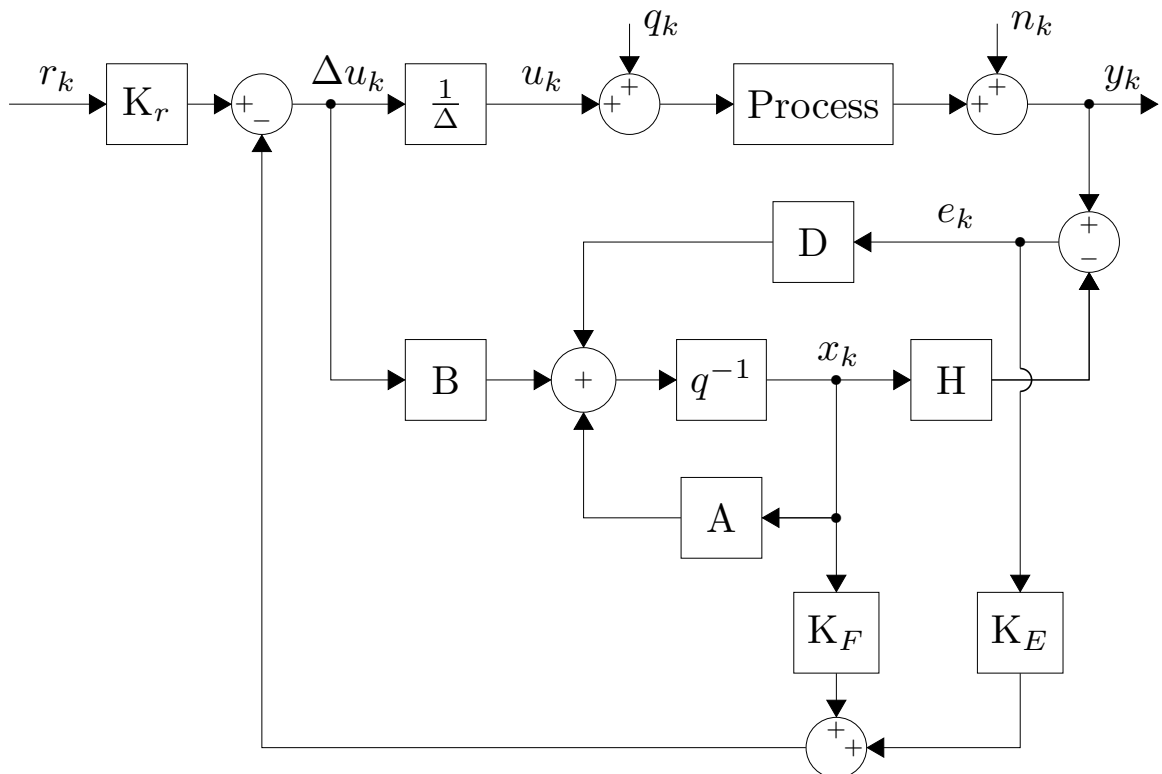
Source: The author.

From (5.3) and (5.11) is obtained the proposed GPC control structure shown in Figure 37. Note that the proposed structure employs a state observer where D is the estimator gain. Matrices K_F and K_E are feedback gains and e_k is the error signal. Therefore, one might

devise the following relationship

$$x_{k+1} = Ax_k + B\Delta u_k + D(y_k - Hx_k). \tag{5.12}$$

Moreover, control moves may be written as

$$\Delta u_k = -(K_F - K_E H)x_k - K_E y_k + K_r r_k. \tag{5.13}$$

Replacing (5.13) into (5.12) leads to

$$x_{k+1} = \left[A - B(K_F - K_E H) - DH \right] x_k + \left[BK_r \quad D - BK_E \right] \begin{bmatrix} r_k \\ y_k \end{bmatrix}.$$

So that, a feedback relationship is established and written as

$$\begin{aligned} x_{k+1} &= \tilde{A}x_k + \tilde{B}\xi_k \\ \Delta u_k &= \tilde{C}x_k + \tilde{D}\xi_k \end{aligned}, \tag{5.14}$$

with $\tilde{A} = \left[A - B(K_F - K_E H) - DH \right]$, $\quad \tilde{B} = \left[BK_r \quad D - BK_E \right]$, $\quad \tilde{C} = -(K_F - K_E H)$, $\quad \tilde{D} = \left[K_r \quad -K_E \right]$ and $\xi_k = \left[r_k \quad y_k \right]^T$. For simplicity, consider the regulator case making $r_k = 0$. Then, a simplified closed loop diagram as the one shown in Figure 38 can be obtained, in which $K_1(z)$ can be calculated from (5.14) as

$$K_1(z) = -(K_F - K_E H) \left[zI - A + B(K_F - K_E H) + DH \right]^{-1}$$
$$(D - BK_E) - K_E.$$

Figure 38 – Simplified closed-loop diagram
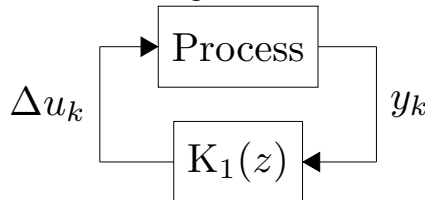
Source: The author.

5.3 Proposed structure analysis

This section presents a DTC structure equivalent to the proposed one. This is valuable in order to analyse performance and robustness properties. Moreover, tuning guidelines for the proposed GPC-based control strategy are derived.

5.3.1 Equivalency with the FSP structure

In this subsection the proposed structure is rewritten in a way that makes it equivalent to the FSP. For simplicity, the analysis considers the process with a common factor time delay d for all transfer functions in the transfer matrix. Thus, the $i-$th process model output (5.2) can be rewritten as

$$\begin{aligned} x_{i_{k+1}} &= \bar{A}_i x_{i_k} + \bar{B}_{i,1} \Delta u_{i_{k-d}} + ... + \bar{B}_{i,m} \Delta u_{m_{k-d}} + \bar{D}_i e_{i_k} \\ y_{i_k} &= \bar{H}_i x_{i_k} + e_{i_k} \end{aligned}. \tag{5.15}$$

Note that differently from the system in (5.2), the delay is explicit in (5.15). Thus, from the superposition principle of linear systems, dynamics and disturbance models may be split leading to the output

$$y_{i_k} = g_{i_{k-d}} + h_{i_k}, \tag{5.16}$$

where $g_{i_{k-d}}$ and h_{i_k} are obtained from the following state-space systems

$$\begin{aligned} v_{i_{k+1}} &= \bar{A}_i v_{i_k} + \bar{B}_{i,1} \Delta u_{1_k} + ... + \bar{B}_{i,m} \Delta u_{m_k} \\ g_{i_k} &= \bar{H}_i v_{i_k} \end{aligned} \tag{5.17}$$

and

$$\begin{aligned} w_{i_{k+1}} &= \bar{A}_i w_{i_k} + \bar{D}_i e_{i_k} \\ h_{i_k} &= \bar{H}_i w_{i_k} + e_{i_k}, \end{aligned} \tag{5.18}$$

for which (5.17) depends entirely on the inputs Δu_j, $j = 1, ..., m$, while (5.18) relates to disturbance e_{i_k} instead. Therefore, (5.17) clearly represents the output of the process model while (5.18) adds the output due to noise. The complete representation including all outputs from 1 to n is given by

$$\begin{aligned} v_{k+1} &= \bar{A} v_k + \bar{B} \Delta u_k \\ g_{ik} &= \bar{H} v_k \end{aligned} \tag{5.19}$$

and

$$\begin{aligned} w_{k+1} &= \bar{A} w_k + \bar{D} e_k \\ h_k &= \bar{H} w_k + e_k \end{aligned}. \tag{5.20}$$

The output prediction is recursively computed using (5.19) and (5.20), yielding

$$\begin{aligned} \hat{y}_{k+d+1} &= \bar{H}\bar{A} v_k + \bar{H}\bar{A}^{d+1} w_k + \bar{H}A^d \bar{D} e_k + \bar{H}\bar{B} \Delta u_k \\ \hat{y}_{k+d+2} &= \bar{H}\bar{A}^2 v_k + \bar{H}\bar{A}^{d+2} w_k + \bar{H}\bar{A}^{d+1} \bar{D} e_k + \bar{H}\bar{A}\bar{B} \Delta u_k + \bar{H}\bar{B} \Delta u_{k+1} \\ &\vdots \\ \hat{y}_{k+d+M} &= \bar{H}\bar{A}^M v_k + \bar{H}\bar{A}^{d+M} w_k + \bar{H}\bar{A}^{d+M-1} \bar{D} e_k + \bar{H}\bar{A}^{M-1} \bar{B} \Delta u_k + ... + \bar{H}\bar{B} \Delta u_{k+M-1}, \end{aligned}$$

where $M = N - d$. The predictions can be written in the compact form

$$\mathbf{Y} = \mathbf{G}\Delta\mathbf{U} + \mathbf{F}_v v_k + \mathbf{F}_w w_k + \bar{\mathbf{E}} e_k, \tag{5.21}$$

where

$$\mathbf{F}_w = \begin{bmatrix} \bar{H}\bar{A}^{d+1} \\ \bar{H}\bar{A}^{d+2} \\ \vdots \\ \bar{H}\bar{A}^{d+M} \end{bmatrix}, \mathbf{F}_v = \begin{bmatrix} \bar{H}\bar{A} \\ \bar{H}\bar{A}^2 \\ \vdots \\ \bar{H}\bar{A}^M \end{bmatrix}, \bar{\mathbf{E}} = \begin{bmatrix} \bar{H}\bar{A}^d\bar{D} \\ \bar{H}\bar{A}^{d+1}\bar{D} \\ \vdots \\ \bar{H}\bar{A}^{d+M-1}\bar{D} \end{bmatrix},$$

$$\mathbf{G} = \begin{bmatrix} \bar{H}\bar{B} & 0 & \dots & 0 \\ \bar{H}\bar{A}B & \bar{H}\bar{B} & \dots & 0 \\ \vdots & \vdots & \ddots & \vdots \\ \bar{H}\bar{A}^{M-1}\bar{B} & \bar{H}\bar{A}^{M-2}\bar{B} & \dots & \bar{H}\bar{B} \end{bmatrix}.$$

In this case, the analytic optimal control is given by

$$\Delta u_k = \bar{\mathbf{K}}(\mathbf{W} - \mathbf{F}_v v_k - \mathbf{F}_w w_k - \bar{\mathbf{E}} e_k), \tag{5.22}$$

where $\bar{\mathbf{K}}$ contains the first m rows of $\left(\mathbf{G}^T\Psi\mathbf{G} + \Lambda\right)^{-1}\mathbf{G}^T\Psi$.

The control signal (5.22) can also be written as

$$\Delta u_k = \bar{K}_r r_k - \bar{K}_v v_k - \bar{K}_w w_k - \bar{K}_E e_k, \tag{5.23}$$

where $\bar{K}_v = \bar{\mathbf{K}}\mathbf{F}_v$, $\bar{K}_w = \bar{\mathbf{K}}\mathbf{F}_w$, $\bar{K}_E = \bar{\mathbf{K}}\bar{\mathbf{E}}$. For the case of constant future trajectory $\bar{K}_r$ is a $n \times m$ constant matrix.

By using (5.19), (5.20), and (5.23) the obtained control structure for analysis is shown in Figure 39.

From Figure 39 note that the output for the nominal case is given by

$$Y(z) = H_r(z)\bar{K}_r\mathbf{R}(z) + [I - H_r(z)V(z)]\mathbf{P}_q(z)\mathbf{Q}(z), \tag{5.24}$$

where

$$H_r(z) = \bar{H}\left(zI - \bar{A} + \bar{B}\bar{K}_v\right)^{-1}\bar{B}z^{-d} \tag{5.25}$$

and

$$V(z) = (\bar{K}_w - \bar{K}_E\bar{H})(zI - \bar{A} + \bar{D}\bar{H})^{-1}\bar{D} + \bar{K}_E. \tag{5.26}$$

Figure 39 – Analysis structure
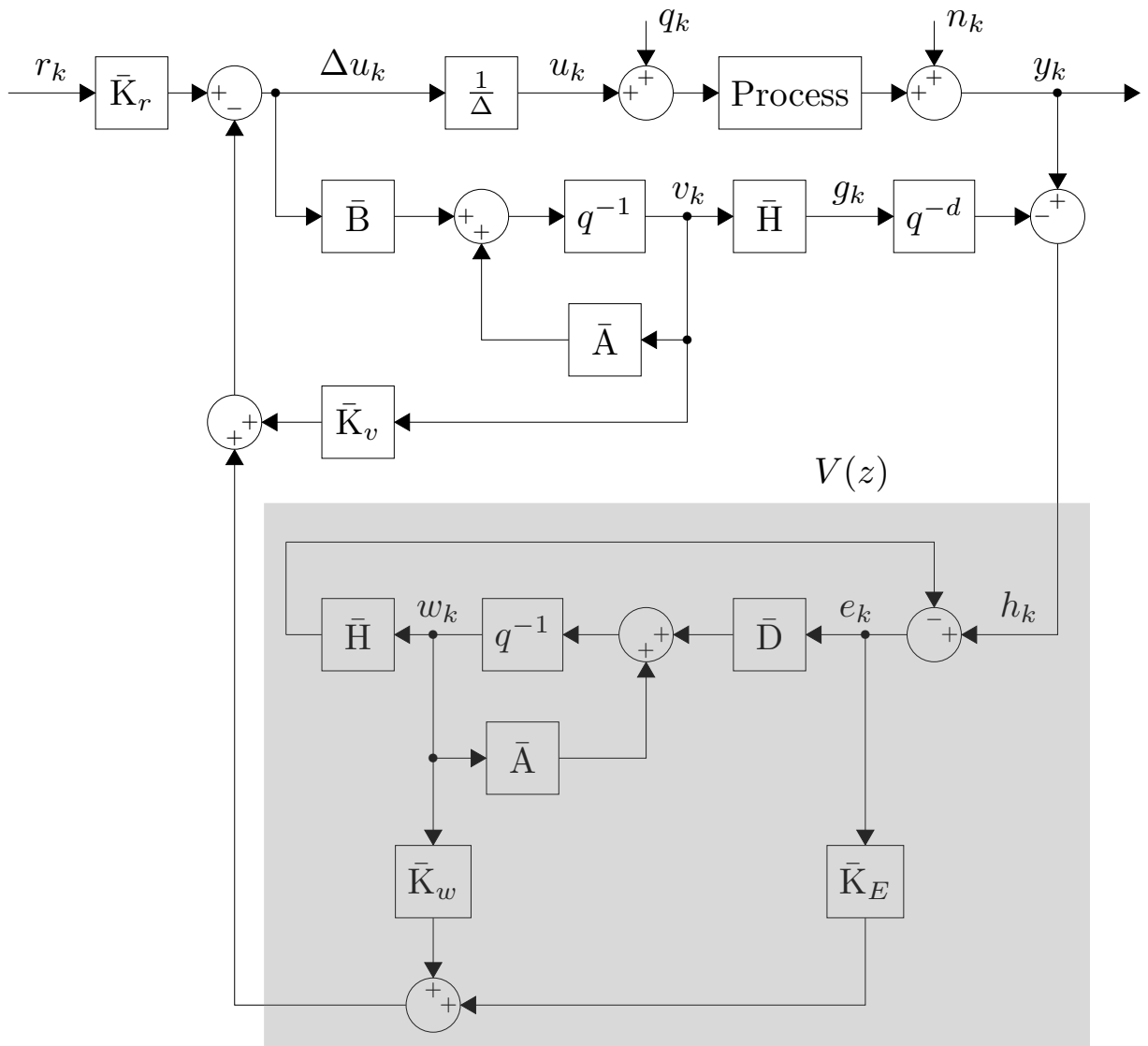
Source: The author.

From (5.24), one can notice that, as in DTC strategies, the dead time has been completely compensated as it no longer appears in the denominator of $H_r(z)$. Also note that $H_r(z)$ has direct influence on the set-point tracking response, whilst filter $V(z)$ only influences disturbance rejection response.

5.3.2 Robustness condition

For robustness analysis let us consider an additive uncertainty

$$\mathbf{P}(z) = \mathbf{P}_n(z) + \Delta\mathbf{P}(z), \tag{5.27}$$

where $\Delta\mathbf{P}(z) = \Omega_2(z)\Delta(z)\Omega_1(z)$, $\|\Delta(z)\|_\infty < 1$. For simplicity, as suggested in (SANTOS *et al.*,

2016) for DTCs, $\Omega_1(z)$ and $\Omega_2(z)$ can be defined as

$$\Omega_1(z) = I \text{ and } \Omega_2(z) = \mathbf{P}(z) - \mathbf{P}_n(z),$$

where $\mathbf{P}(z)$ should include the modelling errors of the static gains, time constants, and delays.

The controller structure from Figure 39 can be represented in the $M - \Delta$ form as in Figure 29, where

$$M(z) = \Omega_1(z)M'(z)\Omega_2(z), \tag{5.28}$$

$$M'(z) = \left[\bar{K}_v \left(zI - \bar{A} + \bar{B}\bar{K}_v \right)^{-1} \bar{B} - I \right] V(z). \tag{5.29}$$

Figure 40 – $\mathbf{M} - \Delta$ structure
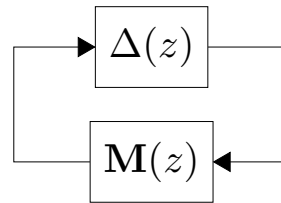
Source: The author.

Then, robust closed-loop stability is given by the condition

$$\bar{\sigma}(\Delta(z)) < \frac{1}{\bar{\sigma}(M(z))}, \qquad z = e^{j\omega T_s}, \qquad \forall \omega = [0, \pi/T_s), \tag{5.30}$$

where $\bar{\sigma}(\cdot)$ is the maximum singular value function.

5.3.3 Considerations on the controller tuning

5.3.3.1 Set-point tracking

A detailed inspection on subsystem $H_r(z)$ reveals that its only adjustable term is the gain $\bar{K}_v$, which depends on the prediction horizon N, the control horizon N_u, and weighting matrices Ψ and Λ.

Prediction horizon N must follow some guidelines. For multiple outputs, different prediction horizons N_i can be defined for each output y_i. Furthermore, it is well known that the prediction window should be bigger than or equal to the maximum input delay $d_i = max(d_{ij})$, where i stands for the output and j for the input. As a practical point of view, one can note that the effective prediction window is given by $\rho_i = N_i - d_i$. Thus, initially ρ_i must be defined, then, Ψ should be built depending on N_i by following the algorithm 1.

Algoritmo 1: Calculate Ψ

    Require: ρ_i, $i = 1,...,n$

    Require: d_{ij}, $i = 1,...,n$, and $j = 1,...,m$

    $d_i \leftarrow max(d_{ij})$

    $N_i \leftarrow \rho_i + d_i$, $i = 1,...,n$

    $N \leftarrow max(N_i)$

    for k = 1 to N **do**

      for i = 1 to n **do**

        if $j > N_i$ **then**

          $\psi(i \cdot k) \leftarrow 0$

        else

          $\psi(i \cdot k) \leftarrow 1$

        end if

      end for

    end for

    $\Psi = diag(\psi)$

For simplicity, the control window is kept constant with $N_u = 1$. This is also an action which can reduce computational efforts due to matrix dimensions. Therefore, the only free parameters left for set-point tracking tuning are ρ_i and λ. The ρ_i parameter has a stronger effect on the speed of the set-point tracking response. That is, bigger ρ_i yield slower poles of $H_r(z)$ and *vice-versa*. On the other hand, the λ parameter has a bigger effect on the system damping, which is over damped for $\lambda = 0$.

5.3.3.2 *Disturbance rejection and robustness*

From (5.24) one can note that disturbance rejection depends on both $H_r(z)$, and $V(z)$. However $H_r(z)$ has been prior adjusted for set-point tracking, leaving $V(z)$ as the only subsystem for disturbance rejection characteristics. A closer look in $M'(z)$ reveals that the poles of $V(z)$ are also part of the poles of $M'(z)$. Furthermore, also note that filter $V(z)$ is the only adjustable subsystem left in $M'(z)$ for the adjustment of the robust stability condition given in (5.30).

A detailed inspection reveals that the poles of subsystem $V(z)$ are given by the eigenvalues of $\bar{A} - \bar{D}\bar{H} = diag(\Phi_1, \Phi_2, ..., \Phi_n)$, which can be written as

$$\Phi_i = \begin{bmatrix} c_{i,1} & 1 & 0 & \dots & 0 \\ c_{i,2} & 0 & 1 & & 0 \\ \vdots & & & \ddots & \vdots \\ & & & & 1 \\ c_{i,p_i} & 0 & 0 & & 0 \end{bmatrix}, i = 1, ..., n,$$

thus the poles of $V(z)$ are equal to the roots of polynomial C_i. Therefore C_i should be adjusted to meet a desired trade-off between disturbance rejection and robustness. In this work, C_i is defined as

$$C_i = (1 - \beta_i z^{-1}) \prod_{j=1}^{\varepsilon} (1 - p_j z^{-1}), \tag{5.31}$$

where p_j are the ε poles of the process model except the undesired ones, which are close to, on or outside the unit circle in the z-plane. Such undesired poles could yield some problems such as internal instability and slow disturbance rejection response. Furthermore, $0 \le \beta_i < 1$ is the user tuning parameter. Thus, $\beta = [\beta_1 \ldots \beta_n]$ is left as the only adjustable parameter for disturbance rejection and robustness characteristics of the proposed controller, which simplifies the controller tuning. Smaller values of β yield faster disturbance rejection while values closer to 1 provide bigger overall system robustness to modelling uncertainties. Therefore, the aforementioned trade-off has to be taken into account when setting the value of β.

5.4 Case studies by simulations

In this section three examples are presented by means of simulations in order to verify the influence of the tuning parameters and to compare the state-space GPC-based DTC (GPC-DTC) with other DTC structures proposed in the literature. By considering a unified state-space approach the proposed structure can deal with SISO/MIMO square/non-square processes. That way, the first example considers a challenging unstable SISO process (SANZ *et al.*, 2018). The second and third examples present non-square stable and square integrative MIMO processes, respectively.

Example 1 − unstable SISO case

Consider the FOPDT model given by

$$P(s) = \frac{1}{s-1} e^{-1.5s}, \tag{5.32}$$

which has recently been studied in (SANZ *et al.*, 2018). As pointed out by the authors of (SANZ *et al.*, 2018), the robust control of this system for such a large delay is considered a challenge in the literature. A discrete-time representation of this process obtained using ZOH is given as

$$P(z) = \frac{0.01}{z-1.01} z^{-150}, \quad T_s = 0.01s. \tag{5.33}$$

For comparison purposes, the GPC-DTC control parameters were adjusted with $\rho = 250$, $\lambda = 0$ and $\beta = 0.985$ selected in order to obtain faster disturbance rejection than the generalized Smith Predictor (GSP) proposed by (SANZ *et al.*, 2018), which is defined as therein. From the equivalency with the FSP structure, and analysis of $H_r(z)$ and $V(z)$, the overall controller order of the GPC-DTC is equal to $d + 2$, which is the same for the GSP, once more showing the equivalency of the proposed controller with other DTC structures. Furthermore, the GPC-DTC tuning is simplified, and takes only three parameters.

Figure 41 shows the nominal performance for the GPC-DTC and the GSP. Note that the GPC-DTC is able to notoriously reach the reference faster than the GSP for both set-point and disturbance rejection phases.

Figure 41 – Output and control signals for the nominal case of example 1
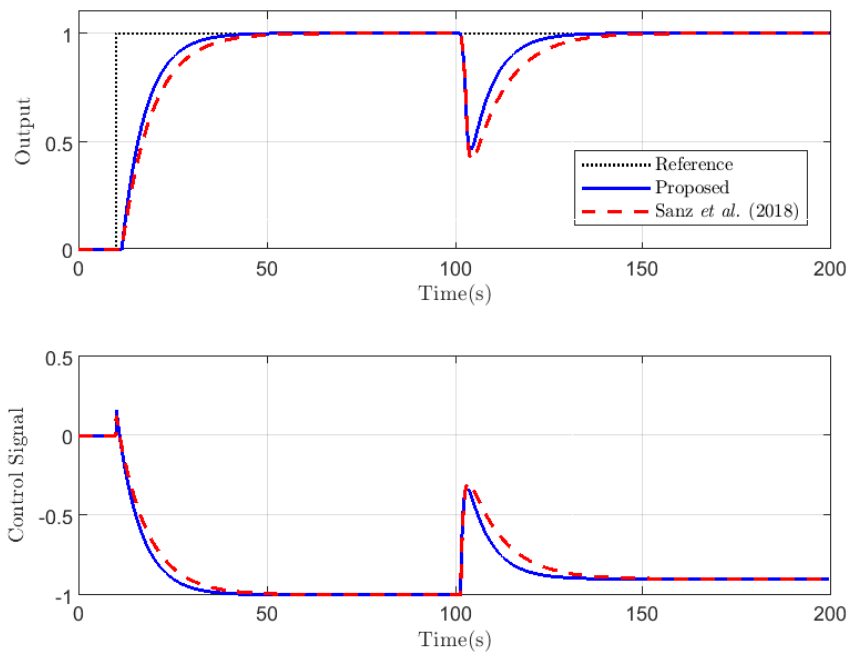
Source: The author.

Consider now that the process gain and process delay are actually 10% lower and 5% higher, respectively, than those of the process model. Figure 42 shows output and control signals obtained for this case for both the GPC-DTC and the GSP. Once again the GPC-DTC was able to reach the reference prior to the GSP, while showing less oscillation both in the output and control signals. This illustrates the robustness characteristics of the proposed strategy.

Figure 42 – Output and control signals for the perturbed case of example 1
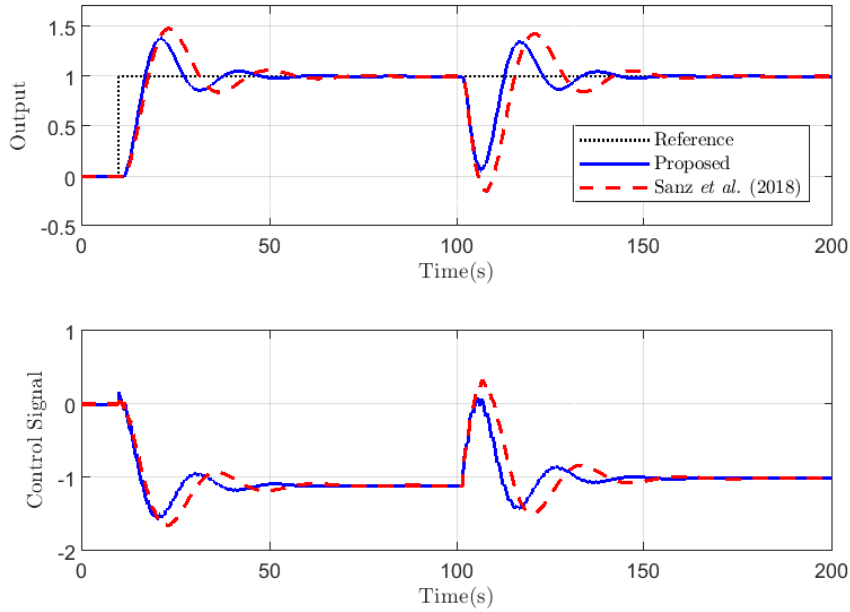
Source: The author.

Example 2 − Modified shell distillation column

A second case study was carried out on the standard Shell heavy oil fractionator problem that was proposed in (RAO; CHIDAMBARAM, 2006) as a 2×3 version with increased delay of the original 5×7 model discussed in (VLACHOS *et al.*, 2002). The Modified shell distillation column is described by:

$$P_n(s) = \begin{bmatrix} \frac{4.05e^{-81s}}{50s+1} & \frac{1.77e^{-84s}}{60s+1} & \frac{5.88e^{-81s}}{50s+1} \\ \frac{5.39e^{-54s}}{50s+1} & \frac{5.72e^{-42s}}{60s+1} & \frac{6.90e^{-45s}}{40s+1} \end{bmatrix}, \tag{5.34}$$

The discrete-time model of (5.34) is obtained using a zero-order-holder with sampling time of $T_s = 1$ min:

$$P_n(z) = \begin{bmatrix} \frac{0.0802z^{-81}}{z-0.9802} & \frac{0.02926z^{-84}}{z-0.9835} & \frac{0.1164z^{-81}}{z-0.9802} \\ \frac{0.1067z^{-54}}{z-0.9802} & \frac{0.09454z^{-42}}{z-0.9835} & \frac{0.1704z^{-45}}{z-0.9753} \end{bmatrix}. \tag{5.35}$$

For this example, the GPC-DTC was compared with the controller proposed by (CHEN *et al.*, 2011) and the simplified MIMO filtered Smith predictor (SMFSP) from (SANTOS *et al.*, 2016). The GPC-DTC control parameters were adjusted with $\rho_1 = 16$, $\rho_2 = 7$, $\lambda = 100$ and $\beta = 0$. Figure 43 shows output and control signals obtained for the nominal model of the plant for a unit step change in the reference. A positive input disturbance of magnitude 0.1 was applied to the control signal u_1 at time 400 s. Note that the proposed GPC-DTC achieves

satisfatory set-point tracking response since y_2 notoriously reach the reference faster than the compared controllers without any overshoot. For output y_1, although some overshoot occurs, the controller achieves similar performance to the compared ones. Furthermore, on what concerns to disturbance rejection and coupling between the process variables the GPC-DTC clearly is superior by showing enhanced response in these situations. Therefore, one might say that the overall response of the GPC-DTC regarding aforementioned characteristics is superior to the compared ones.

Figure 43 – Output and control signals for the nominal case for example 2
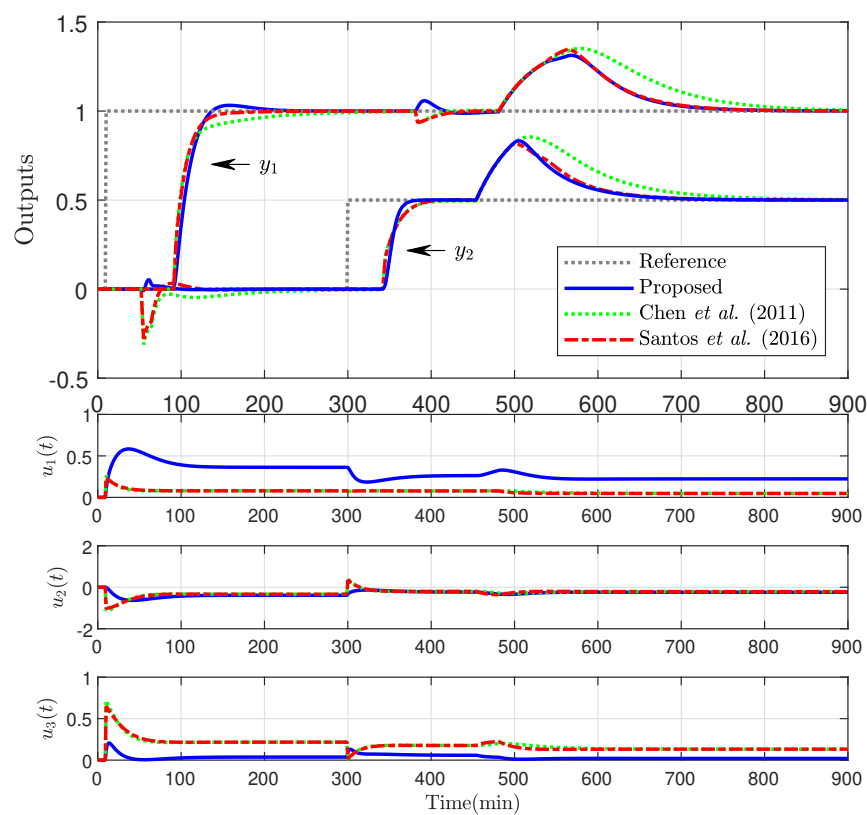
Source: The author.

Figure 44 shows the results obtained when considering uncertainties of 10% in the gain, time constants, and all transport delays of the process. Once again, the GPC-DTC presents good response against the compared controllers. Furthermore, note that the use of the stables poles of the process in the polynomial C_i have been enough to provide robustness and disturbance rejection to the controller.

Figure 44 – Output and control signals for the perturbed case for example 2
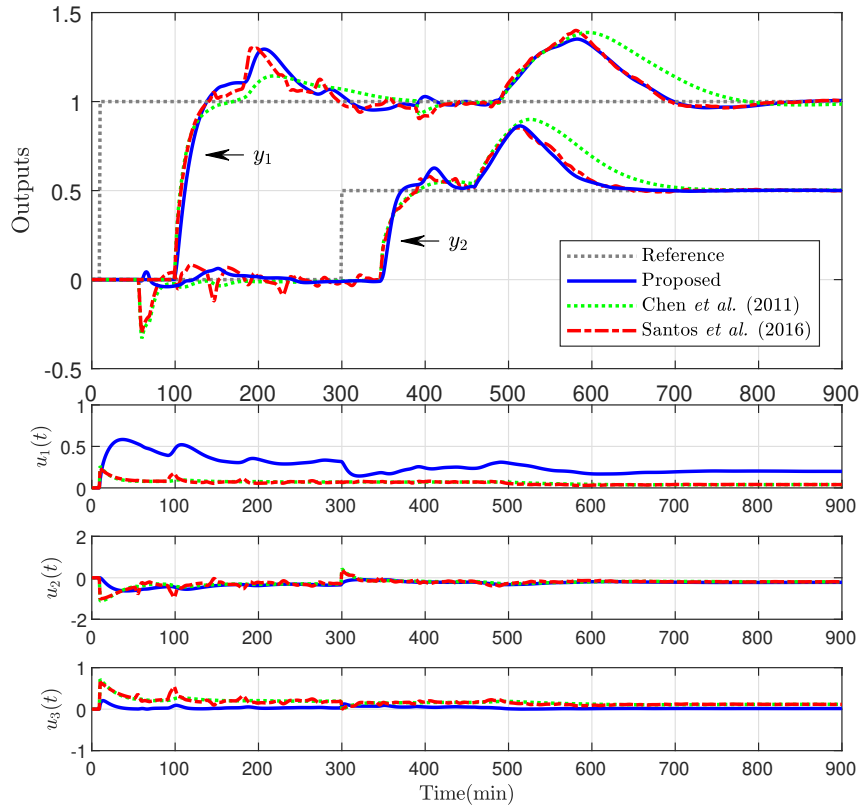
Source: The author.

Example 3 − Three-stage evaporator system

This examples compares the GPC-DTC with the SMFSP from (SANTOS *et al.*, 2016) and the controller presented by (SANTOS *et al.*, 2014) applied to the integrating three-stage evaporator system, which is described by

$$P_n(s) = \begin{bmatrix} \frac{3.5e^{-s}}{s} & \frac{-e^{-5s}}{2s+1} \\ \frac{2e^{-7s}}{1.5s+1} & \frac{-e^{-5s}}{3.2s+1} \end{bmatrix}, P_q(s) = \begin{bmatrix} \frac{3.5e^{-s}}{s} \\ \frac{-4.5e^{-2s}}{2s+1} \end{bmatrix}, \tag{5.36}$$

where $Y(s) = P_n(s)U(s) + P_q(s)Q(s)$.

The discrete-time model of (5.36) is obtained using a zero-order-holder with sampling time of $T_s = 0.2$ min:

$$P_n(z) = \begin{bmatrix} \frac{0.7z^{-5}}{z-1} & \frac{-0.09516z^{-25}}{z-0.9048} \\ \frac{0.2497z^{-35}}{z-0.8752} & \frac{-0.06059z^{-25}}{z-0.9394} \end{bmatrix}. \tag{5.37}$$

For this case, the GPC-DTC parameters were adjusted with $\rho_1 = 0$, $\rho_2 = 15$, $\lambda = 40$ and $\beta = 0$. Once again the use of the stables poles of the plant in the polynomial C_i provided

robustness and disturbance rejection to the controller.

For the GPC-DTC the influence of coupling between outputs is reduced in comparison with the other DTC controllers considered in this example. As shown by Figure 45, when there is a reference change for output y_1, the output y_2 is less affected and *vice-verse*. In addition, when the disturbance $q = 0.05$ was applied in $P_q(s)$ at time 80 min the GPC-DTC also presents better rejection for both outputs. Figure 46 shows the results considering 20% gain mismatch and +0.4 min dead time error. Once more the GPC-DTC is able to achieve the best results among the evaluated strategies.

Figure 45 – Output and control signals for the nominal case for example 3
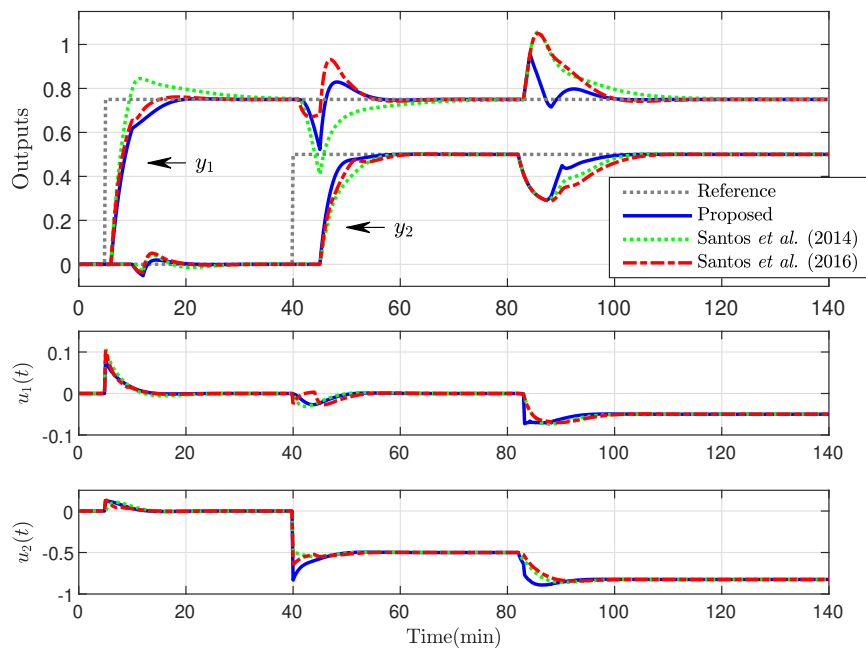
Source: The author.

5.5 Experimental results

A wide range of industrial and commercial processes demand appropriate control of environmental conditions. Greenhouses, neonatal incubators, and warehouses for food storage are a few examples. In this kind of applications comfort and safety, in addition to product quality during production and storage phases are very closely related to a proper control of the internal temperature and the relative humidity. Furthermore, controlling this type of process is a challenging issue due to existing coupling between process variables and associated multiple dead time.

Figure 46 – Output and control signals for the perturbed case for example 3
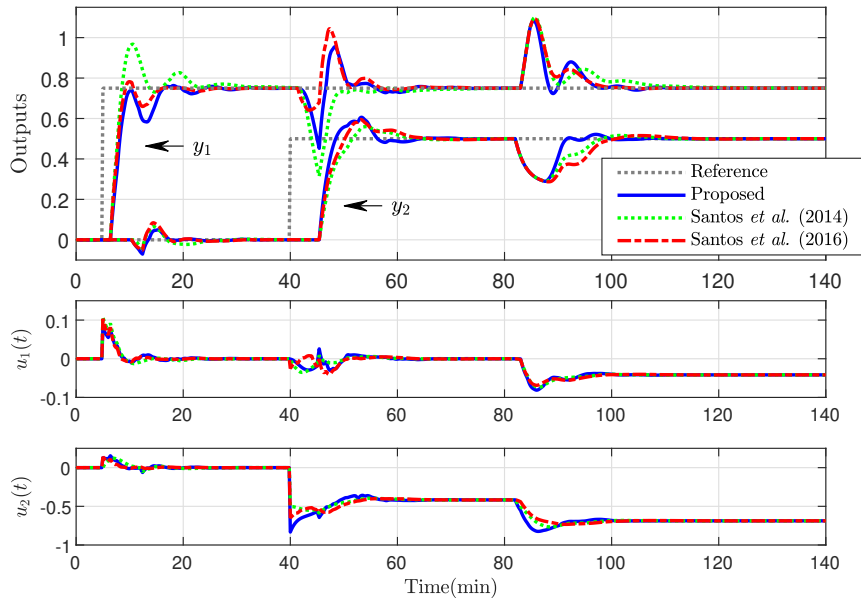
Source: The author.

In this work, an in-house thermal chamber has been used in order to demonstrate the proposed DTC ability to deal with indoor temperature and humidity control.

5.5.1 *In-house thermal chamber and controller setup descriptions*

The proposed strategy was applied for the temperature and humidity control of an in-house thermal chamber, which is shown in Figure 47. The temperature and humidity inside the chamber are controlled by a set of actuators that provide heat and cold steam.

The first actuator is an electrical resistor which provides heat and is situated in an air reservoir right below the acrylic dome. The heat reservoir is separated from the dome only by two openings which allow air to circulate. The power delivered to the heating resistor is controlled by the duty cycle of a switching power supply. Additionally, an ultrasonic humidifier located under the dome outputs the cold steam to the dome through a pipe. The steam flow of the humidifier is controlled using a circuit based on a light dependent resistor.

It is important to highlight that the cold steam increases the control challenge since its effect on temperature opposes the effect of the heating resistor, thus increasing the coupling between the control variables. This set of actuators, in addition to a fan with constant rotational speed that provides the internal air flow, are some know source of delay and nonlinearities in the system.

Furthermore, there are two portholes that when open disturb the internal temperature and humidity by interaction with the external environment. This system can represent a wide variety of industrial and commercial applications, as any of the previously reported ones.

The control inputs are limited by their maximum power, which varies in a scale from 0 to 100%, thus the saturation model is included in the control loop, as shown in the implementation structure for saturated systems located in the bottom of Figure 48. Note that integral action is no longer explicit in the implementation structure for saturated systems, which has been historically related to windup problems.

The controller runs on a supervisory computer. The control signal is sent via Universal Serial Bus (USB) cable to a driving circuit through a Nidaq-USB6009 data acquisition card manufactured by National Instruments. In order to close the control loop, temperature and humidity sensors provide actual measurements inside the chamber to the acquisition card through an analog digital converter (ADC).

Figure 47 – In-house thermal chamber
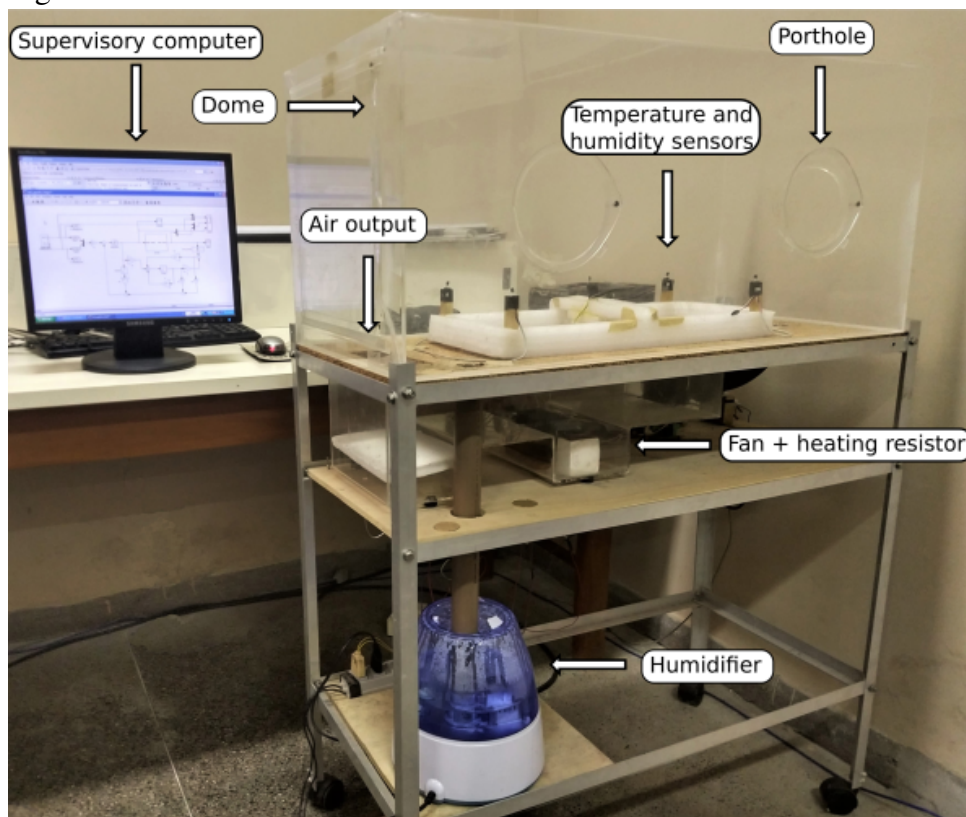
Source: The author.

Figure 48 – In-house thermal chamber schematics and control
diagram
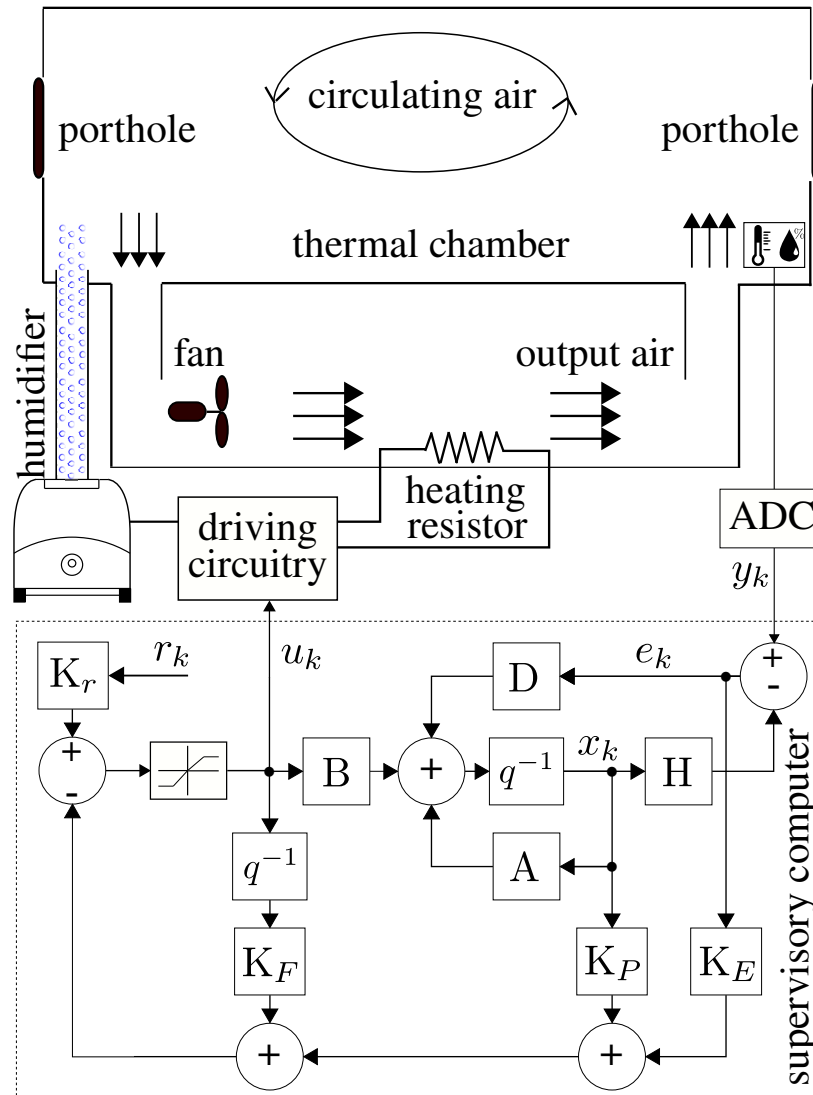
Source: The author.

5.5.2 *Experiments and results*

The in-house thermal chamber has been identified using a open-loop step-test procedure, whose model is given by

$$
\begin{bmatrix} Y_H(s) \\ Y_T(s) \end{bmatrix} = \begin{bmatrix} \frac{10.6e^{-0.22s}}{2.738s+1} & \frac{-7.099e^{-2.73s}}{6.482s+1} \\ \frac{-1.123}{2.829s+1} & \frac{23.66e^{-1.86s}}{36.71s+1} \end{bmatrix} \begin{bmatrix} U_H(s) \\ U_T(s) \end{bmatrix},
\tag{5.38}
$$

where $Y_H(s)$, $U_H(s)$, $Y_T(s)$, $U_T(s)$ are the outputs and control signal related to the humidity and temperature, respectively.

This model was discretized by a zero-order-holder with sampling time of $T_s = 0.2$

min:

$$P(z) = \begin{bmatrix} \frac{0.67445(z+0.1071)z^{-2}}{z-0.9296} & \frac{-0.076251(z+1.829)z^{-14}}{z-0.9696} \\ \frac{-0.076651}{z-0.9317} & \frac{0.09006(z+0.4274)z^{-10}}{z-0.9946} \end{bmatrix}. \tag{5.39}$$

In order to verify robustness and effectiveness, the proposed controller was evaluated under step changes for both temperature and humidity references at different times. This is useful in order to show the anticipating control action which minimizes the effect of the coupling between the process variables. It is important to note that the acrylic dome does not provide a good level of thermal isolation between the internal and external environments. Thus, the external temperature is an unmodeled disturbance.

Figure 49 shows the experimental results for the controller tuned with $\rho_1 = 6$, $\rho_2 = 10$, $\lambda = 0$, and $\beta_1 = \beta_2 = 0.90$. Although the coupling between the output variables is made very clear after each reference step, the controller is able to maintain both at the desired values. Furthermore, the tracking is achieved without any overshoot.

Figure 49 – Experimental results
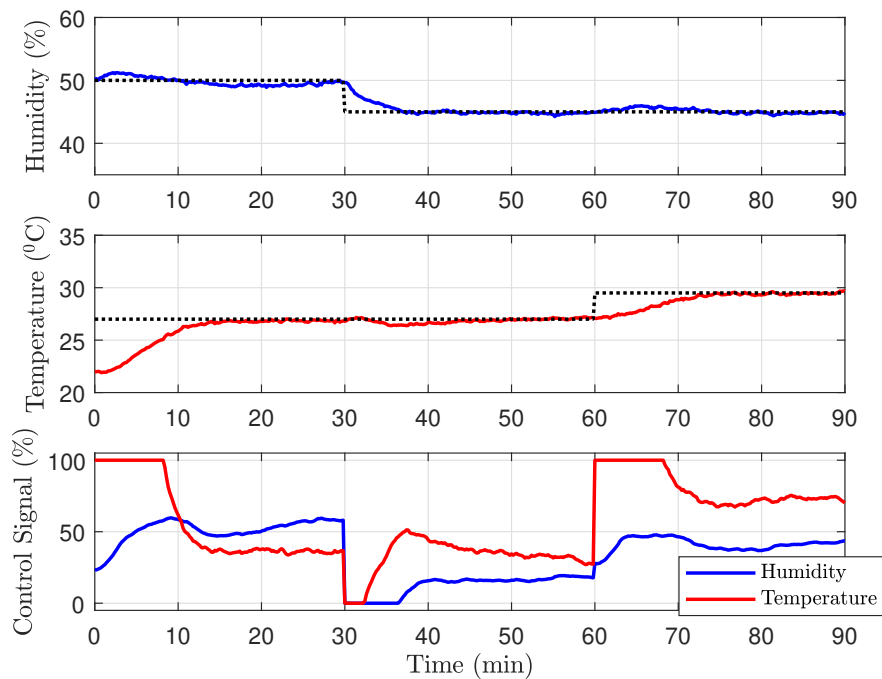
Source: The author.

5.6 Discussion

This work revisits the GPC in order to propose a unified GPC-based (namely GPC-DTC) structure for the control of SISO/MIMO square/non-square dead-time processes. An

equivalent structure to that of a dead-time compensator is used in order to generate simple, intuitive tuning rules. With the reduced number of tuning parameters, it was possible to reach enhanced set-point tracking, robustness, and disturbance rejection characteristics when compared to recently proposed DTC structures for the control of dead-time processes. Furthermore, application to the temperature and humidity control of a thermal chamber is used to assure the real applicability of the proposed strategy effectively. Finally, the control structure has presented very satisfactory results on reducing the effect of coupling between the process variables in the simulation results, while its effect on the experiment was mitigated.

6 A GPC-BASED MID-RANGING CONTROL STRATEGY

This chapter proposes a control input economic approach for Two-Input Single-Output (TISO) processes based on the Generalized Predictive Control (GPC). The proposed strategy is applicable to TISO systems in which the two inputs are from different nature, thus yielding different operating costs. The main idea comes from mid-ranging controllers, where more than one input is used to control one output. The simplicity of the approach lies in the fact that the operating costs of each input do not need to be precisely specified. Actually, one only needs to know which of the inputs is the most expensive. Furthermore, the proposed strategy is able to deal with the problem when the delays from the two inputs to the output are different. An experiment to control the temperature inside a thermal chamber is performed in order to show the effectiveness of the proposal.

6.1 Introduction

Model-based Predictive Control (MPC) belongs to the class of algorithms that explicitly applies a model of the controlled process to predict future outputs, which is then used in the calculation of the control action. Over the few past decades MPC has been applied to control processes in a wide variety of areas, such as in chemical plants, biomedical engineering and robot manipulators (CAMACHO; BORDONS, 2007).

On the other hand, mid-ranging fits into a class of controllers which are used to manipulate one output by using more than one input (usually two). Moreover, another condition is that one of the control variables return to a predefined set-point or midpoint. An extensive comparison between MPC and mid-ranging techniques has been performed in (ALLISON; ISAKSSON, 1998), where it was shown general advantage to MPC. Since then, several mid-range techniques have been proposed. In (JOHNSSON *et al.*, 2015), a modification to the mid-ranging control architecture which enables its use in non-stationary processes is applied to dissolved oxygen control in a bioprocess (JOHNSSON *et al.*, 2015), while in (VELUT *et al.*, 2007) mid-ranging is applied to a bioreactor control. More recently, mid-ranging techniques have been applied to multirotor UAV (Haus *et al.*, 2018), automotive control (Santillo *et al.*, 2016), and macro/mini manipulators (Ma *et al.*, 2015).

However, it does seem that an MPC-based mid-ranging strategy has not yet been proposed. In this paper, we do so motivated by the case in which one of the controlled inputs

is more expensive than the other, and a simple strategy can be used to set its desired setpoint. Moreover, the use of MPC compared to classical mid-ranging strategies yield many advantages, such as the easiness to deal with multiple time-delays, constraints, and model uncertainties.

The classical paradigm for economic and control operation of wide complex plants resides in a multi-layer architecture, in which an upper layer called the real-time optimization (RTO) layer is responsible for defining steady-state set-points for the process variables (ELLIS *et al.*, 2014). Then, a lower-layer feedback control system makes use of simplified linearized process models for output predictions computation and control signal optimization.

However, in recent years, many researchers have shifted focus from the traditional steady-state set-point tracking MPC to the dynamical operation offered by economic Model-based Predictive Control (EMPC). In such a framework, the classical control paradigm which divided the system in different layers is no longer valid. Actually, economical and feedback control layers have been combined in order to obtain a dynamical operation of the system which seeks to minimize global operational costs. Thus, in the EMPC framework, system economics objectives are reflected into the choice of arbitrary cost functions to be minimized (ELLIS *et al.*, 2016). Therefore, set-point tracking is no longer the main priority in such strategies.

In the last few years different approaches have been proposed in the EMPC framework. In (PEREIRA *et al.*, 2015), an economic MPC for periodic systems is applied to the control of a micro-grid through a function that includes the economic cost of operating the plant. In (BAYER *et al.*, 2015) stochastic information is incorporated in order to improve performance in robust economic MPC. In (ALANQAR *et al.*, 2017) a fault-tolerant EMPC strategy is presented.

Although the use of EMPC present many advantages over the traditional control architecture, in many applications (mainly for simpler processes) the traditional steady-state set-point tracking operation is still a valuable option. Therefore, it is important to include some economical aspects for the manipulation of the control inputs in such strategies. In this work, this is done by proposing a modified cost function for the Generalized Predictive Controller (GPC) which includes a mid-ranging strategy.

Therefore, the main goal of this work is to propose a modified cost function for the lower layer feedback control system, based on the GPC, which is able to achieve set-point tracking at steady-state while minimizing the use of the most expensive control input during steady-state operation. That is, the most expensive one is only used to improve the output response during transient phases. Thereby, although the control strategy presented herein

considers some economic aspects, it does not fit the EMPC framework as it is currently defined (see (RAWLINGS *et al.*, 2012)), i.e. an upper layer which defines the set-point target is still necessary, while the economical aspect is only considered in the feedback layer by minimizing the use of the most expensive control input (when multiple outputs are available). This leads to a simple strategy which can be applied to systems with more inputs than outputs. For simplicity, this work considers the case of Two-Input Single-Output (TISO) processes, thus configuring the proposal as a mid-ranging one.

6.2 Problem formulation

Consider a discrete-time LTI system $P(z)$ described by the following equations

$$P(z) \triangleq \begin{cases} x_{k+1} = Ax_k + B_1 u_{1_{k-h_1}} + B_2 u_{2_{k-h_2}} + B_w w_k, \\ y_k = Cx_k, \end{cases} \tag{6.1}$$

where $x_k \in \mathbb{R}^n$ is the plant state vector; $u_{1_{k-h_1}} \in \mathbb{R}$, and $u_{2_{k-h_2}} \in \mathbb{R}$ are the delayed plant inputs; and $y_k \in \mathbb{R}$ is the measured output. A, B_1, B_2, and C are all constant and known matrices of appropriate dimensions. The input delays $h_1 \geq 0$ and $h_2 \geq 0$ are bounded and known. Following assumptions are taken:

Assumption 7. *The pair* $(A, \begin{bmatrix} B_1 & B_2 \end{bmatrix})$ *is controllable.*

Assumption 8. *The unknown disturbance signal is bounded by* $|w_k| < D_w$, *and is locally integrable.*

Assumption 9. *The two inputs are from different nature, thus yielding different operating costs.*

6.2.1 Motivation Example

Consider the desalination process as in (TORRICO *et al.*, 2010), in which the main purpose of the control design was to maintain constant temperature gradient of the collector outlet-inlet. Keeping the constant temperature is important in order to increase the efficiency of the process. Two heating control inputs are available to achieve this goal. One of them is the heat from the solar collector. The second input comes from a smoke-tube gas boiler, which is much more expensive than the solar collector energy. In light of this circumstance, it is desired that during steady-state operation of the plant, only the cheaper input be used in order to reduce

global operation costs. This is just a small example that is conceptually similar to a wide variety of industrial processes where there are many available input sources to achieve the same goal.

6.2.2 Objective

Considering the Assumption 9 we aim at designing a control strategy that reduces the global operating costs in a simple and intuitive way. For this, we introduce the possibility to give a target value to one of the inputs, which can be defined as zero in order to reduce the use of the more expensive one at steady-state operation.

Although the developed strategy might not be suitable to achieve minimal global costs, specially in the case of time-varying costs, introducing this degree of freedom in the control of processes is of practical and theoretical interest because with few information about the process one can introduce a simple and intuitive economic purpose for TISO systems.

6.2.3 Proposal Description

The proposed strategy is applicable to TISO systems in which the two inputs are from different nature, thus yielding different operation costs. The simplicity of the approach lies in the fact that the operation costs of each input do not need to be precisely known. Actually, one only needs to know which of the inputs is the most expensive. Then, it is assumed that the economically optimal steady-state of the inputs happen when the most expensive one reaches zero.

The economic characteristics is introduced in the cost function of a GPC-based controller by adding a term which allows to adjust a desired value for the most expensive input, which is most often desired to be null at steady-state. A novel mid-ranging control structure is obtained, while, in the absence of input or output constraints, predictions are calculated by means of an observer-based structure.

6.3 Observer Based GPC

6.3.1 Prediction model

The CARIMA model for a TISO system is given by

$$\tilde{A} y_k = B_1 \Delta u_{1_{k-h_1}} + B_2 \Delta u_{2_{k-h_2}} + C e_k, \tag{6.2}$$

with

$$\tilde{A} = \Delta A = 1 + a_1 q^{-1} + \ldots + a_{n_a} q^{-n_a},$$

$$B_j = b_{j1} q^{-1} + \ldots + b_{jn_b} q^{-n_b},$$

$$C = 1 + c_1 q^{-1} + \ldots + c_{n_c} q^{-n_c},$$

where y_k is the system output, j is related to the $j-$th input, $u_{1_{k-h_1}}$, and $u_{2_{k-h_2}}$ are the delayed inputs, e_k is a zero mean white noise, q^{-1} is the unit discrete delay operator, and $\Delta = 1 - q^{-1}$ is the differencing operator. The CARIMA model (6.2) can be written as a state space representation in observable canonical form

$$
\begin{aligned}
x_{k+1} &= A x_k + B_1 \Delta u_{1_{k-h_1}} + B_2 \Delta u_{2_{k-h_2}} + D e_k, \\
y_k &= H x_k + e_k,
\end{aligned}
\tag{6.3}
$$

where

$$
A = \begin{bmatrix}
-a_1 & 1 & 0 & \ldots & 0 \\
-a_2 & 0 & 1 & & 0 \\
\vdots & & & \ddots & \vdots \\
& & & & 1 \\
-a_{n_a} & 0 & 0 & & 0
\end{bmatrix}, B_1 = \begin{bmatrix}
b_{11} \\
b_{12} \\
\vdots \\
b_{1n_{b_1}}
\end{bmatrix}, B_2 = \begin{bmatrix}
b_{21} \\
b_{22} \\
\vdots \\
b_{2n_{b_2}}
\end{bmatrix},
$$

$$
D = \begin{bmatrix}
c_1 - a_1 \\
c_2 - a_2 \\
\vdots \\
c_{n_c} - a_{n_a}
\end{bmatrix}, H = \begin{bmatrix} 1 & 0 & \ldots & 0 \end{bmatrix}.
\tag{6.4}
$$

6.3.2 Output predictions

The predicted output $\hat{y}_{k+i}$, $i = 1, \ldots, N$ can be computed recursively from (6.3), where N is the prediction horizon. Since e_k is a white noise with null mathematical expectation, its best predicted value is zero, yielding

$$
\begin{aligned}
\hat{y}_{k+1} &= \bar{H}\bar{A}x_k + \bar{H}\bar{D}e_k + \bar{H}\bar{B}\Delta u_k, \\
\hat{y}_{k+2} &= \bar{H}\bar{A}^2 x_k + \bar{H}\bar{A}\bar{D}e_k + \bar{H}\bar{A}\bar{B}\Delta u_k + \bar{H}\bar{B}\Delta u_{k+1}, \\
&\vdots \\
\hat{y}_{k+N} &= \bar{H}\bar{A}^N x_k + \bar{H}\bar{A}^{N-1}\bar{D}e_k + \bar{H}\bar{A}^{N-1}\bar{B}\Delta u_k + \bar{H}\bar{A}^{N-2}\bar{B}\Delta u_{k+1} + \ldots + \bar{H}\bar{B}\Delta u_{k+N-1},
\end{aligned}
\tag{6.5}
$$

where $\Delta u_k = \begin{bmatrix} \Delta u_{1_k} & \Delta u_{2_k} \end{bmatrix}^T$, and $\bar{A}$, $\bar{B} = \begin{bmatrix} \bar{B}_1 & \bar{B}_2 \end{bmatrix}$, $\bar{D}$, $\bar{H}$ are augmented matrices from (6.4) with appropriated dimensions that incorporate the input delays h_1 and h_2.

The predicted output (6.5) can be written in matrix form as

$$\mathbf{Y} = \mathbf{G}\Delta\mathbf{U} + \mathbf{f}, \tag{6.6}$$

where $\Delta\mathbf{U} = [\Delta u_k \ \Delta u_{k+1} \ \cdots \ \Delta u_{k+N-1}]^T$, and

$$\mathbf{f} = \mathbf{F}x_k + \mathbf{E}e_k,$$

$$\mathbf{Y} = \begin{bmatrix} \hat{y}_{k+1} \\ \hat{y}_{k+2} \\ \vdots \\ \hat{y}_{k+N} \end{bmatrix}, \mathbf{F} = \begin{bmatrix} \bar{\mathbf{H}}\bar{\mathbf{A}} \\ \bar{\mathbf{H}}\bar{\mathbf{A}}^2 \\ \vdots \\ \bar{\mathbf{H}}\bar{\mathbf{A}}^N \end{bmatrix}, \mathbf{E} = \begin{bmatrix} \bar{\mathbf{H}}\bar{\mathbf{D}} \\ \bar{\mathbf{H}}\bar{\mathbf{A}}\bar{\mathbf{D}} \\ \vdots \\ \bar{\mathbf{H}}\bar{\mathbf{A}}^{N-1}\bar{\mathbf{D}} \end{bmatrix}, \mathbf{G} = \begin{bmatrix} \bar{\mathbf{H}}\bar{\mathbf{B}} & 0 & \dots & 0 \\ \bar{\mathbf{H}}\bar{\mathbf{A}}\bar{\mathbf{B}} & \bar{\mathbf{H}}\bar{\mathbf{B}} & \dots & 0 \\ \vdots & \vdots & \ddots & \vdots \\ \bar{\mathbf{H}}\bar{\mathbf{A}}^{N-1}\bar{\mathbf{B}} & \bar{\mathbf{H}}\bar{\mathbf{A}}^{N-2}\bar{\mathbf{B}} & \dots & \bar{\mathbf{H}}\bar{\mathbf{B}} \end{bmatrix}. \tag{6.7}$$

In (6.6), $\mathbf{G}$ represents the system's dynamics matrix and $\mathbf{f}$ is the free response of the system, that is, the part of the response that does not depend on the future control actions (CAMACHO; BORDONS, 2007).

6.3.3 Cost function

The control signal at each sampling time can be obtained by minimizing the following cost function

$$J = (\mathbf{Y} - \mathbf{W})^T \mathbf{Q}(\mathbf{Y} - \mathbf{W}) + \Delta\mathbf{U}^T \mathbf{R}\Delta\mathbf{U}, \tag{6.8}$$

where $\mathbf{W} = \begin{bmatrix} r_{k+1} & r_{k+2} & \cdots & r_{k+N} \end{bmatrix}^T$ is the future reference of output, $\mathbf{Q}$ and $\mathbf{R}$ are weighting matrices of dimensions $N \times N$ and $2N_u \times 2N_u$, respectively, N is the prediction horizon, and N_u is the control horizon. The first term of (6.8) guarantees output setpoint tracking whereas the second ensures that the variation of control signals tends to zero, which ensures that the control signal does not grow indefinitely. Minimization of J for the unconstrained case leads to the optimum control sequence

$$\Delta\mathbf{U} = \left(\mathbf{G}^T \mathbf{Q}\mathbf{G} + \mathbf{R}\right)^{-1} \mathbf{G}^T \mathbf{Q}(\mathbf{W} - \mathbf{f}). \tag{6.9}$$

For the particular case of TISO systems, only the first two rows of $\Delta\mathbf{U}$ are applied to the process, thus

$$\Delta u_k = \mathbf{K}(\mathbf{W} - \mathbf{f}), \tag{6.10}$$

where $\mathbf{K}$ contains the first two rows of $(\mathbf{G}^T \mathbf{Q}\mathbf{G} + \mathbf{R})^{-1}\mathbf{G}^T \mathbf{Q}$.

6.3.4 Control structure

From (6.7) and (6.10) the control input can be written as

$$\Delta u_k = \mathbf{K}(\mathbf{W} - \mathbf{F}x_k - \mathbf{E}e_k). \tag{6.11}$$

Considering that the future reference is constant, that is, $\mathbf{W} = \begin{bmatrix} r_k & r_k & \cdots & r_k \end{bmatrix}^T$, one can write (6.11) as

$$\Delta u_k = \mathrm{K}_r r_k - \mathrm{K}_F x_k - \mathrm{K}_E e_k, \tag{6.12}$$

where $\mathrm{K}_r = \begin{bmatrix} \sum_{i=1}^N \mathbf{K}_{1i} & \sum_{i=1}^N \mathbf{K}_{2i} \end{bmatrix}^T$, $\mathrm{K}_F = \mathbf{KF}$, and $\mathrm{K}_E = \mathbf{KE}$ are constant matrices of dimensions 2×1, $2 \times n_a$, and 2×1, respectively.

A block diagram representation of the observer based GPC approach is the same as in Fig. 37 replacing A, B, D and H with $\bar{\mathrm{A}}$, $\bar{\mathrm{B}}$, $\bar{\mathrm{D}}$ and $\bar{\mathrm{H}}$.

6.4 Proposed Mid-ranging Control Systems

6.4.1 Model for prediction

For the proposed GPC-based mid-ranging control system (GPC-MR), the following CARIMA model of a TISO system is used

$$\tilde{A}y_k = \tilde{B}_1 u_{1_{k-h_1}} + \tilde{B}_2 u_{2_{k-h_2}} + Ce_k, \tag{6.13}$$

with

$$\tilde{A} = \Delta A = 1 + a_1 q^{-1} + \ldots + a_{n_a} q^{-n_a},$$
$$\tilde{B}_1 = \Delta B_1 = b_{11} q^{-1} + \ldots + b_{1n_{b_1}} q^{-n_{b_1}},$$
$$\tilde{B}_2 = \Delta B_2 = b_{21} q^{-1} + \ldots + b_{2n_{b_2}} q^{-n_{b_2}},$$
$$C = 1 + c_1 q^{-1} + \ldots + c_{n_c} q^{-n_c},$$

where y_k is the system output, $u_{1_{k-h_1}}$, and $u_{2_{k-h_2}}$ are the delayed inputs, e_k is a zero mean white noise, q^{-1} is the unit discrete delay operator, $\Delta = 1 - q^{-1}$ is the differencing operator, and n_a, n_{b_1}, n_{b_2}, and n_c are related with the order of the polynomials $\tilde{A}$, $\tilde{B}_1$, $\tilde{B}_2$, and C respectively. The CARIMA model (6.13) can be written as a state space representation in observable canonical form

$$\begin{aligned} x_{k+1} &= \mathrm{A}x_k + \mathrm{B}_1 u_{1_{k-h_1}} + \mathrm{B}_2 u_{2_{k-h_2}} + \mathrm{D}e_k, \\ y_k &= \mathrm{H}x_k + e_k, \end{aligned} \tag{6.14}$$

where

$$
A = \begin{bmatrix} -a_1 & 1 & 0 & \dots & 0 \\ -a_2 & 0 & 1 & & 0 \\ \vdots & & & \ddots & \vdots \\ & & & & 1 \\ -a_{n_a} & 0 & 0 & & 0 \end{bmatrix}, B_1 = \begin{bmatrix} b_{11} \\ b_{12} \\ \vdots \\ b_{1n_{b_1}} \end{bmatrix}, B_2 = \begin{bmatrix} b_{21} \\ b_{22} \\ \vdots \\ b_{2n_{b_2}} \end{bmatrix},
$$

$$
D = \begin{bmatrix} c_1 - a_1 \\ c_2 - a_2 \\ \vdots \\ c_{n_c} - a_{n_a} \end{bmatrix}, H = \begin{bmatrix} 1 & 0 & \dots & 0 \end{bmatrix}.
$$

$$(6.15)$$

6.4.2 Output predictions

The predicted output $\hat{y}_{k+i}$, $i = 1,...,N$ can be computed recursively from (6.14), where N is the prediction horizon. Since e_k is a white noise with null mathematical expectation, its best predicted value is zero, yielding

$$
\begin{aligned}
\hat{y}_{k+1} &= \bar{H}\bar{A}x_k + \bar{H}\bar{D}e_k + \bar{H}\bar{B}u_k, \\
\hat{y}_{k+2} &= \bar{H}\bar{A}^2 x_k + \bar{H}\bar{A}\bar{D}e_k + \bar{H}\bar{A}\bar{B}u_k + \bar{H}\bar{B}u_{k+1}, \\
&\vdots \\
\hat{y}_{k+N} &= \bar{H}\bar{A}^N x_k + \bar{H}\bar{A}^{N-1}\bar{D}e_k + \bar{H}\bar{A}^{N-1}\bar{B}u_k + \bar{H}\bar{A}^{N-2}\bar{B}u_{k+1} + \dots + \bar{H}\bar{B}u_{k+N-1},
\end{aligned}
$$

$$(6.16)$$

where $u_k = \begin{bmatrix} u_{1_k} & u_{2_k} \end{bmatrix}^T$, and $\bar{A}$, $\bar{B} = \begin{bmatrix} \bar{B}_1 & \bar{B}_2 \end{bmatrix}$, $\bar{D}$, $\bar{H}$ are augmented matrices from (6.15) with appropriated dimensions that incorporate the input delays h_1 and h_2.

The predicted output (6.16) can be written in matrix form as

$$
\mathbf{Y} = \mathbf{G}\mathbf{U} + \mathbf{f}, \tag{6.17}
$$

where $\mathbf{U} = \begin{bmatrix} u_k & u_{k+1} & \dots & u_{k+N-1} \end{bmatrix}^T$, and

$$
\mathbf{f} = \mathbf{F}x_k + \mathbf{E}e_k,
$$

$$
\mathbf{Y} = \begin{bmatrix} \hat{y}_{k+1} \\ \hat{y}_{k+2} \\ \vdots \\ \hat{y}_{k+N} \end{bmatrix}, \mathbf{F} = \begin{bmatrix} \bar{H}\bar{A} \\ \bar{H}\bar{A}^2 \\ \vdots \\ \bar{H}\bar{A}^N \end{bmatrix}, \mathbf{E} = \begin{bmatrix} \bar{H}\bar{D} \\ \bar{H}\bar{A}\bar{D} \\ \vdots \\ \bar{H}\bar{A}^{N-1}\bar{D} \end{bmatrix}, \mathbf{G} = \begin{bmatrix} \bar{H}\bar{B} & 0 & \dots & 0 \\ \bar{H}\bar{A}\bar{B} & \bar{H}\bar{B} & \dots & 0 \\ \vdots & \vdots & \ddots & \vdots \\ \bar{H}\bar{A}^{N-1}\bar{B} & \bar{H}\bar{A}^{N-2}\bar{B} & \dots & \bar{H}\bar{B} \end{bmatrix}.
$$

$$(6.18)$$

6.4.3   Cost Function

Considering a TISO process, a cost function is proposed as

$$J = (\mathbf{Y} - \mathbf{W})^T \mathbf{Q}(\mathbf{Y} - \mathbf{W}) + \Delta \mathbf{U}_1^T \mathbf{R}_1 \Delta \mathbf{U}_1 + (\mathbf{U}_2 - \mathbf{U}_r)^T \mathbf{R}_2 (\mathbf{U}_2 - \mathbf{U}_r), \tag{6.19}$$

where $\mathbf{W} = \begin{bmatrix} r_{k+1} & \cdots & r_{k+N} \end{bmatrix}^T$ is the future reference of the output, $\mathbf{U}_r = \begin{bmatrix} u_{r_{k+1}} & \cdots & u_{r_{k+N_u}} \end{bmatrix}^T$ is the future reference of u_2, $\mathbf{Q} = diag(q_1, ..., q_N)$, $\mathbf{R}_1 = diag(r_{11}, ..., r_{1N_u})$ and $\mathbf{R}_2 = diag(r_{21}, ..., r_{2N_u})$ are weighting matrices. In this situation, signal u_2 is an input which is more expensive than input u_{1_k}. Vector $\mathbf{U}_r$ is chosen to force u_2 to reach an interest value. Based on a simple economic context, and considering the simplest case, where costs are not time-varying and there are no performance conditions imposed for the output y_k, the control reference can be chosen as $\mathbf{U}_r = \begin{bmatrix} 0 & 0 & \cdots & 0 \end{bmatrix}^T$. In this case, u_2 will only act in the process when necessary.

Cost function (6.19) can be rewritten as

$$J = (\mathbf{Y} - \mathbf{W})^T \mathbf{Q}(\mathbf{Y} - \mathbf{W}) + (\mathbf{MU}_1 - \mathbf{U}_0)^T \mathbf{R}_1 (\mathbf{MU}_1 - \mathbf{U}_0) + (\mathbf{U}_2 - \mathbf{U}_r)^T \mathbf{R}_2 (\mathbf{U}_2 - \mathbf{U}_r), \tag{6.20}$$

where

$$\mathbf{M} = \begin{bmatrix} 1 & 0 & \cdots & 0 & 0 \\ -1 & 1 & \cdots & 0 & 0 \\ \vdots & \vdots & \ddots & \vdots & \vdots \\ 0 & 0 & \cdots & -1 & 1 \end{bmatrix}, \mathbf{U}_0 = \begin{bmatrix} u_{1_{k-1}} \\ 0 \\ \vdots \\ 0 \end{bmatrix}.$$

Replacing (6.17) in (6.20) and applying some algebraic manipulations, the following quadratic cost function is obtained

$$J = \mathbf{U}^T (\mathbf{G}^T \mathbf{Q} \mathbf{G} + \mathbf{R}) \mathbf{U} + 2((\mathbf{f} - \mathbf{W})^T \mathbf{Q} \mathbf{G} + \mathbf{V}) \mathbf{U} + (\mathbf{f} - \mathbf{W})^T \mathbf{Q}(\mathbf{f} - \mathbf{W}), \tag{6.21}$$

where

$$\mathbf{R} = \begin{bmatrix} r_{11} + r_{12} & 0 & -r_{12} & 0 & 0 & \cdots & 0 \\ 0 & r_{21} & 0 & 0 & 0 & \cdots & 0 \\ -r_{12} & 0 & r_{12} + r_{13} & 0 & -r_{13} & \cdots & 0 \\ 0 & 0 & 0 & r_{22} & 0 & \cdots & 0 \\ 0 & 0 & -r_{13} & 0 & r_{13} + r_{14} & \cdots & 0 \\ \vdots & \vdots & \vdots & \vdots & \vdots & \ddots & \vdots \\ 0 & 0 & 0 & 0 & 0 & \cdots & r_{2N_u} \end{bmatrix}, \tag{6.22}$$

$$\mathbf{V} = -\begin{bmatrix} r_{11} u_{1_{k-1}} & u_{r_k} r_{21} & 0 & u_{r_k} r_{22} & 0 & \cdots & u_{r_k} r_{2N_u} \end{bmatrix}.$$

Minimization of (6.21) for the unconstrained case leads to the optimum control sequence

$$\mathbf{U} = \left(\mathbf{G}^T\mathbf{Q}\mathbf{G} + \mathbf{R}\right)^{-1}\left(\mathbf{G}^T\mathbf{Q}(\mathbf{W} - \mathbf{f}) - \mathbf{V}^T\right). \tag{6.23}$$

For the particular case of TISO systems, only the first two rows of $\mathbf{U}$ are applied to the process, thus

$$u_k = \mathbf{K}(\mathbf{W} - \mathbf{f}) - \mathbf{Ku}\mathbf{V}^T, \tag{6.24}$$

where $\mathbf{K}$ and $\mathbf{Ku}$ contain the first two rows of $\left(\mathbf{G}^T\mathbf{Q}\mathbf{G} + \mathbf{R}\right)^{-1}\mathbf{G}^T\mathbf{Q}$ and $\left(\mathbf{G}^T\mathbf{Q}\mathbf{G} + \mathbf{R}\right)^{-1}$ respectivelly.

6.4.4   Control structure

From (6.18) and (6.24), and assuming that the future references of the output and control signal u_2 are constant, that is, $\mathbf{W} = \begin{bmatrix} r_k & r_k & \cdots & r_k \end{bmatrix}^T$ and $\mathbf{U}_r = \begin{bmatrix} u_{r_k} & u_{r_k} & \cdots & u_{r_k} \end{bmatrix}^T$, the optimal control is given by

$$u_k = \mathbf{K}_r r_k - \mathbf{K}_F x_k - \mathbf{K}_E e_k - \mathbf{K}_P u_{k-1} - \mathbf{K}_{ur} u_{r_k}, \tag{6.25}$$

where

$$\mathbf{K}_r = \begin{bmatrix} \sum_{i=1}^N \mathbf{K}_{1i} & \sum_{i=1}^N \mathbf{K}_{2i} \end{bmatrix}^T, \mathbf{K}_P = -\begin{bmatrix} r_{11}\mathbf{K}_{\mathbf{u}_{11}} & 0 \\ r_{11}\mathbf{K}_{\mathbf{u}_{21}} & 0 \end{bmatrix},$$

$$\mathbf{K}_{ur} = -\begin{bmatrix} \sum_{i=1}^{N_u} r_{2i}\mathbf{K}_{\mathbf{u}_{1(2i)}} & \sum_{i=1}^{N_u} r_{2i}\mathbf{K}_{\mathbf{u}_{2(2i)}} \end{bmatrix}^T,$$

and $\mathbf{K}_F = \mathbf{KF}$, and $\mathbf{K}_E = \mathbf{KE}$ are constant matrices of dimensions 2×1, $2 \times n_a$, and 2×1, respectively.

The implementation structure of the proposed controller is shown in Fig. 50.

6.4.5   Constrained case

Equation (6.23) computes the optimal value of $\mathbf{U}$ only when there is no violation in the process constraints, thus (6.25) does not guarantee the optimum control sequence when constraints are violated (CAMACHO; BORDONS, 2007).

According to (CAMACHO; BORDONS, 2007), when constraints must be taken into account the solution can be obtained by a Quadratic Programming (QP) algorithm. That way, a

Figure 50 – Implementation structure of the proposed controller.
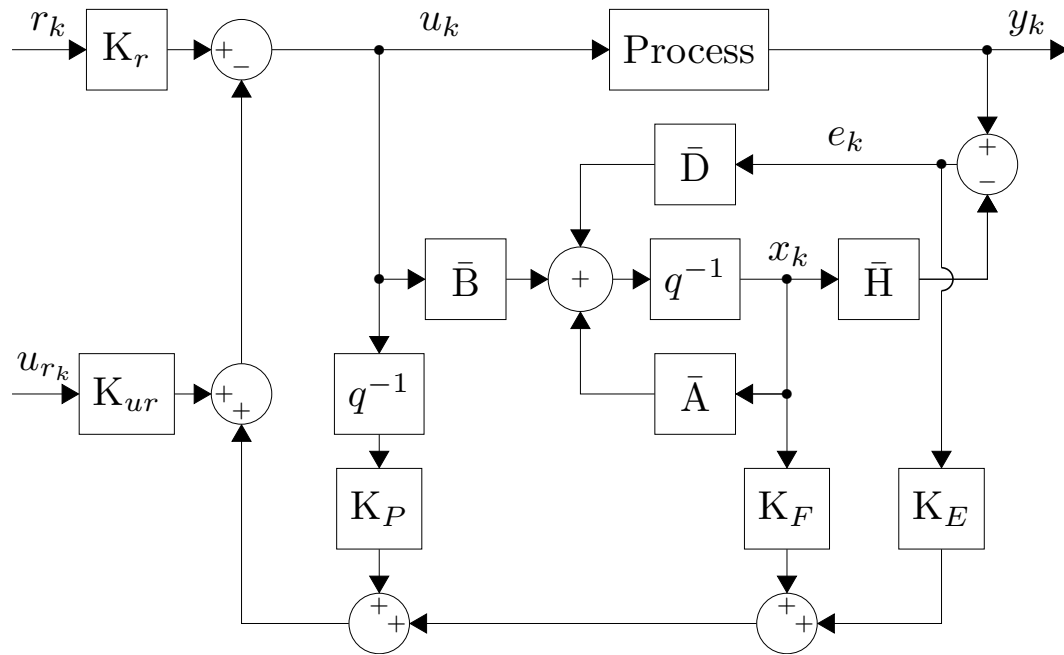
QP algorithm can be used to minimize (6.21) subject to $L\mathbf{U} \leq d$. Considering constraints on the output signals amplitude, slew rate and amplitude limits on the actuator, L and d can be defined as

$$L = \begin{bmatrix} \mathbf{G} \\ -\mathbf{G} \\ \mathbf{M} \\ -\mathbf{M} \\ I \\ -I \end{bmatrix}, d = \begin{bmatrix} \mathbf{Y}_{max} - \mathbf{f} \\ -\mathbf{Y}_{min} + \mathbf{f} \\ \Delta\mathbf{U}_{max} + \mathbf{U}_0 \\ -\Delta\mathbf{U}_{max} - \mathbf{U}_0 \\ \mathbf{U}_{max} \\ -\mathbf{U}_{min} \end{bmatrix},$$

where $\begin{bmatrix} \mathbf{Y}_{max} & \mathbf{Y}_{min} \end{bmatrix}$, $\begin{bmatrix} \Delta\mathbf{U}_{max} & \Delta\mathbf{U}_{min} \end{bmatrix}$, and $\begin{bmatrix} \mathbf{U}_{max} & \mathbf{U}_{min} \end{bmatrix}$ define allowed range of $\mathbf{Y}$, $\Delta\mathbf{U}$, and $\mathbf{U}$.

6.5 Case Study

6.5.1 Simulation results

Let us consider the temperature control of the process presented in (FLESCH *et al.*, 2011)

$$P(z) = \begin{bmatrix} \dfrac{0.1z^{-4}}{z - 0.99} & \dfrac{-0.5z^{-1}}{z - 0.47} \end{bmatrix}. \tag{6.26}$$

This process has two inputs and one output. From (6.26) it can be seen that the transfer function from the second input u_2 to the output presents smaller transport delay and time constant, and higher gain when compared to the first input u_1. Such observations are important as they mean that the output will be more sensitive to changes in u_2.

Consider now that, in an economic context, input u_2 is more expensive than u_1. In this situation u_2 should be kept as close as possible to zero. This goal can be achieved by defining $u_{r_k} = 0$ in (6.25).

Fig. 53 shows results for the proposed GPC-MR and GPC controllers for a reference step change applied to the system at time $t = 1$ *min*. Additionally, an input disturbance of magnitude 1 is applied in u_1 at time $t = 20$ *min*. Both controllers were adjusted to present similar output response when no constraints are considered. The proposed controller was tuned with $N = 12$, $N_u = 5$, $R_1 = diag(0, ..., 0)$, and $R_2 = diag(0.1, ..., 0.1)$. The GPC was tuned with $N = 12$, $N_u = 1$, and $R = diag(0, 0.1, ..., 0, 0.1)$.

Figure 51 – Comparison between the proposed controller and GPC.
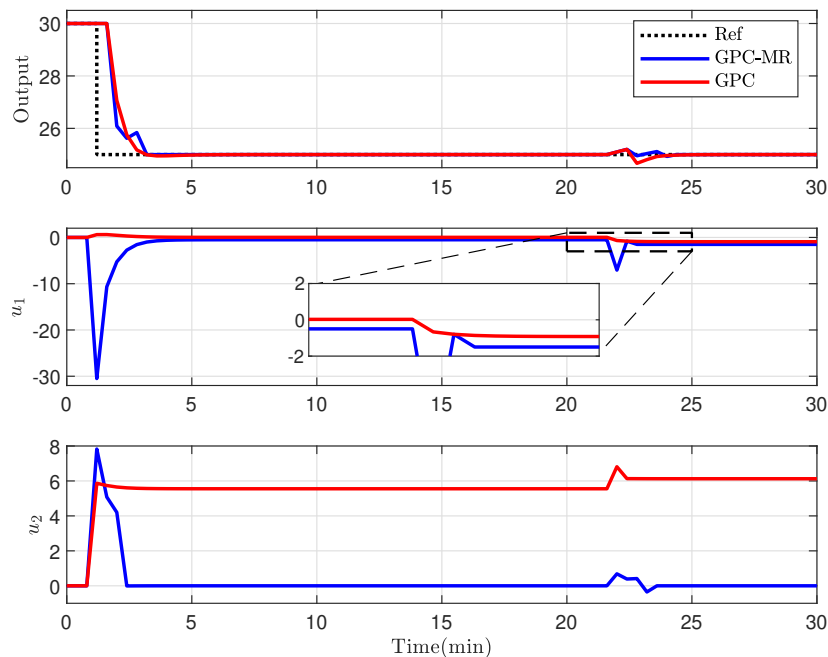
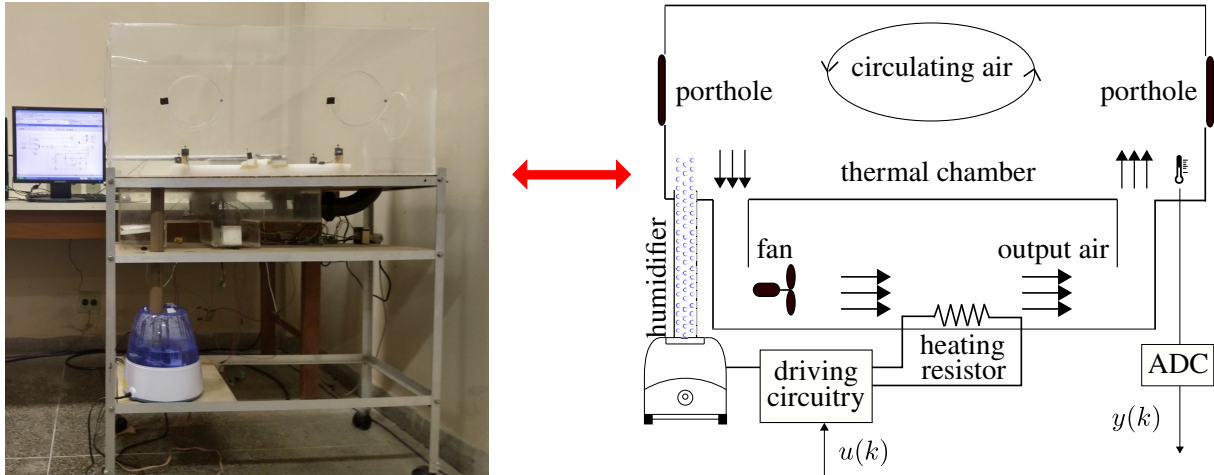Source: The author.

Note from Fig. 51 that for GPC-MR the input u_2 reached the desired value designated by its reference, while for the GPC the signal stabilizes close to 5.5. When the disturbance was applied, the input u_2 increased its steady-state value for the GPC. For the GPC-MR, on the other hand, u_2 quickly returned to zero. This behavior of the GPC-MR is expected since its cost

function allows one to adjust the reference value of u_2.

6.5.2 Experimental results

Figure 52 – Thermal chamber prototype and illustrating diagram.

Source: The author.

Now let us consider the temperature control of the thermal chamber prototype in Fig. 52, which was recently presented in (TORRICO *et al.*, 2018; PEREIRA *et al.*, 2017). The device consists of a rigid boxlike acrylic dome which enclosures the controlled environment. The prototype basically includes an AC-powered heater, an air humidifier, a fan to circulate the warmed air, and relative humidity and temperature transducers. Fresh air is driven by the fan towards the heating element and then the warmed air goes into the chamber. The humidifier is connected directly to the boxlike environment. The power delivered to the heating resistor is controlled by the duty cycle of a switching power supply. Additionally, an ultrasonic humidifier located under the dome outputs the cold steam to the dome through a pipe. The steam flow of the humidifier is controlled using a circuit based on a light dependent resistor.

The process model from the two control inputs to the process variable (temperature in °C inside the chamber) using step tests and an offline least squares identification method is given by

$$P(z) = \left[\frac{0.09006(z+0.4274)z^{-10}}{z-0.9946} \quad \frac{-0.076651}{z-0.9317} \right], \tag{6.27}$$

where the sampling time is $T_s = 0.2$ min. This process has two inputs and one output. The first input u_1 represents the duty cycle of a switching power supply that delivers power to the heating resistor, while the second input u_2 represents the duty cycle used to drive the steam flow of the humidifier.

From (6.27) it can be seen that the transfer function from the second input u_2 to the output presents null transport delay and smaller time constant when compared to the first input u_1, which implies that the output will be more sensitive to changes in u_2. Also note that due to its negative gain, the humidifier can only contribute to speed up the cooling process inside the dome. On the other hand, the heating resistor control signal u_1 plays a bigger role when it is desired to increase the temperature.

Consider now that input u_2 is more expensive than u_1, and similarly to the simulation case, in this situation the economically optimal steady-state of the inputs happen when $u_{r_k} = 0$ in (6.25).

Fig. 53 shows experimental results for the proposed controller for reference step changes applied to the system at times $t = 0$ min and $t = 70$ min. Additionally, the portholes remained opened from $t = 117$ min to $t = 125$ min in order to insert disturbances in the system and assess controller robustness. The proposed controller was tuned with $N = 20$, $N_u = 10$, $R_1 = diag(0.5, ..., 0.5)$, and $R_2 = diag(0.1, ..., 0.1)$.

Figure 53 – Temperature control of thermal chamber using the proposed GPC-MR.
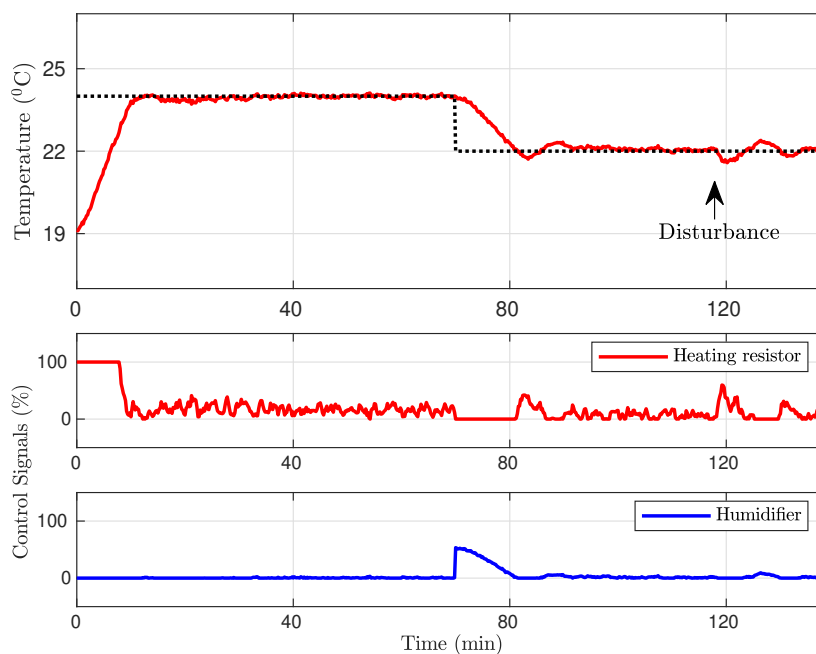
Source: The author.

Note from Fig. 53 that the output was able to reach the desired reference in both step change scenarios, that is, heating and cooling phases. Furthermore, disturbance rejection

was quickly achieved, demonstrating good robustness characteristics of the proposed structure. Furthermore, also note that the input u_2 reached the desired value designated by its reference in all scenarios, even when the disturbance was applied. This behavior of the proposed controller is expected since its cost function allows one to adjust the reference value of u_2. Note that u_1 behaves aggressively because of its lower cost when compared to u_2. Therefore, proposed controller reaches its desired behavior, either in an economic context or when it is desirable to keep one of the inputs at a previously defined steady-state value.

6.6 Discussion

This work presented a GPC-based mid-ranging approach to the traditional steady-state set-point tracking GPC. The GPC is formulated with a cost function that considers output tracking and penalizes the deviation of the control signals, while the proposed approach further considers a cost function which assembles an economic purpose for TISO systems. The proposed cost function is intended to reduce the use of the expensive input by defining its future reference as zero.

From the experimental results it can be observed that the proposed economic cost function achieved the expected results, i.e., the most expensive input is used only during transient phases, while reference tracking to its set-point at steady-state regime is obtained.

This work has shown some preliminary, but promising results toward an observer based economic model predictive approach for TISO systems. Future work is intended in order to consider possible time-varying costs of the inputs and further study stability of the proposal.

7 CONCLUSION

This work presented contributions on model-based controllers applied to the control of dead-time systems. Ease of tuning, and good reference tracking, disturbance rejection, noise attenuation and robustness characteristics are desired to any control system, and these aspects were taken into account in the design of the proposed controllers. This work presented proposals capable of dealing with continuous-time and discrete-time, SISO/MIMO, stable, unstable and integrative dead-time systems. In addition, an important contribution of this work is the extension of the filtered Smith predictor to state-space models with an internally stable structure for open-loop unstable process. Simulations and experiments were carried out in order to show the benefits of the proposed solutions over recent works from literature.

The main contributions of this work are:

1. New tuning method that simultaneously accounts for closed-loop robustness and noise attenuation for stable, unstable and integrative dead-time processes. It was shown that lower order filters are suitable to satisfy design specifications and provide enhanced performance when compared to more complex controllers from recent literature. In case stronger noise attenuation is required, the method allows to monotonically tune the robustness filter while maintaining desired performance characteristics. More specifically:

   - Three different robustness filters are presented. One to deal with FOPDT processes and two which can be tuned for SOPDT industrial processes;

   - Each filter presents two adjustment parameters that allow disturbance rejection and noise attenuation to be individually tuned to meet a desired trade-off, while frequency domain analysis of such characteristics is presente;

   - Such nice decomposition is achieved by using different poles in the robustness filter instead of the traditional design of DTCs which employs multiple repeated poles.

2. The extension of the simplified filtered Smith predictor to state-space models. The proposed structure is simpler than others recently proposed in the literature and can be applied to continuous-time or discrete-time systems. Furthermore, it allows improving rejection of both matched and unmatched disturbances, while also enhancing noise attenuation and robustness characteristics. Finite spectrum assignment (FSA) based implementation is used in order to guarantee the internal stability of the proposed controller. The key

advantages are:

- Simplified design through the SFP approach;
- FSA-based implementation, which provides internal stability for open-loop unstable process;
- Enhanced rejection of disturbances.

3. A general approach for controlling SISO/MIMO dead-time processes using the GPC. The approach employs state-space models for prediction while the control structure is in an observer-based form with two feedback gains, which implies the simplicity of the approach. Furthermore, an equivalent dead-time compensator structure for analysis purposes is presented, which yield some advantages over previously proposed strategies:

- A unified framework for the tuning of SISO/MIMO square/non-square processes with dead time. The controller order of the proposed implementation structure is equivalent to that of other dead-time compensators;
- A simplified tuning approach for the GPC-based strategy. In the proposed strategy, the number of tuning parameters is reduced to three and can be chosen by intuitive rules;
- Such nice obtained tuning rules yield enhanced set-point tracking, robustness, and disturbance rejection properties when compared to recently proposed DTC structures for the control of dead-time processes. Furthermore, results have shown that the effect of coupling between the process variables is reduced in the proposed strategy.

4. A GPC-based mid-ranging approach to the traditional steady-state set-point tracking GPC. The GPC is formulated with a cost function that considers output tracking and penalizes the deviation of the control signals, while the proposed approach further considers a cost function which assembles a simple and intuitive economic purpose for TISO systems. The proposed cost function is intended to reduce the use of the expensive input by defining its future reference as zero.

7.1 Future Work

The following ideas are under development:

1. A proposal to enhance the disturbance rejection of the GPC by including a model of the output disturbance into the control law.

2. Inclusion of event-triggered mechanisms for predictor-based structures applied to the control of dead-time systems.

BIBLIOGRAPHY

ALANQAR, A.; DURAND, H.; CHRISTOFIDES, P. D. Fault-tolerant economic model predictive control using error-triggered online model identification. **Industrial & Engineering Chemistry Research**, v. 56, n. 19, p. 5652–5667, 2017.

ALLISON, B. J.; ISAKSSON, A. J. Design and performance of mid-ranging controllers. **Journal of Process Control**, v. 8, n. 5, p. 469 – 474, 1998. ISSN 0959-1524. ADCHEM '97 IFAC Symposium: Advanced Control of Chemical Processes.

ARTSTEIN, Z. Linear systems with delayed controls: A reduction. **IEEE Transactions on Automatic Control**, v. 27, n. 4, p. 869–879, 1982. ISSN 0018-9286.

ASTRÖM, K. J.; HÄGGLUND, T. **PID controllers: theory, design, and tuning**. [S.l.]: Instrument society of America Research Triangle Park, NC, 1995. v. 2.

BAYER, F. A.; LORENZEN, M.; MüLLER, M. A.; ALLGöWER, F. Improving performance in robust economic mpc using stochastic information. **IFAC-PapersOnLine**, v. 48, n. 23, p. 410 – 415, 2015. ISSN 2405-8963. 5th IFAC Conference on Nonlinear Model Predictive Control NMPC 2015.

BEGUM, K. G.; RAO, A. S.; RADHAKRISHNAN, T. K. Optimal controller synthesis for second order time delay systems with at least one RHP pole. **ISA Trans**, v. 73, p. 181–188, 2018. ISSN 0019-0578.

CAMACHO, E. F.; BORDONS, C. **Model Predictive control**. [S.l.]: Springer London, 2007.

CASTILLO, A.; GARCÍA, P. Predicting the future state of disturbed lti systems: A solution based on high-order observers. **Automatica**, v. 124, p. 109365, 2021. ISSN 0005-1098.

CHEN, J.; HE, Z.-F.; QI, X. A new control method for MIMO first order time delay non-square systems. **Journal of Process Control**, v. 21, n. 4, p. 538–546, 2011. ISSN 0959-1524.

CLARKE, D. W.; MOHTADI, C.; TUFFS, P. S. Generalized predictive control—Part I. The basic algorithm. **Automatica**, v. 23, n. 2, p. 137–148, 1987. ISSN 0005-1098.

CUTLER, C.; RAMAKER, B. Dynamic matrix control - a computer control algorithm. In: **Automatic Control Conference, San Francisco**. [S.l.: s.n.], 1980.

ELLIS, M.; DURAND, H.; CHRISTOFIDES, P. D. A tutorial review of economic model predictive control methods. **Journal of Process Control**, v. 24, n. 8, p. 1156 – 1178, 2014. ISSN 0959-1524. Economic nonlinear model predictive control.

ELLIS, M.; LIU, J.; CHRISTOFIDES, P. D. **Economic Model Predictive Control: Theory, Formulations and Chemical Process Applications (Advances in Industrial Control)**. [S.l.]: Springer, 2016.

FILHO, M. P. de A.; LIMA, T. A.; TORRICO, B. C.; NOGUEIRA, F. G. Observer Based Approach for the Economic Predictive Control of a TISO System. In: IFAC. **6th IFAC Conference on Nonlinear Model Predictive Control, Madison, Wisconsin (USA)**. [S.l.], 2018.

FLESCH, R. C. C.; SANTOS, T. L. M.; NORMEY-RICO, J. E. Unified approach for minimal output dead time compensation in MIMO non-square processes. In: **2012 IEEE 51st IEEE Conference on Decision and Control (CDC)**. [S.l.: s.n.], 2012. p. 2376–2381. ISSN 0191-2216.

FLESCH, R. C. C.; TORRICO, B. C.; NORMEY-RICO, J. E.; CAVALCANTE, M. U. Unified approach for minimal output dead time compensation in MIMO processes. **Journal of Process Control**, v. 21, n. 7, p. 1080–1091, 2011.

FURTAT, I.; FRIDMAN, E.; FRADKOV, A. Disturbance Compensation With Finite Spectrum Assignment for Plants With Input Delay. **IEEE Transactions on Automatic Control**, v. 63, n. 1, p. 298–305, jan 2018.

GARCÍA, P.; ALBERTOS, P. A new dead-time compensator to control stable and integrating processes with long dead-time. **Automatica**, v. 44, n. 4, p. 1062–1071, 2008. ISSN 0005-1098.

GARCÍA, P.; ALBERTOS, P. Dead-time-compensator for unstable MIMO systems with multiple time delays. **Journal of Process Control**, v. 20, n. 7, p. 877–884, 2010.

GARCÍA, P.; ALBERTOS, P. Robust tuning of a generalized predictor-based controller for integrating and unstable systems with long time-delay. **Journal of Process Control**, v. 23, n. 8, p. 1205–1216, 2013. ISSN 0959-1524.

GIRALDO, S. A. C.; FLESCH, R. C. C.; NORMEY-RICO, J. E.; SEJAS, M. Z. P. A Method for Designing Decoupled Filtered Smith Predictor for Square MIMO Systems With Multiple Time Delays. **IEEE Transactions on Industry Applications**, v. 54, n. 6, p. 6439–6449, nov 2018. ISSN 0093-9994.

HÄGGLUND, T. An industrial dead-time compensating pi controller. **Control Engineering Practice**, v. 4, n. 6, p. 749 – 756, 1996. ISSN 0967-0661.

Haus, T.; Ivanovic, A.; Car, M.; Orsag, M.; Bogdan, S. Mid-ranging control concept for a multirotor uav with moving masses. In: **2018 26th Mediterranean Conference on Control and Automation (MED)**. [S.l.: s.n.], 2018. p. 339–344. ISSN 2473-3504.

JOHNSSON, O.; SAHLIN, D.; LINDE, J.; LIDéN, G.; HäGGLUND, T. A mid-ranging control strategy for non-stationary processes and its application to dissolved oxygen control in a bioprocess. **Control Engineering Practice**, v. 42, p. 89 – 94, 2015. ISSN 0967-0661.

KWON, W.; PEARSON, A. Feedback stabilization of linear systems with delayed control. **IEEE Transactions on Automatic Control**, v. 25, n. 2, p. 266–269, 1980. ISSN 0018-9286.

LÉCHAPPÉ, V.; MOULAY, E.; PLESTAN, F.; GLUMINEAU, A.; CHRIETTE, A. New predictive scheme for the control of LTI systems with input delay and unknown disturbances. **Automatica**, v. 52, p. 179–184, 2015. ISSN 0005-1098.

LEE, T. H.; WANG, Q. G.; TAN, K. K. Robust smith-predictor controller for uncertain delay systems. **AIChE Journal**, v. 42, n. 4, p. 1033–1040, 1996.

LIMA, T. A.; de Almeida Filho, M. P.; TORRICO, B. C.; NOGUEIRA, F. G.; CORREIA, W. B. A practical solution for the control of time-delayed and delay-free systems with saturating actuators. **European Journal of Control**, v. 51, p. 53–64, 2020. ISSN 0947-3580.

LIMA, T. A.; TARBOURIECH, S.; GOUAISBAUT, F.; FILHO, M. P. d. A.; GARCÍA, P. G.; TORRICO, B. C.; NOGUEIRA, F. G. Analysis and experimental application of a dead-time compensator for input saturated processes with output time-varying delays. **IET Control Theory and Applications**, Institution of Engineering and Technology, v. 15, n. 4, p. 580–593, mar. 2021.

LIMA, T. A.; TORRICO, B. C.; FILHO, M. P. D. A.; FORTE, M. D. N.; PEREIRA, R. D. O.; NOGUEIRA, F. G. First-order dead-time compensation with feedforward action. In: **2019 18th European Control Conference (ECC)**. [S.l.: s.n.], 2019. p. 3638–3643.

LIU, T.; GAO, F. Enhanced IMC design of load disturbance rejection for integrating and unstable processes with slow dynamics. **ISA Trans.**, v. 50, n. 2, p. 239–248, 2011.

LIU, T.; GARCÍA, P.; CHEN, Y.; REN, X.; ALBERTOS, P.; SANZ, R. New Predictor and 2DOF Control Scheme for Industrial Processes With Long Time Delay. **IEEE Transactions on Industrial Electronics**, v. 65, n. 5, p. 4247–4256, 2018. ISSN 0278-0046.

LIU, T.; TIAN, H.; RONG, S.; ZHONG, C. Heating-up control with delay-free output prediction for industrial jacketed reactors based on step response identification. **ISA Transactions**, v. 83, p. 227–238, 2018. ISSN 0019-0578.

LUAN, X.; CHEN, Q.; ALBERTOS, P.; LIU, F. Compensator design based on inverted decoupling for non-square processes. **IET Control Theory Applications**, v. 11, n. 7, p. 996–1005, 2017. ISSN 1751-8644.

Ma, Z.; Hong, G.; Ang, M. H.; Poo, A. Mid-ranging control of a macro/mini manipulator. In: **2015 IEEE International Conference on Advanced Intelligent Mechatronics (AIM)**. [S.l.: s.n.], 2015. p. 755–760. ISSN 2159-6247.

MANITIUS, A. Z.; OLBROT, A. Finite spectrum assignment problem for systems with delays. **IEEE Transactions on Automatic Control**, v. 24, n. 4, p. 541–552, 1979.

MATAUŠEK, M. R.; MICIĆ, A. D. A modified Smith predictor for controlling a process with an integrator and long dead-time. **IEEE Transactions on Automatic Control**, v. 41, n. 8, p. 1199–1203, 1996. ISSN 0018-9286.

MATAUŠEK, M. R.; RIBIĆ, A. I. Control of stable, integrating and unstable processes by the Modified Smith Predictor. **Journal of Process Control**, v. 22, n. 1, p. 338–343, 2012. ISSN 0959-1524.

MERCADER, P.; BAÑOS, A. A PI tuning rule for integrating plus dead time processes with parametric uncertainty. **ISA Trans**, v. 67, p. 246–255, 2017. ISSN 0019-0578.

MORARI, M.; ZAFIRIOU, E. **Robust Process Control**. [S.l.]: Prentice Hall, 1989.

NOGUEIRA, F. G.; BARREIROS, J. A. L.; BARRA, W.; COSTA, C. T.; FERREIRA, A. M. D. Development and field tests of a damping controller to mitigate electromechanical oscillations on large diesel generating units. **Electr Pow Syst**, v. 81, n. 2, p. 725–732, 2011. ISSN 0378-7796.

NORMEY-RICO, J. E.; BORDONS, C.; CAMACHO, E. F. Improving the robustness of dead-time compensating PI controllers. **Control Engineering Practice**, v. 5, n. 6, p. 801–810, 1997. ISSN 0967-0661.

NORMEY-RICO, J. E.; CAMACHO, E. F. Multivariable generalised predictive controller based on the Smith predictor. **IEE Proceedings - Control Theory and Applications**, v. 147, n. 5, p. 538–546, 2000. ISSN 1350-2379.

NORMEY-RICO, J. E.; CAMACHO, E. F. Robust design of GPC for processes with time delay. **International Journal of Robust and Nonlinear Control**, v. 10, n. 13, p. 1105–1127, 2000.

NORMEY-RICO, J. E.; CAMACHO, E. F. **Control of dead-time processes**. Berlin London: Springer, 2007.

NORMEY-RICO, J. E.; CAMACHO, E. F. Dead-time compensators: A survey. **Control Engineering Practice**, v. 16, n. 4, p. 407–428, 2008. ISSN 0967-0661.

NORMEY-RICO, J. E.; CAMACHO, E. F. Unified approach for robust dead-time compensator design. **Journal of Process Control**, v. 19, n. 1, p. 38–47, 2009.

NORMEY-RICO, J. E.; FLESCH, R. C. C.; SANTOS, T. L. M. Unified dead-time compensation structure for SISO processes with multiple dead times. **ISA Transactions**, v. 53, n. 6, p. 1865–1872, 2014.

NOWAK, P.; CZECZOT, J. Practical verification of active disturbance rejection controller for the pneumatic setup. In: **2017 22nd International Conference on Methods and Models in Automation and Robotics (MMAR)**. [S.l.: s.n.], 2017. p. 19–24.

PALMOR, Z. Stability properties of smith dead-time compensator controllers. **International Journal of Control**, Taylor & Francis, v. 32, n. 6, p. 937–949, 1980.

PALMOR, Z.; HALEVI, Y. On the design and properties of multivariable dead time compensators. **Automatica**, v. 19, n. 3, p. 255 – 264, 1983. ISSN 0005-1098.

PANDA, R. C. Synthesis of PID controller for unstable and integrating processes. **Chem Eng Sci.**, v. 64, n. 12, p. 2807–2816, 2009. ISSN 0009-2509.

PAWLOWSKI, A.; GUZMAN, J. L.; BERENGUEL, M.; NORMEY-RICO, J. E.; DORMIDO, S. Event-Based GPC for Multivariable Processes: A Practical Approach With Sensor Deadband. **IEEE Transactions on Control Systems Technology**, v. 25, n. 5, p. 1621–1633, 2017. ISSN 1063-6536.

PEREIRA, M.; LIMON, D.; ALAMO, T.; VALVERDE, L. Application of periodic economic mpc to a grid-connected micro-grid. **IFAC-PapersOnLine**, v. 48, n. 23, p. 513 – 518, 2015. ISSN 2405-8963. 5th IFAC Conference on Nonlinear Model Predictive Control NMPC 2015.

PEREIRA, R. D.; VERONESI, M.; VISIOLI, A.; NORMEY-RICO, J. E.; TORRICO, B. C. Implementation and test of a new autotuning method for pid controllers of tito processes. **Control Engineering Practice**, v. 58, p. 171 – 185, 2017. ISSN 0967-0661.

RAO, A. S.; CHIDAMBARAM, M. Smith delay compensator for multivariable non-square systems with multiple time delays. **Computers & Chemical Engineering**, v. 30, n. 8, p. 1243–1255, 2006. ISSN 0098-1354.

RAWLINGS, J. B.; ANGELI, D.; BATES, C. N. Fundamentals of economic model predictive control. In: **2012 IEEE 51st IEEE Conference on Decision and Control (CDC)**. [S.l.: s.n.], 2012. p. 3851–3861. ISSN 0191-2216.

RIBIĆ, A. I.; MATAUŠEK, M. R. A dead-time compensating PID controller structure and robust tuning. **J Process Control**, v. 22, n. 7, p. 1340–1349, 2012. ISSN 0959-1524.

RICHALET, J.; RAULT, A.; TESTUD, J.; PAPON, J. Model predictive heuristic control: Applications to industrial processes. **Automatica**, v. 14, n. 5, p. 413 – 428, 1978. ISSN 0005-1098.

ROSSITER, J. A. **Model-Based Predictive Control: A Practical Approach**. [S.l.]: CRC Press, 2003. (Control Series). ISBN 9780203503966.

SÁ, R. C.; SOMBRA, A. K.; TORRICO, B. C.; PEREIRA, R. D.; FORTE, M. D. N.; FILHO, M. P. de A.; NOGUEIRA, F. G. Tuning rules for unstable dead-time processes. **European Journal of Control**, v. 59, p. 250–263, 2021. ISSN 0947-3580.

SANTACESARIA, C.; SCATTOLINI, R. Easy tuning of smith predictor in presence of delay uncertainty. **Automatica**, v. 29, n. 6, p. 1595 – 1597, 1993. ISSN 0005-1098.

Santillo, M.; Magner, S.; Uhrich, M.; Jankovic, M. Mid-ranging control for an automotive three-way catalyst outer loop. In: **2016 American Control Conference (ACC)**. [S.l.: s.n.], 2016. p. 4193–4198. ISSN 2378-5861.

SANTOS, T. L. M. Modified {A}rtstein Predictor for {LTI} Systems with Dead Time and Unknown Disturbances. **Journal of Control, Automation and Electrical Systems**, Springer, v. 27, n. 3, p. 263–273, 2016.

SANTOS, T. L. M.; BOTURA, P. E. A.; N.-R., J. E. Dealing with noise in unstable dead-time process control. **Journal of Process Control**, Elsevier, v. 20, n. 7, p. 840–847, 2010.

SANTOS, T. L. M.; FLESCH, R. C. C.; NORMEY-RICO, J. E. On the filtered Smith predictor for MIMO processes with multiple time delays. **Journal of Process Control**, v. 24, n. 4, p. 383–400, 2014. ISSN 0959-1524.

SANTOS, T. L. M.; FRANKLIN, T. S. Enhanced Finite Spectrum Assignment with disturbance compensation for LTI systems with input delay. **Journal of the Franklin Institute**, v. 355, n. 8, p. 3541–3566, 2018.

SANTOS, T. L. M.; TORRICO, B. C.; NORMEY-RICO, J. E. Simplified filtered {S}mith predictor for {MIMO} processes with multiple time delays. **ISA transactions**, Elsevier, v. 65, p. 339–349, 2016.

SANZ, R.; GARCÍA, P.; ALBERTOS, P. Enhanced disturbance rejection for a predictor-based control of {LTI} systems with input delay. **Automatica**, Elsevier, v. 72, p. 205–208, 2016.

SANZ, R.; GARCÍA, P.; ALBERTOS, P. A generalized smith predictor for unstable time-delay SISO systems. **ISA Transactions**, v. 72, p. 197–204, 2018. ISSN 0019-0578.

SEER, Q. H.; NANDONG, J. Stabilization and PID tuning algorithms for second-order unstable processes with time-delays. **ISA Trans**, v. 67, p. 233–245, 2017. ISSN 0019-0578.

SILVA, W. A.; TORRICO, B. C.; CORREIA, W. B.; REIS, L. L. N. dos. Adaptive Feedforward Control Applied in Switched Reluctance Machines Drive Speed Control in Fault Situations. **Journal of Dynamic Systems, Measurement, and Control**, {ASME} International, v. 140, n. 5, p. 51002, 2017.

SMITH, O. J. M. Closer Control of Loops with Dead Time. **Chem Eng Prog**, v. 53, n. 5, p. 217–219, 1957.

SOMBRA, A. K. R.; PEREIRA, R. D.; FILHO, M. P. de A.; LIMA, T. A.; TORRICO, B. C.; NOGUEIRA, F. G. A dead-time compensator with dead-beat disturbance rejection response. In: **2019 18th European Control Conference (ECC)**. [S.l.: s.n.], 2019. p. 3613–3618.

TORRICO, B. C. **Contribuições ao controle preditivo robusto de sistemas com atraso**. Tese (Tese de doutorado) — Universidade Federal de Santa Catarina, Departamento de Engenharia Elétrica, 2007.

TORRICO, B. C.; CAVALCANTE, M. U.; BRAGA, A. P. S.; NORMEY-RICO, J. E.; ALBUQUERQUE, A. A. M. Simple tuning rules for dead-time compensation of stable, integrative, and unstable first-order dead-time processes. **Industrial & Engineering Chemistry Research**, ACS Publications, v. 52, n. 33, p. 11646–11654, 2013.

TORRICO, B. C.; CORREIA, W. B.; NOGUEIRA, F. G. Simplified dead-time compensator for multiple delay SISO systems. **ISA Transactions**, v. 60, p. 254–261, 2016.

TORRICO, B. C.; de Almeida Filho, M. P.; LIMA, T. A.; do N. Forte, M. D.; SÁ, R. C.; NOGUEIRA, F. G. Tuning of a dead-time compensator focusing on industrial processes. **ISA Transactions**, v. 83, p. 189–198, 2018. ISSN 0019-0578.

TORRICO, B. C.; de C. Almeida, R. N.; REIS, L. L. N. dos; SILVA, W. A.; PONTES, R. S. T. Robust Control Based on Generalized Predictive Control Applied to Switched Reluctance Motor Current Loop. **Journal of Dynamic Systems, Measurement, and Control**, {ASME} International, v. 136, n. 3, p. 31021, 2014.

TORRICO, B. C.; FILHO, M. P. de A.; LIMA, T. A.; SANTOS, T. L.; NOGUEIRA, F. G. New simple approach for enhanced rejection of unknown disturbances in lti systems with input delay. **ISA Transactions**, 2019. ISSN 0019-0578.

TORRICO, B. C.; NORMEY-RICO, J. E. 2DOF Discrete Dead-time Compensators for Stable and Integrative Processes with Dead-time. **J Process Control**, v. 15, n. 3, p. 341–352, 2005.

TORRICO, B. C.; ROCA, L.; NORMEY-RICO, J. E.; GUZMAN, J. L.; YEBRA, L. Robust nonlinear predictive control applied to a solar collector field in a solar desalination plant. **IEEE Transactions on Control Systems Technology**, v. 18, n. 6, p. 1430–1439, Nov 2010. ISSN 1063-6536.

VELUT, S.; MARé, L. de; HAGANDER, P. Bioreactor control using a probing feeding strategy and mid-ranging control. **Control Engineering Practice**, v. 15, n. 2, p. 135 – 147, 2007. ISSN 0967-0661.

VLACHOS, C.; WILLIAMS, D.; GOMM, J. B. Solution to the Shell standard control problem using genetically tuned PID controllers. **Control Engineering Practice**, v. 10, n. 2, p. 151–163, 2002. ISSN 0967-0661.

WANG, D.; LIU, T.; SUN, X.; ZHONG, C. Discrete-time domain two-degree-of-freedom control design for integrating and unstable processes with time delay. **ISA Trans.**, v. 63, p. 121–132, 2016. ISSN 0019-0578.

WANG, L. **Model Predictive Control System Design and Implementation Using MATLAB**. 1st. ed. [S.l.]: Springer Publishing Company, Incorporated, 2009.

WANG, Z.; BAI, Y.; WANG, J.; WANG, X. Vehicle Path-Tracking Linear-Time-Varying Model Predictive Control Controller Parameter Selection Considering Central Process Unit Computational Load. **Journal of Dynamic Systems, Measurement, and Control**, {ASME} International, v. 141, n. 5, p. 51004, jan 2019.

WATANABE, K.; ITO, M. A process-model control for linear systems with delay. **IEEE Transactions on Automatic Control**, v. 26, n. 6, p. 1261–1269, 1981.

ZHENG, Q.; GAO, Z. Predictive active disturbance rejection control for processes with time delay. **ISA Trans.**, v. 53, n. 4, p. 873–881, 2014. ISSN 0019-0578.

ZHONG, Q. C. On distributed delay in linear control Laws-part I: discrete-delay implementations. **IEEE Transactions on Automatic Control**, v. 49, n. 11, p. 2074–2080, 2004. ISSN 0018-9286.